University of Alberta

Molecular characterization of bacterial communities associated with a high Arctic polythermal glacier

by

Maya Pilar Bhatia

A thesis submitted to the Faculty of Graduate Studies and Research in partial fulfillment of the requirements for the degree of Master of Science

Departments of Earth and Atmospheric Sciences and Biological Sciences

Edmonton, Alberta

Fall 2004

Your file Votre référence
ISBN: 0-612-95707-1
Our file Notre référence
ISBN: 0-612-95707-1

Acknowledgements

First I would like thank my supervisors Martin Sharp and Julia Foght for their exceptional insight and constant support. Without your range of expertise covering glaciology and microbiology, and your efficiency and organization, this thesis would not have been possible. I could not have asked for a better combination of supervisors, and I am deeply indebted to you both for my academic and personal growth throughout my time in Edmonton.

Funding for this research was provided by NSERC Research Grants to Martin Sharp and Julia Foght. Funding for field research was supplemented by two grants from the Canadian Circumpolar Institute, a Circumpolar/Boreal Alberta Research Grant Award and a Northern Scientific Training Program Grant Award. Logistical support in the field (Resolute Bay and Ellesmere Island) was provided by the polar continental shelf project. Additional support was provided by a Province of Alberta Graduate Scholarship.

Corey Davis and Hardeep Rai kindly offered invaluable insight into the mechanics of T-RFLP analysis for which I am truly grateful. Without their assistance things would have been much harder. Thanks also to Pat Murrey and Lisa Ostafichuk in the Molecular Biological Service Unit for their assistance running gels.

I would also like to thank the Arctic and Alpine Research group and the Foght and Fedorak Lab groups for sharing their expertise and for their friendship. In particular, I owe a large thank-you to Joel Barker for analyzing the hydrochemistry data and to Stephanie Cheng for all of her help in the lab. Also, to Joel Barker and Melissa Lafreniere for being fantastic office mates, and to friends in Edmonton who made my time here so enjoyable (Sam Barker, Dave Burgess, Fiona Cawkwell, Nigel Atkinson, Lana Bzdel, Gabe Wolken, Chantel Nixon, Sarah Hill, Adrienne Price, Zabrina Gibbons, Brian Smerdon, Meg and Jay Cabaj, Dan and Marilyn Roth, Dave Roth, Kaston Leung, and Cam Stevens). It is hard for me to express in words how thankful I am to each of you.

A special thanks to Vanessa Hall-Patch, for her friendship and support. I feel fortunate to have had a best friend as a roommate throughout this degree.

Finally, my sincerest gratitude to my family (mom, papa, and amar), for always being my rock. Your unconditional love and support makes everything possible.

Table of Contents

List of Tables

List of Figures

List of Acroynms and Abbreviations

B-C	basal ice cave
B-F	basal ice fox junction
bp	base pairs
B-S	basal ice snout
dd	doubly distilled water
DI	deionized water
DIC	dissolved inorganic carbon
DNA	deoxyribonucleic acid
rDNA	DNA encoding rRNA genes (*rrn*)
DOC	dissolved organic carbon
EC	electrical conductivity
JEG	John Evans Glacier
P	proglacial environment
PAGE	polyacrylamide gel electrophoresis
P-R	proglacial sorted rock polygons
P-S	proglacial sands and gravels
PCA	principal component analysis
PCR	polymerase chain reaction
M-N	nunatak mud
RFU	relative fluorescence unit
RNA	ribonucleic acid
rRNA	ribosomal ribonucleic acid
SB	subglacial environment
SB-AF	subglacial artesian fountain
SB-IB	subglacial initial burst
SB-OC	subglacial outburst channel
SP	supraglacial environment
SP-IS-a	supraglacial surface ice stream A
SP-IS-b	supraglacial surface ice stream B
SP-ML-a	supraglacial marginal lake A
SP-ML-b	supraglacial marginal lake B
SP-MLS-a	supraglacial marginal lake stream A
SP-MLS-b	supraglacial marginal lake stream B
T-RFs	terminal restriction fragments
T-RFLP	terminal restriction fragment length polymorphism

Chapter 1. Introduction

1.1. Thesis Objectives

The objective of this thesis is to characterize and discern the relationships among the bacterial populations, beneath, on, and adjacent to a high Arctic polythermal glacier, so as to infer the source of the subglacial bacterial communities. The study site is John Evans Glacier (JEG), Ellesmere Island, Canada. Previous investigations have discovered that microbial communities are present in the subglacial waters and debris-rich basal ice, and that they may facilitate redox reactions and chemical weathering at the glacier bed (Sharp *et al.,* 1999; Skidmore *et al.,* 2000). Although it has been demonstrated by Skidmore *et al.* (2000) that the subglacial microbes at JEG can be cultured at near *in situ* conditions, the source and molecular characterization of these newly discovered communities have not been yet been fully determined. In order to gain insight into the source, phylogenetic uniqueness, and biogeochemical function of subglacial microbial communities, this thesis proposes to: (a) characterize and compare the genetic patterns of bacterial communities in the subglacial (the basal ice layer and subglacial waters), supraglacial (snow and ice on top of the glacier), and proglacial (sediments adjacent to the glacier) environments and (b) investigate whether the water chemistry of the surrounding environment reflects microbially mediated geochemical reactions. The first objective will be achieved by using a physical lysis technique and molecular analyses. The second objective will be achieved by collecting corresponding snow, ice, and water samples from the subglacial and supraglacial sites, and comparing the hydrochemical analyses with the molecular community composition results. The research hypothesis is that the subglacial, supraglacial, and proglacial bacterial communities at JEG are different, heterogeneously distributed across the different glacial environments, and correlated to site-specific environmental parameters. This would imply that some members of the subglacial community are unique to that environment.

The results of this study will allow us to infer whether (a) the subglacial community is unique, as would be expected if the subglacial environment has existed for some time and supports a stable ecosystem or (b) the subglacial community is primarily composed of selected components of the proglacial and supraglacial communities that have been overridden during glaciation or transported into the subglacial environment by surface-derived melt waters or downwards advection in glacier ice by glacier flow. The latter would be expected if the subglacial community is young, and perhaps, is impacted on a regular basis by addition of new inoculum from the soils or the surface. In this way, we can infer the source of the subglacial bacterial communities, and assess whether the subglacial environment is selectively favoring part of the soil or surface communities or whether it favors organisms distinct from those in the proglacial and supraglacial environments. The wide differences in physical factors such as ambient temperature, light, water, nutrient availability, and temperature fluctuations among the subglacial, proglacial, and supraglacial environments suggest that bacterial community composition may vary significantly among the three different locations. By assessing if the community compositions differed in relation to the hydrochemistry we may be able to gain some insight into the potential causes of differing microbial activity at JEG. This research is valuable because it will provide increased understanding of a newly discovered microbial niche, the limitations of life on Earth, and, possibly, analogues for extraterrestrial life.

1.2. Thesis Scope and Rationale

Until recently, the subglacial environment was considered to be devoid of microbial life (Raiswell, 1984; Raiswell and Thomas, 1984). Furthermore, many workers previously assumed that there was no subglacial weathering based on the assumption that there is no atmospheric CO_2 source to generate acidity (Gibbs and Kump, 1984; Kump and Alley, 1994). However, recent investigations have discovered evidence of microbial communities in the refrozen lake water above Antarctic subglacial lakes (Priscu *et al.*, 1999), and at the beds of alpine (Sharp *et al.*,

1999) and high Arctic (Skidmore *et al.*, 2000) glaciers. These communities are interesting as they exist in extreme cold, dark, oligotrophic environments that exclude many other organisms, and possibly provide the closest Earthly analogues to extraterrestrial environments such as ice-covered areas of Mars and Europa (Anderson *et al.*, 1998; Skidmore *et al.*, 2000). Therefore, by characterizing their composition, distribution, and biogeochemical function we will extend our understanding of the limitations to life on Earth, and the types of life that may be present elsewhere in the solar system.

Recent studies (Tranter *et al.*, 1994; Sharp *et al.*, 1999; Skidmore *et al.*, 2000; Bottrell and Tranter, 2002; Tranter *et al.*, 2002; Wadham *et al.*, 2003) have determined that microbially mediated reduction-oxidation (redox) reactions facilitate subglacial chemical weathering because microbes can generate CO_2 from the oxidation of organic C and because microbially mediated oxidation of sulfides generates sulfuric acid. The presence of subglacial microbial communities and subglacial chemical weathering may have important implications for variations in the global carbon cycle on glacial-interglacial timescales (Sharp *et al.*, 1999; Skidmore *et al.*, 2000). Moreover, the water chemistry in a subglacial environment reflects the geochemical reactions that occur there, and these in turn may be related to the types of microbes found at the glacier bed (Sharp *et al.*, 1999; Lanoil *et al.*, 2001; Skidmore *et al.*, in preparation). For example, iron and sulfide oxidizing bacteria are present in water samples beneath glaciers where microbially mediated sulfide oxidation is an important process for producing sulfate (e.g. Bench Glacier, Alaska), but are absent where sulfate is primarily derived from evaporite sources (e.g. John Evans Glacier, Nunuvut) (Lanoil *et al.*, 2001; Skidmore *et al.*, in preparation). Thus, the presence of different bacterial communities may explain variations in glacial water chemistry.

Previous studies in the laboratory have successfully established the presence and viability of microbes and the production of redox reaction products from subglacial microbes at near *in situ* conditions (Sharp *et al.*, 1999; Skidmore *et al.*, 2000; Foght *et al.*, 2004). However, these studies consisted primarily of culture-based experiments that are limited because many organisms

in the natural community are unresponsive to cultivation (Amann *et al.*, 1995). Laboratory culture experiments do not necessarily indicate *in situ* activity or provide information concerning the source or composition of the communities, and the inability to simulate actual *in situ* conditions may result in an altered apparent community composition (Amann *et al.*, 1995). An alternative method to culture-based experiments, which would more fully characterize the microbial communities at JEG and possibly determine the source of the subglacial microbes, would be to conduct molecular based studies.

Preliminary molecular analyses have been conducted by Lanoil *et al.* (2001) and Skidmore *et al.* (in preparation) on the subglacial microbial communities at JEG. However, it is interesting to note that while they indicate a predominance of Gram-negative bacteria, culture studies using the same samples grew primarily Gram-positive bacteria (Balakrishnan, 2000). This discrepancy may be explained by the fact that Lanoil *et al.* (2001) and Skidmore *et al.* (in preparation) used a relatively gentle chemical lysis procedure that may have been biased towards extracting DNA from Gram-negative cells, which are easier to lyse than Gram-positive cells. In order to circumvent this problem, this study used a more severe physical cell disruption technique.

The study site for the project is John Evans Glacier, Ellesmere Island, Canada, (Figure 1.1) which is a high Arctic polythermal glacier. A polythermal glacier consists of a core of ice at the pressure melting point, surrounded by an outer layer of cold ice. Cold ice is defined as ice that is below the pressure melting point (Blatter and Hutter, 1991). The core of warm ice at the pressure melting point is located at and immediately above the glacier bed, and is overlain by cold ice that may extend all the way to the bed in areas surrounding the warm core. Melting occurs at the warm core of the glacier, providing liquid water, which may serve as a foundation for microbial life. The general *in vitro* growth conditions for subglacial microbes are known from the previous culture experiments (Balakrishnan, 2000; Skidmore *et al.*, 2000), and from this work it has been possible to extrapolate to the specific functional types of microbes that exist in the

subglacial environment at JEG (Skidmore *et al.*, 2000). However, no analysis comparing the subglacial, proglacial, and supraglacial communities on a molecular level has been performed here or elsewhere. Such an analysis would be useful as it could determine the source of the subglacial microbes, whether they are allochthonous microbes (originating from adjacent environments) or autochthonous (indigenous populations unique and adapted to the subglacial environment). If the subglacial populations are distinct from the proglacial and supraglacial communities, it implies the existence of a functioning ecosystem with biogeochemical significance in the subglacial environment. Additional issues that can be addressed include the species distribution and diversity of glacial bacteria, thus providing a more complete understanding of the extent of bacteria distribution in glacial environments and of subglacial community composition. Finally, the creation of an inventory of bacteria present at JEG and their distributions throughout the subglacial, supraglacial, and proglacial environments may aid future identification of the major microbial groups that facilitate subglacial biogeochemical reactions.

The remainder of this chapter consists of a literature review of previous studies of subglacial microbes, subglacial water chemistry, work at JEG, and limitations and biases associated with molecular techniques used to assess environmental microbial populations.

1.3. Literature Review

1.3.1. Subglacial environments – Temperate alpine glaciers

Active microbial communities have recently been documented at the beds of two Swiss alpine valley glaciers, Glacier de Tsanfleuron and Haut Glacier d'Arolla (Sharp *et al.*, 1999). Sharp *et al.* (1999) investigated microbial communities inhabiting supraglacial and subglacial meltwaters, borehole meltwaters, glacier ice and debris-rich basal ice, and melt-out till at these glaciers. The primary purpose of this study was simply to determine if microbes were present in the subglacial environment and if so, at what numerical levels. This study was motivated by observations of hydrochemistry that pointed to the occurrence of reactions that would be

considered microbially mediated in subaerial environments. Microbes were found in all the samples, and the numbers were of a size comparable to those previously documented in the active layer of permafrost (10^7-10^9/g) (personal communication from D. Gilichinsky cited by Sharp *et al.*, 1999), and much larger than communities previously found in Antarctic ice cores (>10^3/mL) (Abyzov, 1993). Generally, the microbial numbers were greater in the Tsanfleuron ice and sediment (mean 9.6 x 10^6/mL, range 9.3 x 10^5 to 5.9 x 10^7/mL) than in the Arolla waters (mean 2 x 10^5/mL, range 5.3 x 10^4/mL to 1.8 x 10^6/mL). If the microbes were merely associated with subglacial waters that subsequently refroze to the glacier sole, it would be expected that the numbers in the ice and sediment would be similar to those in the waters, unless microbes are rejected during freezing along with solute and sediment. The fact that the numbers were much greater in the Tsanfleuron ice and sediment suggests that the Tsanfleuron microbes may have represented *in situ* communities because the sediment may serve as a substrate for growth. However, the differences in the numbers of the microorganisms found between the Tsanfleuron ice and sediment and the Arolla waters may also have been a consequence of the different environmental conditions beneath the two glaciers.

The numbers of microorganisms found were positively correlated with sediment concentration suggesting that the metabolic processes of subglacial microbes may involve the oxidation of reduced minerals or organic carbon in the sediments (Sharp *et al.*, 1999). Furthermore, thawed basal ice samples from Glacier de Tsanfleuron incubated at 4°C for 2 months exhibited a 4- to 6-fold increase in microbial numbers and the production of a significant amount of sulfate (3190 μeq/L and 520 μeq/L in two samples). The observed sulfate yield was two orders of magnitude greater than that expected for strictly abiotic reactions (Sharp *et al.*, 1999).

Sharp *et al.* (1999) provided strong evidence that microbes exist beneath the beds of temperate Alpine glaciers, and argued that microbially mediated redox reactions at the glacier bed

(e.g. sulfide oxidation, oxidation of organic carbon) might drive subglacial chemical weathering processes. This finding is significant because it challenges the previously accepted notion that subglacial chemical weathering arises from purely abiotic reactions. This idea is discussed in detail in the next section (1.3.2.). Additionally, the presence of large, active subglacial microbial communities may affect carbon cycling in soils that accumulated organic carbon during interglacial periods and were thereafter overridden by the last major glaciation.

Recent investigations have also discovered active bacterial communities at the beds of two glaciers in the Southern Alps of New Zealand using culture-based methods. Foght *et al.* (2004) analyzed unfrozen subglacial sediments and overlying glacier ice and found total numbers (2-7 x 10^6 cells g^{-1} dry weight) similar to those documented by Sharp *et al.* (1999) in the Swiss Alps. Viable counts in the New Zealand subglacial sediments were generally 3 – 4 orders of magnitudes higher than those in glacier ice, supporting the correlation with sediment concentrations suggested by Sharp *et al.* (1999). Additionally, nitrate-reducing and ferric iron-reducing bacteria were detected in the Southern Alps subglacial sediments, but were limited in the glacier ice samples. Foght *et al.* (2004) also employed a culture-based community technique using 16S rRNA gene amplification, the typical method used for microbial community analysis (discussed further in section 1.3.8.2). Restriction fragment analysis of 16S rDNA amplified from pure cultures resolved 23 different groups, some representing bacteria associated with permanently cold environments. Notably, similar types of bacteria were found in both the subglacial sediments and overlying glacier ice, though the subglacial sediments did possess the communities in greater abundance. However, because the glacier ice sampled in this study directly overlaid the subglacial sediments, the glacier ice may have had a basal component due to inter-folding of the two ice types close to the bed.

1.3.2. Subglacial water chemistry in alpine glaciers and its implications for subglacial microbial life

Subglacial chemical weathering is the fragmentation or loss of material when minerals in the rocks and soils react with acidic and oxidizing substances at the glacier bed (Schlesinger, 1991). Historically, subglacial chemical weathering was thought to consist of a series of inorganic reactions that occurred in oxic environments (Raiswell and Thomas, 1984). The dissolution of atmospheric CO_2 or biologically derived CO_2 via carbonation provides the main proton source fueling geochemical weathering in surface environments, and thus it was assumed that subglacial chemical weathering occurred by a similar mechanism (Raiswell, 1984, Schlesinger, 1991; Tranter *et al.,* 1993). Sulfide oxidation and carbonate dissolution were recognized as the primary reactions (Equations 1 and 4, Table 1.1) (Raiswell, 1984; Tranter *et al.,* 1993). The protons required to dissolve carbonate (HCO_3^-), in addition to those derived from sulfide oxidation, were produced by the dissociation of carbonic acid (H_2CO_3) from the dissolution of CO_2 in water (Equation 2, Table 1.1) (Reynolds and Johnson, 1972; Raiswell, 1984; Tranter *et al.,* 1993). However, the source of the CO_2 in the subglacial environment was unknown, because unlike surface environments, the glacier bed is isolated from the atmosphere and there was assumed to be little or no organic C in subglacial sediments (Fairchild *et al.,* 1994; Skidmore, 2001). Thus, the rate of subglacial chemical weathering generally was believed to be insignificant because access to atmospheric CO_2 was restricted (Reynolds and Johnson, 1972; Tranter, 1982; Gibbs and Kump, 1994; Kump and Alley, 1994).

However, there were anomalies in data collected from the Swiss Alps (Glacier de Tsanfleuron and Haut Glacier d'Arolla) that led researchers to speculate that subglacial geochemical weathering may be microbially mediated (M. Sharp, personal communication, 2002). Firstly, analysis of the ^{13}C isotope chemistry of secondary calcite rocks at Glacier de Tsanfleuron revealed that the isotopic signatures of the calcites were lighter than expected if the rocks were being precipitated solely from DIC derived from the carbonate bedrock (Fairchild *et al., 1993*). The light calcite signature signifies that the dissolved inorganic carbon (DIC) in the water from which the precipitation took place was also isotopically light, thus indicating that a

component of the DIC probably originated from organic carbon (Fairchild *et al.*, 1993). The source of this organic C may be microbial respiration (Equation 3, Table 1.1), which forms HCO_3^- that precipitates into the secondary calcite rocks.

Secondly, sulfide oxidation is an important weathering process in glacial systems, given that subglacial meltwaters are sulfate rich relative to non-glacial waters, however, the levels of sulfide oxidation observed were not explicable if only abiotic reactions were considered. Analysis of the meltwater chemistry of 17 boreholes at Haut Glacier d'Arolla during the 1993 and 1994 melt seasons, revealed that the borehole meltwaters had extremely high concentrations of sulfate (up to 1200 μeq/L), which exceeded the upper limit of sulfate present if the sulfides were being oxidized strictly chemically by oxygen (ca. 414 μeq/L) (Tranter *et al.*, 2002). Thus, either the input waters to the subglacial drainage system were 250% saturated in comparison to atmospheric O_2, which is unlikely, or there was a source of oxidizing agents at the glacier bed, which facilitated sulfide oxidation under anoxic conditions (Brown *et al.*, 1994; Tranter *et al.*, 2002). Microbial activity most likely catalyses the oxidation of ferrous iron (Fe^{2+}) to ferric iron (Fe^{3+}), which thus replaces oxygen as the terminal electron acceptor (TEA) in sulfide oxidation under anoxic conditions at the glacier bed (Tranter *et al.*, 2002; Sharp *et al.*, 1999). Subsequent analysis of sulfate oxygen isotopic composition of bulk meltwaters from Haut Glacier d'Arolla confirmed that anoxic conditions were present at the glacier bed (Bottrell and Tranter, 2002). Sulfate in the bulk glacial meltwaters from the early melt season (May), was ^{18}O-depleted, whereas the sulfate in the meltwaters from later in the season (July, August) was ^{18}O-enriched. Depleted ^{18}O values indicate that the oxygen in the sulfate was derived from the water molecule rather than from dissolved oxygen in the water, which implies a lack of dissolved oxygen in the early melt season waters (i.e. sub-oxic or anoxic conditions).

Additionally, Tranter *et al.*, (2002) found that some of the borehole meltwater samples had an excess of bicarbonate with respect to sulfate. If, as previously believed, carbonate

dissolution and sulfide oxidation were the primary abiotic reactions occurring in the subglacial environment, it would be expected that the protons derived from sulfide oxidation would equate to the bicarbonate generated from carbonate dissolution (Tranter *et al.*, 2002; M. Sharp, personal communication, 2002). Though some bicarbonate (ca. 200 μeq/L) can also be generated from carbonate hydrolysis (Equation 6, Table 1.1) without protons, Tranter *et al.* (2002) illustrated that there is more bicarbonate present in the borehole meltwaters than can be accounted for by dissolving calcite using solely the protons derived from sulfide oxidation. Consequently, the calcite must be weathered using protons from another source. Tranter *et al.* (2002) suggested that microbial respiration of organic C (Equation 3, Table 1.1) could provide this proton source as it generates carbonic acid, which then dissociates to supply protons.

Finally, measurements of nitrate concentrations in supraglacial and subglacial streams from 1989, 1992, and 1993 indicated periods during which nitrate was present in the supraglacial runoff, but decreased to non-detectable concentrations in the bulk runoff coming out from under the glacier (Tranter *et al.*, 1994; Tranter *et al.*, 2002). It was speculated that nitrate reduction might be occurring at the glacial bed, and microbes might be present that use nitrate as a TEA to oxidize organic carbon to CO_2 when the subglacial oxygen supply became exhausted (Tranter *et al.*, 1994; Sharp *et al.*, 1999; Bottrell and Tranter, 2002; Tranter *et al.*, 2002). Tranter *et al.* (2002) proposed that the subglacial geochemical weathering progresses from carbonate and silicate hydrolysis (Equation 5, Table 1.1) to coupled carbonate dissolution and sulfide oxidation, initially using oxygen and nitrate or ferric iron as the TEA, which instigates further carbonate and silicate weathering. Furthermore, sulfide oxidation and microbial respiration both preferentially utilize oxygen, thus resulting in sub-oxic conditions at the bed. However, subglacial chemical weathering persists, as it is not dependent on the appropriation of large amounts of atmospheric CO_2. Instead it is controlled by the O_2 content of the subglacial waters and microbial activity, which catalyze sulfide oxidation by increasing the rate of oxidation of ferrous iron (Tranter *et al.*, 2002).

The discovery of microbial communities at the base of Haut Glacier d'Arolla (Sharp *et al.,* 1999) offered an explanation for the light calcite signatures in secondary calcite precipitates, the proton source fueling subglacial gecochemical weathering, and the periodic decreases in nitrate concentrations to below detectable levels. Thus, the findings at Haut Glacier d'Arolla from subglacial water chemistry studies are significant as they provide a separate realm of evidence apart from culture or molecular studies, indicating that microbial communities are likely present and active at glacier beds. Furthermore, they illustrate how subglacial microbial activity could drive subglacial chemical weathering thereby resolving many previously unexplained anomalies in the water chemistry data.

1.3.3. Field Site Description: John Evans Glacier

JEG (79° 40' N; 74° 00' W) is a high Arctic polythermal valley glacier located on the eastern coast of Ellesmere Island, Nunavut. JEG is about 20 km long, terminates on land, and occupies a 220 km^2 basin, which is 75% glaciated (Woodward *et al.,* 1997). The glacier bed is composed of an Ordovician/Silurian carbonate/evaporite sequence with a small clastic component (Kerr, 1972). JEG extends in elevation from 100 m to 1500 m, and ranges in thickness from ~150 m in the terminus region to ~ 400 m at the equilibrium line (~ 750 m). From 1997 to 1999, the mean annual air temperatures were -14.3 °C at the terminus (~ 200 m), -15.2°C at 850 m, and -14.8 °C in the upper accumulation region (~ 1150 m). Temperatures measured 15 m deep in the ice from the accumulation and upper ablation areas ranged from -7 to -15°C. Radio-echo sounding indicates that JEG is composed primarily of temperate ice in the ablation area, and cold ice in the accumulation area. In the upper ablation area (4-7 km up glacier from the terminus), temperate ice is present only at the bed. However, in the lower ablation area (the lowest 4 km of the glacier) where the ice is approximately 200 m deep, the temperate ice layer can be up to 20 m

thick. Exceptions to the general pattern are that the ice is cold-based at the glacier margins and over a prominent bedrock bump in the ablation region (Copland and Sharp, 2001).

1.3.4. The supraglacial, subglacial, and proglacial environments at JEG

The supraglacial environment comprises the snow, ice, and water on the glacier's surface. Glacier ice constitutes the majority of ice masses, and is usually formed by the metamorphosis of snow into ice via firnification processes near the surface of glaciers and ice sheets (Hubbard and Sharp, 1989). Supraglacial waters are found in meltwater streams and lakes that form on the glacier surface during the summer, originating from melt of the supraglacial snow and glacier ice. JEG supraglacial snow, ice and waters typically have low electrical conductivity (EC; a measure of dissolved solutes in water) (<10 μS/cm) and low sediment concentrations (<0.01 g/liter) (Skidmore *et al.*, 2000).

The subglacial environment includes the basal ice layer, waters that are in contact with the glacier bed, and subglacial sediments. Basal ice underlies the glacier ice, and constitutes a relatively thin layer of the ice mass, though it may extend vertically to tens of meters (Figure 1.2). The basal ice layer is chemically and physically distinct from the glacier ice as it contains substantial amounts of basally derived sediment, and is formed by processes that occur at the glacier bed (Skidmore *et al.*, 2000; Hubbard and Sharp, 1989). Basal ice typically has much higher solute and sediment concentrations than glacier ice, due to the incorporation of glacially overridden material and basally derived sediment. Surficial debris is not typically incorporated into the basal ice layer. Theoretically, the basal ice layer can be formed by various mechanisms, including folding, basal accretion of subglacial waters (water freezing directly onto the glacier sole), or refreezing of ice onto the bedrock in calcites (Hubbard and Sharp, 1989). At JEG, the refreezing of ice onto the glacier bed, or the accretion of super-cooled waters to the ice at the bed interface most likely formed the debris-rich basal ice layers. These layers are several meters thick

and are accessible for sampling as they are widely exposed at the glacier margins (Skidmore, *et al.*, 2000).

At JEG, subglacial waters originate as supraglacial waters that reach the bed through crevasses and moulins in summer, and subsequently mix with small amounts of groundwater and basal melt water at the glacier base. Since subglacial waters interact with the rock and sediments that underlie the ice they have high EC concentrations (>100 μS/cm) and high suspended sediment concentrations (>0.1 g/liter) (Skidmore *et al.*, 1999).

The proglacial environment includes the sediments in front of and adjacent to the glacier. These sediments have been exposed by retreat of the glacier or deposited by proglacial melt streams after deglaciation. They represent potentially more biologically developed areas, possibly containing light-based microbial communities (Welker *et al.*, 2002).

1.3.5. Previous hydrological work at JEG – Evidence for a subglacial drainage system

The summer melt season at JEG typically begins in early June and persists until early August, and during this time complex supraglacial and subglacial drainage systems form (Skidmore and Sharp, 1999). Skidmore and Sharp (1999) conducted the first study analyzing subglacial water released from the glacier, and found that a subglacial drainage system forms annually beneath JEG. Chemical analyses of the subglacially derived waters indicated that they are distinct from the supraglacial waters, as they have much higher degrees of rock:water contact. The subglacial streams have much higher concentrations of ionic species indicative of silicate weathering (Na^+, K^+, and Si) (Equation 5, Table 1.1) and dissolution of the gypsum bedrock (Ca and SO_4^{2-}), while solute in the supraglacial streams consisted predominantly of Ca and HCO_3^-. The differing chemistries between the two waters illustrate that the waters exiting from beneath the glacier contain more solute and a different mix of solute species than waters entering the glacier from the surface. This implies that the subglacial waters have acquired solute by rock:water interaction during transit through the glacier, thus suggesting they have come into

contact with the glacier bed since glacier ice contains very low concentrations of sediment (Skidmore and Sharp, 1999).

In the early melt season, supraglacial runoff from the central basin penetrates into the glacier interior through a large crevasse field located 4 km from the glacier terminus (Skidmore and Sharp, 1999). These waters accumulate in a subglacial reservoir, until a threshold pressure is reached which is great enough to break through the boundary of cold ice frozen to the glacier bed that initially impedes outflow. The presence of this cold ice barrier may delay the initiation of subglacial drainage from the reservoir after the onset of the summer melt season. However, once outflow commences, the discharge patterns are usually determined more by the drainage conduit properties (i.e. openings and closings), than the supraglacial meltwater input to the reservoir. Previously, discharge from the reservoir has been observed to occur via a succession of distinct outflow events. The first outflow event is characterized by the formation of an artesian fountain on the glacier surface, followed by upwelling of waters through subglacial sediments at the glacier margins. After a period of time the second event commences in which the outflow becomes much larger and channelized, and the water is released via an outburst channel, forming the subglacial stream (Skidmore and Sharp, 1999). Though the work by Skidmore and Sharp (1999) described only two years of flow (1994 and 1996), an analysis of aerial photography of JEG from 1959 and field observations in 1995 and 1998 indicate that the two outflow events occur annually (excluding 1999 and 2001). The presence of a subglacial drainage system fed by supraglacially derived meltwaters is surely important to subglacial microbial life as the annual input of surface water replenishes the subglacial environment with dissolved gases, nutrients, and liquid water.

1.3.6. Previous cultural studies at JEG

The initial paper documenting microbial life beneath glaciers by Sharp *et al.* (1999) and the subsequent analyses of borehole meltwater chemistry by Tranter *et al.* (2002) presented strong

evidence that microbes are present beneath Alpine temperate glaciers, and that their presence explains many anomalies in subglacial water chemistry. However, the *in situ* activity and the ability to culture subglacial microbes was not established by either of these studies. Skidmore *et al.* (2000) attempted to advance the investigation of subglacial microbial populations by addressing these concerns. The objectives of that study were to: (1) establish the presence of subglacial microbes beneath a high Arctic polythermal glacier (JEG), (2) examine the potentially different microbial activities in the supraglacial and subglacial environments, (3) determine the viability of subglacial microbes under near *in situ* conditions, and (4) assess the effects of microbial activity on biogeochemical processes.

Culture studies and transmission electron microscopy (TEM) conducted on supraglacial and subglacial samples indicated that microbes could be cultured from the basal ice and that these microbes were biogeochemically active at near *in situ* temperatures (Skidmore *et al.*, 2000). The supraglacial and subglacial samples examined by Skidmore *et al.* (2000) were collected aseptically during the 1996, 1997, and 1998 summer seasons. The 1996 experiments consisted of qualitative studies on the supraglacial and subglacial meltwater samples in order to assess the presence of microbial communities. The results of the 1996 experiments on the subglacial and supraglacial meltwaters suggested that the subglacial environment at JEG contained viable populations of aerobes, anaerobes, pscychrophiles ("cold-loving" organisms whose optimal growth occurs at < 15°C) and psychrotolerant organisms (organisms that can grow at near-freezing temperatures, but whose optimal growth typically occurs at 25-30°C).

The purpose of the 1997 experiments was to examine the microbial diversity and biogeochemical activity in thawed samples of glacier and basal ice from JEG. The results of the 1997 experiments clearly indicated that viable metabolically diverse anaerobic bacteria, including nitrate reducers, sulfate reducers, and methanogens were present in the basal ice and active in cultures incubated at 4°C.

Whereas the 1997 ice samples were amended with organic supplements and incubated at higher temperatures (4°C and 8°C) than those expected in the natural subglacial environment, the 1998 ice samples were incubated aerobically under near *in situ* conditions (≤ 0.3°C) (Skidmore *et al.*, 2000). Microbial activity in minimally amended and unamended basal and glacier ice samples was assessed under aerobic conditions by quantifying the mineralization of radiolabeled acetate to $^{14}CO_2$. During the subsequent 91-day incubation period at 0.3°C, acetate mineralization was detected in both the amended and unamended basal ice and the amended glacier ice samples. Mineralization of the radiolabeled acetate was not detected in the unamended glacier ice or the sterile control samples. The addition of a dilute organic amendment greatly increased the microbial activity observed in the glacier ice samples, whereas it did not significantly alter the results from the basal ice samples. This indicated that the microbes in the glacier ice were more nutrient starved than those in the basal ice or that there was no C limitation on the growth of the subglacial communities. These observations were confirmed by measurements of the organic carbon (OC) and dissolved organic carbon (DOC) concentrations in the basal and glacier samples. It was found that there was more sediment and correspondingly more OC and DOC in the basal ice samples than in the glacier ice samples. The initial source of the OC is most likely the soils, plant material, and cyanobacterial mats which were overridden during glacial advance. TEM experiments confirmed that viable, morphologically diverse microbial cells were present in the uncultured basal ice and the unamended basal ice cultures incubated at 0.3° and 4°C. These cells were observed (by TEM) to be associated with the debris-rich sediment in the basal ice layers, though not exclusively attached to them (Skidmore *et al.*, 2000).

Balakrishnan (unpublished, 2000) performed additional culture studies and taxonomic tests on basal ice samples collected from 1997-1999 (Skidmore *et al.*, 2000) in order to determine the predominant culturable genera and major types of organisms that comprise the microbial

ecosystem at JEG. The number of colonies with distinct cell morphologies was positively correlated with the sediment concentrations in the basal ice samples, thus supporting the results of Skidmore *et al.* (2000) and Sharp *et al.* (1999) that higher sediment concentrations equate to larger, more diverse microbial communities. Taxonomic tests revealed that the majority of the bacteria cultured were Gram-positive. Most of the microbes did not respire anaerobically or were facultative fermenters. The results obtained from a qualitative aerobic growth experiment agreed with those obtained by Skidmore *et al.* (2000) in that most bacteria were restricted to growing between 4°C – 22°C, and though some psychrophilic bacteria were successfully isolated, the majority of the cultured bacteria were psychrotolerant. Finally, preliminary evidence was found suggesting that both nitrogen-fixing and fermentative bacteria were present in the basal ice layer at JEG. The presence of these types of organisms supports the inferences by Skidmore *et al.* (2000) and Sharp *et al.* (1999) that subglacial communities contribute to primary nutrient cycling.

Currently the culture experiments conducted on samples from JEG by Skidmore *et al.* (2000) and Balakrishnan (unpublished, 2000) have illustrated that (1) viable microbes exist in the supraglacial and subglacial environments, (2) microbial activity is positively correlated with increasing sediment concentrations, (3) the basal ice layer contains numerous types of culturable microbes including aerobic heterotrophs, nitrate and sulfate reducers, fermenters, nitrogen-fixers, and methanogens, and (4) the microbes are viable and active in the basal ice samples at near *in situ* conditions. It is possible that the microbes present in the basal ice layer may not be representative of *in situ* populations, but were washed into the subglacial area from the supraglacial environment. However, the experiments conducted by Skidmore *et al.* (2000) and Balakrishnan (unpublished, 2000) suggest that the subglacial environment with its debris-rich basal ice and subglacial sediments possesses the necessary nutrients and organic carbon to sustain a viable microbial community. In order to fully characterize and determine the source of the microbes present in the basal ice layer it is necessary to conduct studies at a molecular level.

1.3.7. Preliminary molecular studies at JEG

Preliminary molecular analyses comparing the subglacial microbial communities found at JEG to those at Bench Glacier (BG) Alaska have been conducted to elucidate the remaining questions concerning microbial community composition and its relationship to subglacial geochemical processes. Lanoil *et al.* (2001) and Skidmore *et al.* (in preparation) used restriction fragment length polymorphism (RFLP) and sequencing to analyze 233 16S rDNA clones from BG and JEG. The majority of the rDNAs (97/100) from BG were shown to be members of the Proteobacteria group, and most of these (64/100) belonged to the β-subgroup. The majority of the rDNAs (82/133) from JEG were also related to the β-Proteobacteria group, but the remainder of the rDNAs from JEG were more diverse than those found at BG. These molecular analyses also illustrate that the types of microbes found at the glacier bed reflect the different water chemistries at JEG and BG. This implies that there is a different balance of weathering mechanisms and solute sources at the two sites. Iron and sulfide oxidizing bacteria were present in the subglacial water samples at BG, where microbially mediated oxidation of sulfides in the bedrock is an important process for producing sulfate, but were essentially absent from JEG, where sulfate is primarily produced from evaporite sources (e.g. gypsum or anhydrite). Currently, Lanoil and colleagues are continuing their molecular comparison of BG and JEG by constructing group-specific phylogenetic probes for the abundant rDNAs and conducting quantitative dot blot hybridizations of multiple samples at each glacier (Lanoil *et al.*, 2001; Skidmore *et al.*, in preparation). These data will help link the site geochemistry to the detection of certain microbial genera with known metabolic capabilities such as iron or sulfide oxidation.

1.3.8. Nucleic acid analysis of glacial microbes

1.3.8.1. Limitations of culture studies in microbial ecology

Traditionally, culture-based techniques were the primary methods used to study microbial ecology, however, culture experiments are limited because many organisms present in the natural community are believed to be unresponsive to cultivation (Amann *et al.,* 1995; Rappe and Giovannoni, 2003). The culturability of bacteria is described as the percentage of bacteria that can be successfully cultured compared to the total cells present in sample (as determined by fluorescence microscopy) (Roose-Amsaleg *et al.,* 2001). In natural terrestrial and marine habitats, the culturability of bacteria is extremely low, estimated at 0.03% and 0.001% respectively (Roose-Amsaleg *et al.,* 2001). Many microorganisms enter a non-culturable state once removed from ambient environmental conditions, and the inability to simulate precise *in situ* conditions results in an altered apparent community composition and underestimation of microbial diversity (Amann *et al.,* 1995; Rappe and Giovannoni, 2003). If the natural populations are low and specifically adjusted to specific environmental parameters, such as in oligotrophic environments, microbial diversity may be severely underestimated, as it may be impossible to detect these rare microbes among other faster growing, more adaptable species on a conventional plate culture (Amann *et al.,* 1995; Roose-Amsaleg *et al.,* 2001). Furthermore, laboratory culture experiments do not necessarily reflect *in situ* activity or provide information concerning the source or overall composition of the natural communities (Amann *et al.,* 1995; Liu *et al.,* 1997; Roose-Amsaleg *et al.,* 2001).

The recent application of molecular techniques to microbial ecology provides a powerful new analytical tool for directly studying microbes in their natural environment, free of the biases inherent in more traditional cultivation techniques that require microbial growth before analyses can be performed (Amann *et al.,* 1995; Martin-Laurent *et al.,* 2001). Furthermore, molecular approaches can be used to establish the presence and biogeochemical impact of particular populations, metabolic activities, or specific genes in an environment (Frostegard *et al.,* 1999). However, molecular methods also have their own biases that influence insights into community

composition and ecological activity (Amann *et al.*, 1995; Wintzingerode *et al.*, 1997; O'Donnell and Gorres, 1999), discussed in detail below.

1.3.8.2. Applications and limitations of nucleic acid analysis to microbial ecology

Nucleic acids (i.e. DNA and RNA) communicate the genetic information essential for growth and multiplication. Thus, the direct extraction of nucleic acids from the natural environment can provide information concerning microbial composition and activity (Amann *et al.*, 1995). Genetic information is transmitted from one generation to the next in the form of DNA; however, DNA must be transcribed into three types of RNA in order to build proteins, the basis of cellular metabolic functions. The messenger RNA (mRNA) is translated into protein, whereas the transfer RNA (tRNA) and ribosomal RNA (rRNA) assist in protein synthesis. The genes encoding rRNA (*rrn*), have been conserved throughout evolutionary time although they mutate at a constant rate that constitutes the "molecular clock". The amplified *rrn* genes are rDNA. The highly conserved aspect of rDNA ensures that it is present in all cellular biota, but the variations in its nucleic acid sequences allow it to be used as a measure of phylogenetic diversity (Wintzingerode *et al.*, 1997; Karp, 1999). In this way, the regions of the rDNA that vary slowly may be used to infer associations among broader taxonomic classifications (Bacteria, Eukarya, and Archaea), whereas the most variable regions may yield discrimination between organisms at the genus and species level (Madsen, 2000). Typically, the gene sequences of the small subunit of the ribosome (16S rDNA in prokaryotes and its equivalent 18S rDNA in eukaryotes) are studied as they are highly conserved yet taxonomically distinct, and public databases exist for comparative purposes (e.g. Ribosomal Database Project II; http://rdp.cme.msu.edu/html) (Cole *et al.*, 2003). The use of rDNA genes has some inherent limitations in that it cannot specifically determine the metabolic activity or the biogeochemical impact of a gene, such as analysis of mRNA might provide (Karp, 1999). Despite the limitations intrinsic to nucleic acid analyses, molecular techniques are still powerful tools that can be used to

complement culture studies. However, it is necessary to minimize the biases inherent in the extraction, amplification, and analyses of the nucleic acids in order to maximize the potential contribution of molecular approaches to microbial ecology. These biases are discussed in the following sections.

1.3.8.3. Applications and limitations of Bead-Beater™ cell lysis and nucleic acid extraction

Nucleic acid extraction directly from environmental samples can be achieved by a variety of physical and chemical approaches, each with their own inherent limitations and biases. In order to optimize the extraction procedure it is necessary to compromise between the maximum recovery of microbial DNA that will render the most representative estimation of community structure and diversity, and the highest quality of the DNA extracted that will optimize subsequent molecular analyses (Zhou *et al.,* 1996; Martin-Laurent *et al.,* 2001; Roose-Amsaleg *et al.,* 2001). The primary goal in nucleic acid extraction is to lyse all cells completely and isolate the nucleic acids from the cellular debris (proteins, membranes, cell walls) and environmental matrix (rock, clay, silt, sand, humic acids) (More *et al.,* 1994; Madsen, 2001). Cell extraction methods require that the microbial cells first be separated from their environmental matrix before the cells are lysed and the nucleic acids are released. However, this approach is time-consuming, and imposes an additional bias in that only DNA from cells that are successfully isolated will be extracted (Frostegard *et al.,* 1999; Roose-Amsaleg *et al.,* 2001). Conversely, direct lysis methods do not require cell isolation, and thus tend to be more representative of the *in situ* microbial community because they are able to lyse cells that are aggregated to the environmental matrix (More *et al.,* 1994; Frostegard *et al.,* 1999; Roose-Amsaleg *et al.,* 2001).

A crucial step in nucleic acid extraction is the manner in which the cells are lysed, as it directly influences the apparent phylotype abundance and overall picture of microbial community composition (O'Donnell and Gorres, 1999; Martin-Laurent *et al.,* 2001). Cell lysis can be accomplished by chemical, enzymatic, or physical methods (Miller *et al.,* 1999; Roose-Amsaleg

et al., 2001). Chemical and enzymatic lysis are comparatively gentle approaches, which typically produce higher quality DNA with minimal shearing (Roose-Amsaleg *et al.*, 2001). Chemical lysis usually involves a detergent (e.g. sodium dodecyl sulfate) or high alkaline solutions, incubation at high temperatures, a phenol/chloroform extraction, and the addition of chelating agents (e.g. EDTA or Chelex 100) in order to inhibit nucleases and separate soil particles (Miller *et al.*, 1999). Enzymatic lysis normally involves lysozyme digestion to weaken bacterial cell walls (Miller *et al.*, 1999). However, potentially significant limitations and biases persist in both chemical and enzymatic lysis with regard to the representation of the *in situ* community, primarily due to incomplete or preferential cell lysis or the incorporation of nucleic acids into the environmental matrix (Wintzingerode *et al.*, 1997; Martin-Laurent *et al.*, 2001; Roose-Amsaleg *et al.*, 2001). Physical lysis typically yields a more uniform, complete representation of the natural microbial community as it more effectively lyses the cells from a greater array of microbial groups, particularly those organisms with more resistant cell walls, such as Gram-positive bacteria, or endospores (More *et al.*, 1994; Frostegard *et al.*, 1999; Miller *et al.*, 1999; Roose-Amsaleg *et al.*, 2001).

The Bead-Beater™ (Biospec Products, Bartlesville, OK) is a physical cell disruption apparatus that directly lyses the cells *in situ* by colliding them with small (e.g. 0.1 mm and 2.5 mm diameter) zirconium beads moving at high velocities (5000 reciprocations per minute.[rpm]). Previous studies have shown that the bead-beater homogenization technique yields almost twice as much DNA as chemical lysis methods (More *et al.*, 1994; Zhou *et al.*, 1996; Miller *et al.*, 1999). More *et al.* (1994) found that a relatively high proportion (62%) of the total DNA in a 19 μg sample was extracted using the bead-beater lysis method. Furthermore, a comparison between chemical freeze-thaw procedures and bead-beater illustrated that 94% of *Bacillus subtilis* endospores remained viable (i.e. were not lysed) using the chemical lysis methods whereas only 2% of the endospores were viable after bead-beater homogenization, thus indicating that the

remaining 98% were effectively lysed after bead-beater homogenization (More *et al.,* 1994). Microscopic examination of a sediment sample after bead-beater homogenization revealed that 6% of the total cells remained intact in a sediment sample, mostly small coccoid cells (More *et al.,* 1994). Thus, though bead-beater homogenization circumvents the inherent biases in culture and chemical lysis methods by effectively lysing different types of cells (Gram-negatives, Gram-positives, endospores), until all cells in a community can be equally lysed, even severe treatments such as bead-beater homogenization will present a biased representation of the *in situ* population (More *et al.,* 1994; Frostegard *et al.,* 1999).

The primary limitations associated with the bead-beater technique are the incorporation of humic acids into the extracted DNA and increased shearing of the nucleic acids as compared to chemical lysis (More *et al.,* 1994; Wintzingerode *et al.,* 1997; Miller *et al.,* 1999). Though the incorporation of humic acids can inhibit subsequent Polymerase Chair Reaction (PCR) amplification of extracted DNA, and is the principal deterrent from using physical lysis methods in many environments (Miller *et al.,* 1999; Roose-Amsaleg *et al.,* 2001), it is probably not an obstacle in glaciated environments such as JEG, where the humic acid content of the environmental matrix is very low (M. Sharp, personal communication, 2002). However, shearing of the nucleic acids is still problematic, as it reduces the quality of the DNA product, and inhibits subsequent analyses. Generally, the longer the homogenization times the greater the DNA yield, and the smaller the DNA fragment size. However, DNA from more easily lysed microbes may become amalgamated with the soil colloids during longer homogenization periods, thus biasing the community representation from the extracted DNA towards cells which are harder to lyse (Miller *et al.,* 1999). Bead-beater homogenization can shear DNA into lengths of 5 to 10 kilobase pairs (kb) or less (Zhou *et al.,* 1996; Miller *et al.,* 1999). If the DNA is to be cloned, it is necessary to have larger fragments of DNA to reduce the number of clones required to represent the community, and thus gentler methods such as chemical lysis should be employed. If the DNA is to be used in PCR, larger fragments are less important than a high DNA yield, and thus more

severe physical lysis may be used (Miller *et al.*, 1999). Greater homogenization speeds also produce increasingly larger DNA yields, up to a maximum speed, after which DNA yield substantially decreases as the nucleic acids are sheared (Miller *et al.*, 1999). Additionally, smaller fragments have a greater tendency to produce chimeras (i.e. PCR products arising from more than once piece of template DNA). Chimeras form when two distinct, homologous (high sequence similarity) DNA molecules anneal during PCR amplification when the nucleic acid strands compete with primers (Becker *et al.*, 2000), and subsequent analysis of chimeric DNA yields inaccurate information. Thus, for each environmental sample, the speed and duration of the bead-beater homogenization conditions must be optimized to obtain the greatest yield of DNA with minimal shearing (Zhou *et al.*, 1996; Wintzingerode *et al.*, 1997; Miller *et al.*, 1999; Becker *et al.*, 2000).

1.3.8.4. Applications and limitations of PCR amplification of the extracted nucleic acids

PCR is a molecular technique that can be used to amplify specific DNA sequences quickly and exponentially from small amounts of environmental sample without cloning (Griffiths *et al.*, 1997; Wintzingerode *et al.*, 1997). In PCR, a heat resistant polymerase (e.g. from *Thermus aquaticus; Taq* polymerase) is used to catalyze the amplification of a particular region using specially designed primers (Griffiths *et al.*, 1997; Karp, 1999). Primers are short DNA fragments (oligonucleotides) with sequences complementary to the binding sites at both 3' ends of the target sequence (i.e. "forward" and "reverse" primers). Initially the extracted DNA is heated to 92°-94°C, causing the double-stranded helix to separate into its two complementary strands. The temperature is then decreased, allowing the primers (present in excess) to anneal (hybridize) to their complementary binding sites on the 3' ends of each of the strands. Subsequently, the *Taq* polymerase catalyzes the extension of the primers by adding nucleotide bases (A, T, C, or G) to the primers in the 5' direction, thus copying the target gene by creating new complementary DNA strands. This cycle is repeated numerous times (e.g. 30), doubling the

amount of target DNA each cycle, and therefore creating many copies of the target sequence in a few hours.

Though PCR amplification of nucleic acids extracted directly from an environmental matrix is the basis of many molecular studies, there are numerous implicit limitations and biases associated with this approach (Wintzingerode *et al.*, 1997; Becker *et al.*, 2000). Apart from preferential amplification as a result of the quality of the extracted nucleic acids (i.e., shearing or the presence of humic acids), the base pair composition of the DNA and competition between DNA templates also results in differential amplification (Wintzingerode *et al.*, 1997; Becker *et al.*, 2000; Roose-Amsaleg *et al.*, 2001; Sheridan *et al.*, 2003). DNA containing low proportions of guanidine (G) and cytosine (C) is preferentially amplified compared to DNA with higher G+C percentages, in which the strands do not dissociate as easily in the denaturation step of the PCR amplification (Wintzingerode *et al.*, 1997; Roose-Amsaleg *et al.*, 2001). Furthermore, differential hybridization efficiency of the PCR primers may bias the amplification of specific target DNA in mixed DNA templates (Wintzingerode *et al.*, 1997; Becker *et al.*, 2000). If the nucleic acid strands have identical primer target sequences, competition between the DNA templates for primer binding results in reduced amplification efficiency and an underestimation of the target DNA (Becker *et al.*, 2000). Conversely, non-specific amplification may also result in an overestimation of the target DNA in the presence of a large background of phylogenetically similar DNA with comparable target sequences, as some of the oligonucleotides will non-specifically bind (mismatch) to these untargeted sequences (Becker *et al.*, 2000).

Point mutations in the PCR products may affect community analysis, because during strand synthesis the *Taq* DNA polymerase has an inherent misincorporation rate, which results in base pair substitutions ranging from one error per 290 to 5411 nucleotides (Wintzingerode *et al.*, 1997). Such errors can give the appearance of unique organisms, thus erroneously increasing the apparent diversity of the community. Finally, PCR-based approaches may also be affected by amplification of contaminating DNA from reagent-borne microbes, thus biasing subsequent

analyses of community composition and diversity within the environmental sample (Wintzingerode *et al.,* 1997; Madsen, 2000). Thus, though PCR amplification is a powerful tool, which allows specific genes to be targeted and populations to be identified, it does possess intrinsic biases that limit and may misrepresent the natural microbial community. It should be noted that all of the biases inherent in PCR amplification and nucleic acid extraction necessarily influence subsequent molecular analyses performed using the amplified nucleic acids.

1.3.8.5. Applications and limitations of Terminal Restriction Fragment Length Polymorphism community analysis

Terminal Restriction Fragment Length Polymorphism (T-RFLP) analysis is currently one of the most powerful culture-independent molecular techniques by which entire communities can be resolved and analyzed. It is used to assess community composition and similarity to other communities in different environmental samples, to establish the primary differences between communities, and to test hypotheses based on sample comparisons (Madsen, 2000; Dunbar *et al.,* 2001; Roose-Amsaleg *et al.,* 2001; Blackwood et al., 2003). The principal advantage of T-RFLP analysis is that it rapidly elucidates the relative changes in community composition that occur over space or time or in response to environmental perturbations (Madsen, 2000; Osborn *et al.,* 2000; Engebretson and Moyer 2003). Thus the microbial diversity within and among numerous environmental samples can be much more efficiently studied using T-RFLP than by generating "clone libraries", which is extremely time-consuming (Osborn *et al.,* 2000). In T-RFLP, the "forward" PCR primer is fluorescently tagged, and the resultant labeled PCR products are digested with restriction enzymes. Sequence variation of the rRNA genes (*rrn*) among different species results in the restriction enzymes generating T-RFs of different lengths (Dunbar *et al.,* 2001). The digested fragments are subsequently separated by electrophoresis and resolved on a gel on which only the terminal restriction fragments (T-RFs) (i.e., fluorescently labeled 5' ends)

are detected with an automated DNA sequencer by excitation of the fluor (Liu *et al.*, 1997; Osborn *et al.*, 2000; Roose-Amsaleg *et al.*, 2001; Blackwood et al., 2003). Theoretically, each different band on the gel represents a different species. The lengths of the T-RFs are precisely determined using an automated DNA sequencer, which has internal size standards in every profile (Dunbar *et al.*, 2001). The differential conservation of restriction site positions in 16S rDNA often reduces the resolution of the T-RFs obtained from the species level to that of higher order phylogenetic groups, thus limiting the complexity of T-RFLP profiles (Liu *et al.*, 1997; Dunbar *et al.*, 2001; Engebretson and Moyer 2003). However, T-RFLP analyses serve as effective screening precursors to facilitate subsequent labor-intensive DNA sequencing.

The number and abundance of unique T-RFs ("ribotypes") detected by the automated DNA sequencer provide a quantitative estimate of species richness and diversity in a community (Liu *et al.*, 1997; Dunbar *et al.*, 2001). However, since the ribotypes are resolved from amplified genes from the total community DNA, organisms whose DNA comprises a minor proportion of the total DNA may not appear in the T-RFLP profile because the more abundant template will dominate the profile (Liu *et al.*, 1997; Osborn *et al.*, 2000). Additionally, the PCR primers and restriction enzymes used and the occurrence of PCR errors during amplification affect the number of unique ribotypes obtained, possibly resulting in an underestimation of overall community diversity (Liu *et al.* 1997; Osborn *et al.*, 2000). In order to maximize the number of unique ribotypes obtained from the greatest number of rDNA sequences it is necessary to optimize the combination of PCR primers and restriction enzymes employed in the T-RFLP analysis (Liu *et al.*, 1997; Osborn *et al.*, 2000). Despite these efforts, T-RFLP may inherently underestimate the microbial diversity as phylogenetically similar organisms can have T-RFs of identical size (Liu *et al.*, 1997; Osborn *et al.*, 2000; Miteva *et al.*, 2004). Conversely, *rrn* sequence variation (estimated to be within 0-5% among strains from the same species) may result in T-RFs from the same species having different T-RFs, possibly providing an overestimation of community diversity (Liu *et al.*, 1997; Crosby and Criddle, 2003). Additionally, *rrn* sequence redundancy

may result in one organism having multiple copies of the *rrn* operon, thus generating multiple signals for a single organism and producing an overestimation of that organism (Crosby and Criddle, 2003). The community diversity may also be overestimated if the amplified 16S rDNA genes are not fully digested by the restriction enzymes, as these partially digested fragments may appear as additional ribotypes on the T-RFLP profile (Osborn *et al.,* 2000). Finally, though amplification of 16S rDNA genes is commonly performed using "universal" primers, they do not hybridize equally well to all Eukaryal, Bacterial, and Archaeal sequences. Therefore, the extent of phylogenetic information obtained from T-RFLP analyses is implicitly dependent upon the actual ability of the primers to amplify all sequences (Liu *et al.,* 1997; Dunbar *et al.,* 2001). Nonetheless, T-RFLP is a powerful technique for rapidly assessing and comparing diversity and community origin in complex or previously unquantified microbial ecosystems (Liu *et al.,* 1997). Moreover, previous studies (Dunbar et al. 2001; Blackwood et al. 2003; Engebretson and Moyer 2003) have demonstrated that T-RFLP analysis is especially useful for analyzing communities with low to intermediate levels of species richness, thus making this technique ideal to study oligotrophic environments like JEG.

Table. 1.1. Subglacial chemical weathering reactions (Skidmore, 2001).

Proton Sources	
(1) Sulfide Oxidation	
$4FeS_{2\,(s)} + 15O_{2\,(aq)} + 14H_2O_{\,(l)} \rightarrow 16H^+_{\,(aq)} + 8SO_4^{2-}{}_{(aq)} + 4Fe(OH)_{3\,(s)}$	
pyrite	ferric oxyhydroxides
(2) Carbonation	
$CO_{2\,(g)} + H_2O_{\,(l)} \leftrightarrow H_2CO_{3\,(aq)} \leftrightarrow H^+_{\,(aq)} + HCO_3^-{}_{(aq)}$	
Atmospheric	
(3) Microbial Respiration – oxidation of organic Carbon	
$C_{\,(s)} + O_{2\,(aq)} + H_2O_{\,(l)} \rightarrow H_2CO_{3\,(aq)} \leftrightarrow H^+_{\,(aq)} + HCO_3^-{}_{(aq)}$	
Organic	
Proton Sinks	
(4) Carbonate Dissolution	
$CaCO_{3\,(s)} + H^+_{\,(aq)} \leftrightarrow Ca^{2+}_{(aq)} + HCO_3^-{}_{(aq)}$	
Calcite	
(5) Silicate Weathering	
$CaAL_2Si_2O_{8\,(s)} + 2H^+_{\,(aq)} \leftrightarrow Ca^{2+}_{\,(aq)} + H_2Al_2Si_2O_{8\,(s)}$	
Anorthite (Ca-feldspar)	weathered feldspar surfaces
Other Weathering Reactions	
(6) Carbonate Hydrolysis	
$CaCO_{3\,(s)} + H_2O_{\,(l)} \rightarrow Ca^{2+}_{\,(aq)} + HCO_3^-{}_{(aq)} + OH^-_{\,(aq)}$	
(7) Gypsum Dissolution	
$CaSO_4.H_2O_{\,(s)} + H_2O_{\,(l)} \leftrightarrow Ca^{2+}_{\,(aq)} + SO_4^{2-}{}_{(aq)} + 3H_2O_{\,(l)}$	

Figure 1.1. John Evans Glacier, Ellesmere Island, Nunuvut, Canada (Photo courtesy of M. Sharp).

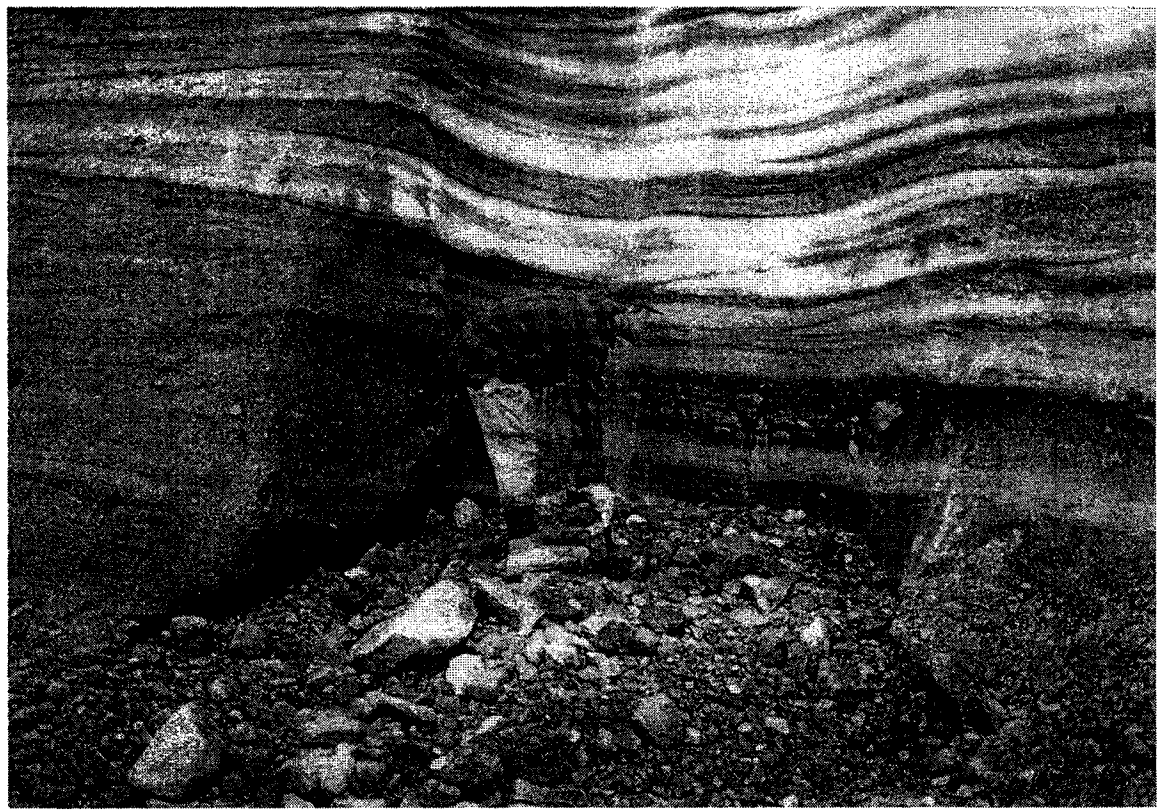

Figure 1.2. Basal ice deposits interspersed with clean glacial ice deposits at Skaare Fjord, Axel Heiberg Island, Canada. The basal ice layers are distinguished by their high sediment content and dark color (Photo courtesy of M. Sharp).

Chapter 2. Materials and Methods

2.1. Description of sampling environments, snow, ice, and water types and sample collection

Sampling was conducted throughout the summer melt season from May 21 to August 1, 2002 using the protocol described by Skidmore *et al.* (2000). The primary objective was to aseptically collect an array of samples from the supraglacial, subglacial, and proglacial environments at JEG for molecular (T-RFLP) and hydrochemical analysis (Figure 2.1 and Table 2.1).

2.1.1. Supraglacial environment

Snow samples and melt water on the glacier surface were collected. Samples of dry snow (snow at sub-freezing temperatures that has not yet experienced seasonal melting) were collected aseptically from the upper part of the glacier by digging a snow pit (Figure 2.2.a) and cleaning the pit face with an ethanol (EtOH)-flame-sterilized trowel. Samples were taken aseptically, using the sterile trowel, from the wind-crusted snow layer and transferred without handling to new 3.0-mil thick, 69-oz sterile plastic bags (WhirlPak™, Nasco Products, New Hambury, Ontario, Canada). The wind-crusted layer was approximately 11 cm below the surface and was specifically chosen because it was denser than the other snow horizons. Temperatures of the wind-crusted layer ranged from –4 to –10°C. The snow samples were melted on-site in the WhirlPak™ bags in a warm water bath (~ 30°C) and then vacuum-filtered in 150-mL increments through an EtOH-sterilized, disposable analytical filter unit with a removable 0.2 μM cellulose nitrate membrane (09-740-21A Nalgene, Rochester, New York) (Figure 2.2.b). Using EtOH-sterilized forceps, the filter membrane was removed from the unit, placed in a sterile plastic bag (WhirlPak™) (Figure 2.2.c) and stored frozen. Wet snow samples from the middle and lower

parts of the glacier were collected in Ziploc™ bags for hydrochemical analyses. Unfortunately, parallel wet snow samples were not collected for molecular analyses.

Melt water samples were collected from two different streams for microbial analysis; one stream drained a catchment composed entirely of glacier ice (surface ice stream A [SP-IS-a]) (Figure 2.3). The second stream catchment drained a meltwater lake, fed by two ice marginal channels that transported sediment from an exposed nunatak, into the marginal lake fed stream A [SP-MLS-a] (Figure 2.4). Thus, the SP-MLS-a waters had contact with ice marginal sediments and bedrock before draining onto the glacier, while those in the SP-IS-a stream did not. Samples were collected aseptically in twice-autoclaved 1-L polypropylene screw closure bottles (11-825-B, Nalgene). The bottles were new, and prior to autoclaving were washed in soap and doubly distilled (dd) water, and rinsed in deionised (DI) water. Subsequently, the bottles were wrapped in foil and autoclaved on two successive days to kill any endospores. Samples were stored on ice in coolers at $\leq 4°C$ for up to 22 d in the field, transported to a laboratory (72 h) at $\leq 4°C$, and frozen at -20°C in the original bottles until processed for chemical and microbial analyses. One bottle from SP-IS-a was stored at 4°C upon arrival at the laboratory until processed 64 d later. Samples from the ice marginal lake (SP-ML-a) feeding SP-MLS-a were also collected for hydrochemical analysis. Two additional supraglacial streams were also sampled for hydrochemical analysis: a third stream catchment which also drained a catchment composed entirely of glacier ice (surface ice stream B [SP-IS-b]), and a fourth catchment draining another meltwater lake, marginal lake fed stream B (SP-MLS-b). Samples from the meltwater lake (SP-ML-b) feeding SP-MLS-b were also collected for hydrochemical analysis.

2.1.2. Subglacial environment

To represent the subglacial environment, basal ice samples were collected from three specific locations. The first was accessible in late May before the onset of the melt season,

whereas the other two locations only became accessible in late June and July. The first site was at the terminus (snout) of the glacier ("basal ice snout" [B-S]); the second site was in an ice cave at the glacier's west margin, which was exposed due to a stream cutting into the glacier bed ("basal ice cave" [B-C]) (Figure 2.5); and the third site was at the junction between JEG and a tributary glacier (Fox glacier) where the basal ice was exposed ("basal ice Fox junction" [B-F]). Samples were collected aseptically using EtOH-flame-sterilized ice axes. A few centimeters of the surface ice was chipped away prior to sampling to ensure that the samples were not exposed to atmospheric contamination. Subsequently, samples were chipped into flame-sterilized metal collection trays and transferred without handling into sterile plastic bags (WhirlPak™). Samples were stored on ice in coolers for up to 30 d in the field, transported frozen to a laboratory (72 h), and stored frozen and undisturbed in the original sterile bags until processed for analysis. In addition to basal ice, frozen mud (M-N) from the nunatak lake (ice marginal lake A) was collected in a similar manner to the basal ice collection protocol above.

Subglacially-derived water samples were collected from three different sources. The first set of subglacial water samples (three bottles) was collected on June 30 at 19:00 h when the water that had been stored in the subglacial environment over-winter burst at the glacier front from the ice in a pressurized horizontal flow ("subglacial initial burst" [SB-IB]) (Figure 2.6). Samples were then collected each hour for the next 20 hours to determine when the over-winter stored water became diluted by the addition of the new season's melt. Sometime during this 20 h period, (between 4:00-8:00 AM on July 1) the subglacial flow shifted from the glacier front to an artesian fountain on the glacier surface, between 1.4 – 2.0 m high; samples were collected from this fountain ("subglacial artesian fountain" [SB-AF]) (Figure 2.7). The SB-IB outflow ceased once the SB-AF outflow started. The artesian fountain persisted for one week (until July 7), during which period the subglacial outflow shifted to a channelized flow (July 4 – August 1) at the glacier front ("subglacial outburst channel" [SB-OC]) (Figure 2.8). Thus the SB-AF and SB-OC outflows overlapped for about three days. Presumably the waters draining from the channel

(SB-OC) were more diluted with supraglacial inflow than those associated with SB-IB. The SB-IB waters represent those that have been stored at the base over-winter, whereas the SB-OC waters represent those from later in the melt season when supraglacial inflow from the surface has penetrated to the bed. Samples were collected from this channel until the end of the field season (August 1). All subglacial water samples were collected aseptically in sterile plastic 1-L bottles (Nalgene). Samples were stored on ice in coolers at $\leq$ 4°C for up to 8 d in the field, transported to a laboratory (72 h) at $\leq$ 4°C, and frozen at -20°C in the original bottles until processed for chemical and microbial analyses. No salt precipitates were observed in the bottles, indicating that the freezing process did not substantially affect the water chemistry. Two bottles of SB-IB were stored at 4°C upon arrival at the laboratory until processed 7 d and 84 d later, respectively.

2.1.3. Proglacial environment

Sediment samples were collected from fine sands and gravels exposed in stream bank cuts directly in front of the glacier terminus (P-S) (Figure 2.9). Samples were also collected from sorted rock polygons adjacent to the glacier (P-R) (Figure 2.10), on which incipient soils were developed. Specifically, these polygons had a thin black algal crust on the surface of the fine sediments in the center of the polygons. Some plants were also growing on these sediments (e.g. Arctic poppy, purple saxifrage). There was little sign of soil development. Samples were collected in July, which was sufficiently late in the melt season to ensure that the sediment samples were unfrozen and exposed. Samples were collected aseptically using an EtOH-flame-sterilized trowel. Subsurface samples (ca 20-40 cm) were collected to avoid surface and atmospheric contamination, and were shoveled without handling directly into sterile plastic bags (WhirlPak™). Samples were stored in coolers for up to 16 d in the field, transported frozen to a

laboratory (72 h), and stored frozen and undisturbed in the original sterile bags until processed for experiments.

2.2. Hydrochemical Analyses

Samples of supraglacial and subglacial waters were processed on-site for measurements of electrical conductivity (EC), pH, major anions (nitrate [NO_3^-] and sulfate [SO_4^{2-}]), and dissolved organic carbon (DOC) content using the protocols described by Skidmore and Sharp (1999), Lafreniere and Sharp (2002; 2003). Samples for EC, pH, and ion chromatography were collected from streams in 1-L polyethylene wide-mouth bottles (Nalgene) that had been rinsed in DI water and the sample stream (three times each) prior to sampling. Separate bottles were designated for supraglacial and subglacial stream sampling to avoid cross-contamination between the two water types. Subglacial ice samples were similarly processed in the laboratory (filtered and analyzed), when the samples were thawed for microbial analysis, using the protocol described by Skidmore and Sharp (1999) and Lafreniere and Sharp (2002; 2003).

2.2.1. Electrical Conductivity (EC)

The EC of a liquid is a measure of its ability to transmit an electrical current. This ability increases as the concentration of ions in solution increases. Thus, EC can be used as a measure of total dissolved solutes in a water sample. EC concentrations were measured in the field for all supraglacial and subglacial water samples within 1 h of collection using an Orion 128 conductivity meter (Thermo Electron, Waltham, MA) with automatic temperature compensation to 25°C. Before measuring the EC of samples, the conductivity meter was calibrated using 2 conductivity standards (10 μS/cm and 100 μS/cm) (Fisher Scientific, Nepean, Ontario). After the meter was calibrated, the EC of a 50 mL aliquot of unfiltered sample was measured in a clean plastic cup which had previously been rinsed three times with DI and sample water. Supraglacial samples for EC analysis were collected from wet snow, ice streams A and B, lake streams A and

B, and ice marginal lake A. Subglacial samples for EC analysis were collected from the basal ice locations B-S, B-C, and B-F, and from the subglacial waters SB-IB, SB-AF, and SB-OC.

2.2.2. pH and ion chromatography

The pH of a water sample is the negative log of the concentration of hydrogen ions in the sample. The pH was measured using a Ross Sure-flow electrode connected to an Orion 290A digital pH meter with automatic temperature compensation calibrated using Orion low ionic strength buffers (pH 4, 6, and 10 standards) (Thermo Electron). A 500-mL aliquot of sample water was vacuum filtered on-site through a 0.45 μM cellulose nitrate membrane (Whatman International Ltd., Maidstone, England) in a plastic filtration chamber (Nalgene). Prior to each use, the filtration chamber was rinsed with DI and sample water three times. After filtration, the pH of a 50-mL aliquot of the filtrates was measured immediately in a clean plastic cup, which had previously been rinsed with DI and filtered sample three times, and to which a 10% volume (0.05 mL) of ionic strength adjustor (pHisa solution) (Thermo Electron) had been added. The pH readings were recorded once the meter had stabilized. The pH electrode was immersed in DI water between samples. From the remaining filtrate, two 20-mL samples were collected for laboratory analysis of major anions by liquid ion chromatography in polyethylene scintillation vials, which had been pre-rinsed three times with filtered sample. Samples were stored at $\leq 4°C$ for up to 22 d in the field, transported to a laboratory (72 h) at $\leq 4°C$, and refrigerated until analysis after 140 d. Anion concentrations were analyzed using a Dionex DX500 ion chromatograph with a Dionex Ionpac AS4 column and 1.7 mM sodium carbonate/1.8 mM sodium bicarbonate eluent (Dionex Corporation, Sunnyvale, CA). The uncertainty in ion concentrations was estimated from analyses of duplicate samples run on separate days following the protocol described by Lafreniere and Sharp (2003). Supraglacial samples for pH and ion chromatography analysis were collected from the same areas as for EC analysis (excluding wet

snow which was omitted due to time constraints). Subglacial samples for pH and ion chromatography analysis were collected from the sites listed above for EC analysis.

2.2.3. Dissolved Organic Carbon (DOC)

Stream samples for DOC analysis were collected in 250-mL amber glass bottles, and filtered on-site using a glass filtration apparatus and 0.7-μm-pore-size GF/F filters (Whatman). Filtrates were transferred to 40 mL amber glass EPA vials containing 25 µL concentrated HCL to acidify the samples to pH 2 for storage preservation until analysis and to remove dissolved inorganic carbon (DIC). Prior to sampling, the sample bottles, filtration apparatus, and EPA vials were soaked in 2M HCL, rinsed with DI water, and combusted overnight at 550°C to burn off any organic carbon residue. The GF/F filters were similarly combusted overnight at 550°C. On-site, the sample collection bottles and filtration apparatus were soaked and rinsed in 2M HCL, DI water, and sample water between each use. Samples were stored at $\leq$ 4°C for up to 22 d in the field, transported to a laboratory (72 h) at $\leq$ 4°C, and refrigerated until analysis 97 d later. DOC was measured as non-purgeable organic carbon by high temperature (680°C) combustion with a Shimadzu TOC 5000A analyzer equipped with a high sensitivity platinum catalyst (Shimadzu, Columbia, MD). Potassium hydrogen phthalate was used to prepare standards for a five-point calibration curve from 0 – 1.2 ppm. Any samples with values outside the calibration curve were diluted with DI water. Each sample was measured three times, and the reading was deemed reliable if the coefficient of variation was not greater than 1.2% (J. Barker, personal communication, 2004). Supraglacial and subglacial samples for DOC analysis were collected from the sites listed for EC analysis.

2.3. Molecular Analyses

2.3.1. Laboratory Precautions

All sample manipulations were conducted in a UV-sterilized biohazard safety cabinet with HEPA filtered airflow. All tools and containers (forceps, spatulas, beakers) were washed in soap and doubly-distilled water, rinsed in DI water, covered with foil, and autoclaved twice on successive days before use. Forceps and spatulas were also rinsed in 5% bleach prior to use. All samples were kept in an ice bucket in between the procedures. Disposable latex gloves (Evolution One, Microflex, Reno, Nevada) were worn throughout all procedures and changed frequently.

2.3.2. Sample Processing

For an overview of protocols for processing the subglacial and supraglacial water samples, the basal ice samples, the proglacial sediment samples, and the cell lysis and nucleic acid extraction procedure, see the flowcharts in Appendices 1, 2, 3, and 4 respectively.

2.3.2.1. Subglacial and Supraglacial Water Samples

Frozen water samples were thawed at 4°C in their original bottles for 1-2 d, and processed for microbial analyses. The thawed 1-L water samples were vacuum filtered through a sterile 0.2 μm pore size analytical filter unit (Nalgene). The filters were used for T-RFLP analysis, and the filtrates were collected in clean plastic bottles for EC, pH, and ion analysis, and in combusted glassware for DOC analysis.

The "standard protocol" after filtration is described below. Firstly, the filter chamber was disassembled and the membrane was cut into sections (halves, quarters, or eighths) using a fresh pre-sterilized, disposable scalpel blade. Each section was transferred with twice autoclaved, bleach-rinsed forceps into a pre-sterilized 2.0-mL polypropylene screw-cap microcentrifuge tube with an o-ring seal and conical-bottom (Biospec Products, Bartlesville, OK). Each tube contained

approximately 0.5 g each of sterile 0.1 mm and 2.5 mm diameter zirconium-silica beads (3.7 g/cc) (Biospec Products). The selection of bead material and size were determined by following the manufacturer's recommendation for disrupting bacterial cells. The proportion of beads to cell suspension was determined according to the method described by Foght *et al.* (2004). Prior to sample processing, the tubes were filled with beads in the biosafety cabinet and subsequently autoclaved on two successive days. After the membrane filter section had been transferred, the bead-filled tubes were immediately placed on ice and then stored at –70°C, until the cell lysis and nucleic acid extraction procedure.

Of the subglacial water samples collected, 4 bottles of SB-IB (19:00 h, June 30), 1 bottle of SB-IB (23:00 h, June 30), 1 bottle of SB-AF (11:00 h, July 1), and 1 bottle of SB-OC (July 4) were processed for molecular analysis (Table 2.1). Of the supraglacial water samples collected, 2 bottles of SP-IS-a (June 16), 1 bottle of SP-IS-a (July 5), 1 bottle of SP-MLS-a (June 28), and 1 bottle of SP-MLS-a (July 5) were processed for molecular analysis (Table 2.1).

2.3.2.2. Basal Ice Samples

Basal ice samples were thawed by careful transfer from original sample bags to covered sterile beakers in a biohazard safety cabinet (section 2.3.1), and stored at 4°C until the sample had completely melted (1-3 d). Once thawed, the beaker was swirled to thoroughly mix the sediment and water layers from the basal ice, and simultaneously vacuum filtered through a 0.2 μm pore size analytical filter unit (Nalgene). The filtrates were collected in clean plastic bottles for EC, pH, and ion analysis, and in combusted glassware for DOC analysis. After filtration, the standard protocol (section 2.3.2.1) was followed. Any remaining sediment or slurry of sediment and water in the beaker after filtration was also measured into bead-filled tubes, using twice-autoclaved, bleach-rinsed spatulas, in 0.50 g and 500 µL increments respectively, and stored at –70°C until extraction; these amounts were chosen according to the method described by Foght *et al.* (2004).

Of the basal ice samples collected, 2 bags of B-C and 2 bags of B-F were processed for molecular analysis (Table 2.1). Additionally, 1 bag of M-N was also processed for molecular analysis.

2.3.2.3. Proglacial Sediment Samples

In order to process the proglacial sediment samples for microbial analyses, the original WhirlPak™ sample bags were carefully opened and, using twice autoclaved, bleach-rinsed spatulas, small sub-samples of sediment were carefully transferred to a covered sterile beaker. The original sample bag was then immediately re-sealed and returned to storage at -20°C. The sediment sub-sample was carefully measured from the beakers into sterile bead-filled tubes in approximately 0.5 g increments. After the proglacial sediment sub-sample had been transferred, the bead-filled tubes were immediately placed on ice, then stored at –70°C until the cell lysis and nucleic acid extraction procedure. Of the proglacial samples collected, 1 bag of P-S and 1 bag of P-R were processed for molecular analysis (Table 2.1).

2.3.3. Cell lysis and nucleic acid extraction

DNA in each sample was extracted using a Mini-BeadBeater™ (Biospec Products) using a modification of a method previously described by Foght *et al.* (2004), and presented below. Stock solutions of all extraction reagents, with exception of the chloroform-isoamyl alcohol mixture, were made in bottles that had been washed in soap and doubly distilled water and rinsed in DI water. Stock solutions were made using bottles of reagents that were separated from general use reagents and had not been touched with spatulas. The powders were tapped into disposable plastic trays to weigh out the correct amounts into glass bottles (Whatman) and prepared in DI water. Once made, the stock solution was sterilized by autoclave. DNA-free filter-barrier micropipette tips (Fisher Scientific) were used exclusively for all steps in the extraction procedure. Microfuge tubes (Rose Scientific, Edmonton, Alberta) were new, sterilized

by autoclave, and handled only with gloves. The chloroform:isoamyl alcohol was made fresh before each extraction in a sterile microfuge tube. Samples were kept on ice throughout the entire extraction process.

Three hundred microliters each of phosphate buffer (100 mM Na-phosphate buffer, pH 8), 10% sodium dodecyl sulfate (SDS) lysis buffer (100 mM NaCl, 500 mM Tris pH 8, 10% [wt/vol] SDS), and chloroform-isoamyl alcohol (24:1 v:v) were added to each sample tube. Samples were then homogenized for 40-60 seconds at 5000 reciprocations per minute (rpm) after which the samples were clarified in a microfuge at 13,000 x g for 5 min at room temperature. The supernatant (approximately 650 μL) was transferred to a new sterile microfuge tube, and 7M ammonium acetate was added to achieve a final concentration of 2.5 M (approximately 360 μL). The samples were then gently mixed by inversion and clarified at 13,000 x g for 5 min at room temperature. Subsequently, the supernatant (approximately 580 μL) was transferred to a new microfuge tube, 54% volume of isopropanol was added, and the sample was incubated at -20°C for at least 30 min. The precipitated DNA was recovered at 14,000 x g for at least 15 min at room temperature. After precipitation, the isopropanol was discarded, the genomic DNA pellet was dissolved in 40 μL of heat-sterilized DI water, and stored at -20°C until used in the DNA amplification procedure.

Before the bead-beater homogenization method described above was used on the new glacial samples collected in 2002, the technique was optimized using pure colonies and subglacial mud samples previously collected from JEG (Appendix 4). First it was ascertained that the extraction method could be used to successfully extract genomic DNA directly from pure colonies of JEG bacteria, previously collected mud samples, and from the Nalgene cellulose-nitrate filter membranes in the filter units used in the sample processing of the water (2.3.2.1) and basal ice samples (2.3.2.2). Once this had been established, the optimum time to homogenize the samples was determined by subjecting pure colonies, environmental samples, and filter

membranes to a range of homogenization times (0 seconds to 2 minutes), and comparing the intensity of the PCR bands by gel electrophoresis. It was determined that 40 – 60 seconds was sufficient to attain a strong amplicon (the amplified segment of DNA) band for the JEG pure colonies (gram negative and gram positive cells), environmental samples, and filter membranes.

2.3.4. PCR conditions

Following DNA extraction, PCR was used to amplify only the Bacterial 16S rDNA gene (1500 bp) using the universal Bacterial primers FAM-PB36 (5'-AG(AG)GTTTGATC(AC)TGG CTCAG-3') and PB38 (5'-G(GT)TACCTTGTTACGACTT-3'), corresponding to the *E. coli* 16S rRNA gene positions 8-27 and 1492-1509, respectively (numbering per Brosius *et al.*, 1981). The forward primer, FAM-PB36, was purchased (MWG Biotech, High Point, North Carolina) with the 5' end labeled with a fluorescein phosphoramidite dye. To prevent quenching of the fluorescent tag, the samples were kept in a covered container on ice during the PCR and restriction enzyme digestion preparations and the lights in the laboratory were switched off. Generally, the reaction mixtures for PCR used 5 μL of template DNA and contained each deoxynucleoside triphosphate at a concentration of 200 μM, each primer at a concentration of 10 μM, and 5 U/μL of *Taq* polymerase with 1x concentration of supplied buffer (Roche Diagnostics, Laval, Quebec, Canada) in a final volume of 50 μL. For some samples, either 5% or 2.5% dimethyl sulfoxide (DMSO) was added to stabilize the reaction and obtain a better amplicon. DNA amplification was performed with a Techne Flexigene thermal cycler (Techne Flexigene, Princeton, New Jersey) using the following program (Foght *et al.*, 2004): a 3-min initial denaturation at 94°C, followed by 30 cycles of denaturation (45 s at 94°C), annealing (30 s at 53°C) and extension (90 s at 72°C), and finally 7 min at 72°C to stabilize the reaction after the cycles were complete. Amplified DNA was visualized by gel electrophoresis of aliquots of PCR mixtures (5 μL) in 1.5% agarose (ICN Biomedicals Inc., Aurora, OH) in 1 x TAE buffer (0.04 M

Tris, 0.001 M EDTA, 0.95 M acetate). The concentration of the amplified product was estimated by comparing the intensity of amplicon bands to a 100-bp ladder (DNA molecular weight marker XIV, Roche) of known mass. The PCR reaction was conducted in new, pre-sterilized 0.2 mL tubes (Rose Scientific), exclusively using DNA-free filter-barrier micropipette tips (Fisher Scientific) for all steps.

2.3.5. 16S rDNA T-RFLP

Following successful amplification, aliquots (60 ng) of the fluorescently labeled PCR products were separately digested with *Hae*III and *Hha*I (Roche), according to the manufacturer's instructions in 1.5 mL new, autoclaved, microfuge tubes (Rose Scientific). Tests were conducted comparing different enzyme quantities and incubation conditions and times to determine the optimum digestion protocol. The precise lengths of the T-RFs from the amplified rDNA products were determined in the Molecular Biology Services Unit (Biological Sciences Department, University of Alberta, Edmonton, Canada) by polyacrylamide electrophoresis with a model 377 XL automated sequencer (Applied Biosystems Instruments (ABI), Foster City, Calif.) in the GeneScan mode. Aliquots (6 ng) of each digested product were mixed with 1 μL of DI formamide and loading buffer (ABI) and 0.5 μL of DNA fragment length standard (TAMRA 2500, ABI), which contained 28 DNA fragments of precisely 37, 94, 109, 116, 172, 186, 222, 233, 238, 269, 286, 361, 470, 490, 536, 827, 1115, 1181, 1722, 2008, 2162, 2465, 2481, 2860, 4529, 4771, 5099, and 14,079 bp. (The first gel was run using the DNA fragment length standard TAMRA 500, which contained 16 DNA fragments of precisely 35, 50, 75, 100, 139, 150, 160, 200, 250, 300, 340, 350, 400, 450, 490, and 500 bp.) The entire mixture was then denatured at 94°C for 5 min and immediately chilled on ice prior to loading. Aliquots (2 μL) were loaded onto a 36-cm 5% denaturing polyacrylamide gel (Figure 2.11). Tests were conducted comparing different aliquot volumes to determine the optimum amount of digested DNA to load on to a gel.

The odd numbered wells were loaded, the even numbered wells were flushed out with a Pasteur pipette, and the odd numbered wells were run into the gel for 2 minutes. Subsequently, all of the wells were flushed out, the even numbered wells were loaded, the odd numbered wells were flushed out, and the even numbered wells were run into the gel. These precautions were taken to prevent spill over and well-to-well contamination. Electrophoresis proceeded for 6 hours (2.5 h for the TAMRA 500 gel) with a standard voltage of 2.4 kV. In total, one 500 bp gel and sixteen 2500 bp gels were successfully run and analyzed. These gels were designated PAGE 1 – 17. PAGE 1 was the 500 bp gel, and PAGE 2 – 17 were the 2500 bp gels.

After electrophoresis, the lengths of the fluorescently labeled T-RFs were determined by comparison with the internal standard (TAMRA 2500 or TAMRA 500) in each lane using GeneScan™ software (version 3.1, ABI). GeneScan™ interprets the gel fragments by converting the raw fluorescence signal of the T-RFs into discrete base pair sizes, as calculated by the standard curve developed for the internal lane standards. The protocol used is a modification of the method described at http://biowe.usus.edu/wolf/aflp_protocol.htm. First the lanes were tracked using the GeneScan™ autotracker; if the auto-tracker confidence level for the gel was less than 70%, the straight tracking option was used instead and the tracking was adjusted manually to align with the gel lanes. All the lanes were then extracted from the gel file into the GeneScan™ analysis software. The size standards (TAMRA 2500 or 500) were separately defined for the odd and even lanes by selecting a lane in which only the standard had been loaded, defining the standard peaks in this lane, and applying this definition to the entire gel. If a peak was split, the right-hand peak was always defined. If GeneScan™ missed any peak or could not define the standard in any lane using the global definition, the minimum peak amplitude was re-set for a lower relative fluorescence unit (RFU) or the standard in that lane was individually defined. After bp sizes were assigned to all the peaks in each lane, the standard data in each lane were scored. Scoring entails analyzing the data to ensure that each of the defined standard peaks in the odd and even lanes line up with each other (± approximately 50 scan lines), as the software

is using these peak definitions as a reference point from which to define the base pair values in the T-RFs. Thus, if the wrong standard peak is defined in any lane, the base pair size calling for the T-RFs in that lane will not be comparable with the other lanes or other gels. Scoring the standard data compensates for the fact that the gels and individual lanes run slightly differently by standardizing the base pair size calling between lanes and gels, therefore allowing inter- and intra- gel comparison. The standard was scored by importing it into the GenoTyper™ software (version 2.0, ABI), labeling the peaks by rounded base pair integer (always defining the right-hand peak if the peak was split) and scan number, and viewing the standard in each lane by scan line, to ensure that GenoTyper™ was assigning the correct base pair value to the peak. GenoTyper™ allows higher order fragment analysis in that it takes the output from GeneScan™ and plots electropherograms that can be analyzed against varying criteria and exported to other statistical programs. If any lanes had peaks that did not line up within ~50 scan lines, the standard was redefined specifically for that lane in GeneScan™, and re-imported back into GenoTyper™ for scoring. If the standard baseline in any lane was above approximately 15 RFU that lane was discounted. For TAMRA 2500, peaks were only defined up to 1722 bp because the 16S rDNA gene has a total size of 1500 bp.

Once the standard lanes had been scored, the T-RFs from the samples were analyzed. An absolute minimum RFU threshold level (peak height) was established as the basic criterion used to eliminate background peaks, and identify the valid peaks in all samples on all gels. Each valid peak represents a base pair category that corresponds theoretically to a different organism. The absolute minimum peak height fluorescence threshold, above which all peaks were considered valid, was set at 100 RFU, and the minimum peak amplitude for import into GenoTyper™ set at 50 RFU. To determine the minimum RFU level, the lanes on one gel (PAGE 2) with samples from the supraglacial, subglacial, and proglacial environments was analyzed. Dunbar et al. (2001) found that although setting a high threshold value may eliminate much of the background noise in a T-RFLP profile and increase the validity of the results, the fluorescence threshold is

specific to each dataset and cannot be determined *a priori*. First, a graph of the number of unique base pair categories defined versus a scale of threshold values ranging from 15 to 3000 RFU was produced, for all T-RFs ranging from 94 bp to 1181 bp (the largest fragment was 1009.66 bp) (Figure 2.12). The minimum value of 15 RFU was the lowest level at which the GeneScan™ software could analyze the dataset without exceeding the maximum peak detection limit of 250 peaks per lane. The resulting relationship was exponential, with the maximum number of categories (1000) defined at 15 RFU due to the incorporation of background signal. No categories were defined at the upper value of 3000 RFU. Secondly, each of the T-RFs from PAGE 2 that were assigned bp values by GeneScan™ were individually analyzed in GenoTyper™, at a threshold of 40 RFU (the lowest RFU level at which the GenoTyper™ software could analyze the T-RFs without exceeding the maximum category number of 128 for individual file export) with minimum peak import amplitude at 15 RFU, to ascertain if they were valid categories or simply background. Using these criteria, 117 unique peaks (categories) were identified by GenoTyper™ (peaks that were assigned bp values within ± 0.5 bp of each other were grouped in the same category). A valid category for the purposes of this fluorescence test was rigorously defined as each peak within the category being consistently present in every sample in which peaks from that category were identified. After individual visual analysis of every peak, 42 categories were confirmed as valid, which corresponded to a fluorescence threshold of approximately 100 RFU on Figure 2.12. It was also determined that the minimum peak amplitude for import of 15 RFU was too low, as the individual peaks assigned bp values consisted primarily of background, and thus this value was adjusted to the GeneScan™ default of 50 RFU. The fluorescence threshold is necessarily more rigorous than the minimum peak amplitude for import because the former is defining the basic criterion of a valid base pair category, whereas the latter refers to the minimum height for a peak to be recognized as a peak by GenoTyper™ and placed into a category if it is within the category tolerance level of a peak that fluoresces above 100 RFU. Some of the individual peaks in these categories may be weak (i.e.

<100 RFU) as peak height is dependent on the initial amount of template DNA, but if at least one peak in any of the samples is above the threshold (100 RFU) then that peak defines a valid base pair category in all the samples.

For each gel, all the peaks in all the samples above the absolute minimum peak height fluorescence threshold (100 RFU) were labeled by bp size, representing the valid bp categories for that gel. Only fragments at least 80 bp long (TAMRA 2500 gels) or 50 bp long (TAMRA 500 gel) were analyzed in an attempt to represent the realistic resolving power electrophoresis technology, as the bp size assignment of small bp fragments is inaccurate due to the fact that they diffuse through the gel (Engebretson and Moyer, 2003). Subsequently, all of the remaining peaks (of at least 50 RFU) were also labeled by size and placed into the appropriate bp category bins, thus examining all the samples for all the valid categories. The category tolerances (i.e. acceptable variation in a calculated bp size within a category) were established by analyzing various replicate samples to account for the variation within a gel, between different gels, and the fact that the size-calling margin of error inherently increases logarithmically with base pair size, due to the manner in which larger fragments migrate through the gel (Engebretson and Moyer, 2003; Liu *et al.*, 1997). If the category tolerance is too narrow, false categories are created and diversity is overestimated. Conversely, if the category tolerance is too broad, diversity is underestimated as peaks representing unique organisms with similar T-RFs are grouped together. The variation within a gel represents the size-calling margin of error between replicated peaks on the same gel from samples that underwent the same extraction process but different amplification and digestion processes. The variation between different gels represents the margin of error between replicated peaks on different gels from identical samples (same extraction, amplification, and digestion). Comparative analysis revealed that the variation between replicated peaks run on different gels was greater than the variation resulting from different amplification and digestion processes. Thus, the variation between replicated peaks on different gels was used to calculate the category tolerance levels and establish a more conservative guideline for category

differentiation. The average variations among 341 replicated peaks from 150 replicated samples on 6 different gels from identical samples (same extraction, amplification, and digestion) per bp range was graphed (Figure 2.13) and a function was fit to the resulting logarithmic curve ($y = 0.0487e^{0.0034x}$, $R^2 = 0.8371$). The category tolerances per bp range were calculated using this function as: 0-300 bp = ± 0.1 bp; 300-400 bp = ± 0.2 bp; 400-500 bp = ± 0.3 bp; 500-600 bp = ± 0.4 bp; 600-700 bp = ± 0.5 bp; 700-800 bp = ± 0.7 bp; 800-900 bp = ± 1.0 bp; 900-1000 bp = ± 1.5 bp; 1000-1100 bp = ± 2.0 bp; 1100-1200 = ± 3.0 bp; 1200-1300 bp = ± 4.0 bp. Generally, the category tolerances derived with the function were similar to the observed average variation between replicated peaks for each 100-bp range.

A master category list was created, composed of all the valid categories (peaks fluorescing above 100 RFU) in each of the gels, using the appropriate category tolerances for the varying T-RFs bp ranges. Some of these categories were duplicated among the different gels, and thus the list was edited to consolidate these overlapping categories. In Microsoft Excel™ (version 9.0.0.3822), the master category list was sorted by ascending bp size, and the difference between successive category bp sizes (rows) was calculated. If the difference between two successive categories (rows) was greater than twice the category tolerance for that bp range then the categories were considered to be discrete. Conversely, if the difference between two successive categories was less than twice the category tolerance for the bp range, the categories were considered to overlap and represent the same peaks. In this manner, the category list was consolidated by clustering values that fit within empirically determined margins of error, whilst accounting for the fact that the average margin of error within and between gels differed depending on bp value. The overlapping categories were grouped into one consolidated category, which was redefined as the minimum bp value in the overlapping category set minus the category tolerance for that bp range to the maximum value in the set plus the category tolerance for that bp range (consolidated category = [minimum bp value in category set] – [category tolerance for bp range] to [maximum bp value in category set] + [category tolerance for bp range]). Once all of

the overlapping categories in the entire list were consolidated, the list was rechecked and any of the newly defined categories that differed by less than twice the tolerance for the bp range were combined, finally resulting in a list of categories with discrete bp sizes. The accuracy of the category tolerances predicted by the function was established as the electropherograms of the minimum and maximum bp values from the same gel in an overlapping set were visually inspected to ensure that the categories should be consolidated. Using this method of verification, it was observed that the category tolerances estimated by the function were generally correct in predicting the appropriate breaks in the category list between discrete peaks. Subsequently, each gel file was imported separately into GenoTyper™, and the T-RFs were analyzed (peaks with bp sizes within the category definition tolerances were labeled) using the consolidated master category list. The labeled peaks representing the valid T-RFs were then scored to ensure the accuracy of the category groupings predicted by the function-derived category tolerances, and to ensure that no valid peaks were missed or invalid peaks were labeled. Thus, every peak used in further downstream analysis was visually checked for accuracy. The consolidated master category list was edited accordingly as a result of scoring, and the new edited consolidated master category list was used to reanalyze the gel for which the changes were made and for the next gel. Once all of the gels had been analyzed in this manner, the peaks in each of the gels were checked again to ensure that the changes to the master category list did not affect the category calling in each of the gels. Once this had been verified, the peak information (bp values of valid T-RFs in each category for each sample site) was exported to Microsoft Excel™, where it was converted to a binary data table (1 if a peak was present in a category, 0 if it was not), and used in statistical analyses.

2.3.6. Controls and Replicate Samples

Extraction controls (bead-filled tubes containing only extraction reagents) were included with each extraction procedure and subsequently amplified to certify that the reagents and beads

were DNA-free. A water filter control, consisting of autoclaved, DI water filtered and processed in the same manner as the subglacial and supraglacial water samples was used to confirm that the Nalgene filter unit, cellulose nitrate membrane (Nalgene), and DI water were DNA-free.

PCR negative controls (containing autoclaved DI water as "template") were used in every PCR reaction to certify that the reagents were DNA-free. The extraction negative controls and PCR water controls were also digested, loaded onto the polyacrylamide gel, and analyzed in the same manner as the fluorescently labeled T-RFs to check for possible contamination by extraneous DNA.

Sub-samples were taken from each sample bottle or bag, and placed in bead-filled tubes. The majority of these sub-samples were replicated in at least two separate amplification, digestion, and polyacrylamide gel electrophoresis (PAGE) steps (Appendices 5 and 6).

2.3.7. Statistical Analysis

Principal component analysis (PCA) and cluster analysis were used to analyze the sample T-RF peak information (bp values of valid T-RFs in each category for each sample site) using Statistica™ (version 5, 1997 edition, StatSoft Inc., Tulsa, OK). The *Hae*III and *Hha*I datasets were each analyzed separately, generating two independent sets of statistical results. Both PCA and cluster analysis are types of multivariate statistical methods, which reduce the complexity of a dataset by identifying the combinations of variables that best summarize the sample information (PCA) and the groups of individual samples most similar to each other (cluster analysis) (Fowler *et al.*, 1998). Thus, in this study, these statistical methods were used to generate groups of samples that contained similar assemblages of T-RFs to determine if all the samples represented similar environments.

PCA creates statistically independent variables (called principal components or factors) that are linear combinations of the original variables (in this case, samples), which summarize the majority of the variation within the dataset. Thus by summarizing the inter-relationships between

the samples, the complexity of the dataset is reduced from every sample in the original dataset (141 for the *Hae*III dataset and 102 for the *Hha*I dataset) to a smaller, more manageable number of factors (15 each for *Hae*III and *Hha*I). Each sample is treated as being equally important, and the factors are derived from the entire dataset so that the first factor summarizes the largest possible amount of sample information; the second factor is uncorrelated with the first factor and summarizes the second largest amount of sample information, and so forth. Successive factors explain increasingly smaller fractions of the total variance within the dataset. Theoretically, there are as many factors as the number of original samples. The number of factors used in the final analysis was chosen to be the number that explained a large proportion (> 70%) of the total variance in the dataset. Associated with each factor are a group of "loadings" of each sample on the factor. The factor loadings represent how strongly each original sample is correlated with each factor.

Cluster analysis was conducted using the PCA factor loadings of each sample in the *Hae*III and *Hha*I datasets, to group the samples into clusters so that samples sharing the same terminal restriction fragments (T-RFs) or groups of T-RFs were in the same class. Samples were clustered using an agglomerative hierarchical method with generalized Euclidean distances as a measure of similarity between samples (Statistica™). The Euclidean distance was calculated as the differences between every samples' factor loadings for every principal component. The squared differences between each pair of samples on all possible principal components was summed, and the square root of the total was the value of distance between any two samples. Once the distance between every pair of samples had been calculated for every component using a uniform distance measure (e.g. Euclidean distance), the entire dataset was clustered using an agglomerative hierarchical method that amalgamated samples based on the Euclidean distance. In this way, the samples that are most closely related (i.e. loaded most similarly on the PCA factors) are clustered together first. The analysis is complete when all of the clusters link together at the highest Euclidean distance in a single cluster. The results of cluster analysis are then

depicted as a dendrogram, summarizing as much of the variability in the dataset as possible, in which Euclidean distance is displayed on the vertical axis and the samples on the horizontal axis (Blackwood *et al.*, 2003). At the beginning of the analysis, each sample is independent; samples that are merged at zero on the distance scale had the same factor loadings on every principal component, while samples linked at progressively higher Euclidean distances had increasing dissimilar loadings on each principal component.

PCA and cluster analysis (using the factor loadings from the independent PCA of each environment) were also performed on each environment separately to determine if the factors identified and clusters within each environment were different when the other environments were not considered. However, it was found that individual multivariate analysis of the environments did not lend a greater sensitivity to determining the intra-environmental variability, as the factors and clusters created were the same for each environment as those identified by analyzing the entire dataset simultaneously.

Table 2.1. Transport and storage conditions of samples collected (summer 2002) and analyzed with T-RFLP. Samples were stored on ice in coolers at JEG. Water samples were stored at ≤ 4°C in Resolute Bay, Nunuvut, Canada. Basal ice and proglacial sediment samples were stored at –20 °C upon arrival in Resolute Bay. All samples (water, ice, and sediment) were shipped from Resolute Bay to Edmonton, Alberta, Canada at ≤ 4°C (72 h).

Sample	Sample Type	Date (2002) and time collected	No. of days at JEG	Storage in Edmonton	Date processed	No. of days until processed from the collection date
SUBGLACIAL (section 2.1.1)						
B-C	Basal ice cave	June 15 (17:30 h)	23 d	-20°C	B-C1 – 9/25/02 B-C2 – 11/18-19/02	30 d 157 d
B-F*	Basal ice fox junction	July 31	1 d	-20°C	B-F1 – 9/24/02 B-F2 – 11/18-20/02	55 d 112 d
M-N	Nunatak mud	May 27	11 d	-20°C	9/25/02	121 d
SB-IB	Subglacial initial burst waters	June 30 (19:00 h)	8 d	S-IB1, 2: 4°C S-IB3, 4: -20°C	S-IB1 – 7/22/02 S-IB2 – 10/07/02 S-IB3 – 11/29/02 S-IB4 – 5/24/03	22 d 99 d 152 d 328 d
SB-IB	Subglacial initial burst waters	June 30 (23:00 h)	8 d	-20°C	5/24/03	328 d
SB-AF	Subglacial artesian fountain waters	July 1 (11:00 h)	7 d	-20°C	5/23/03	326 d
SB-OC	Subglacial outburst channel waters	July 4 (12:45 h)	4 d	-20°C	5/23/03	323 d
SUPRAGLACIAL (section 2.1.2)						
Dry snow	Dry snow (wind-crust layer)	June 5	33 d	-20°C	9/19/02	106 d
SP-IS-a	Supraglacial ice stream A	June 16	22 d	BM1: 4°C BM2: -20°C	BM1 – 9/17/02 BM2 – 11/29/02	93 d 147 d
SP-IS-a	Supraglacial ice stream A	July 5	3 d	-20°C	11/03/03	486 d
SP-MLS-a	Supraglacial marginal lake stream A	June 28	10 d	-20°C	5/23/03	329 d
SP-MLS-a	Supraglacial marginal lake stream A	July 5	3 d	-20°C	5/23/03	322 d
PROGLACIAL (section 2.1.3)						
P-S*	Proglacial subsurface sediments	July 16	16 d	-20°C	10/07/02 11/19/02	87 d 127 d
P-R*	Proglacial rock polygons	July 6	3 d	-20°C	11/03/03	485 d

* indicates sample was collected by M. Sharp

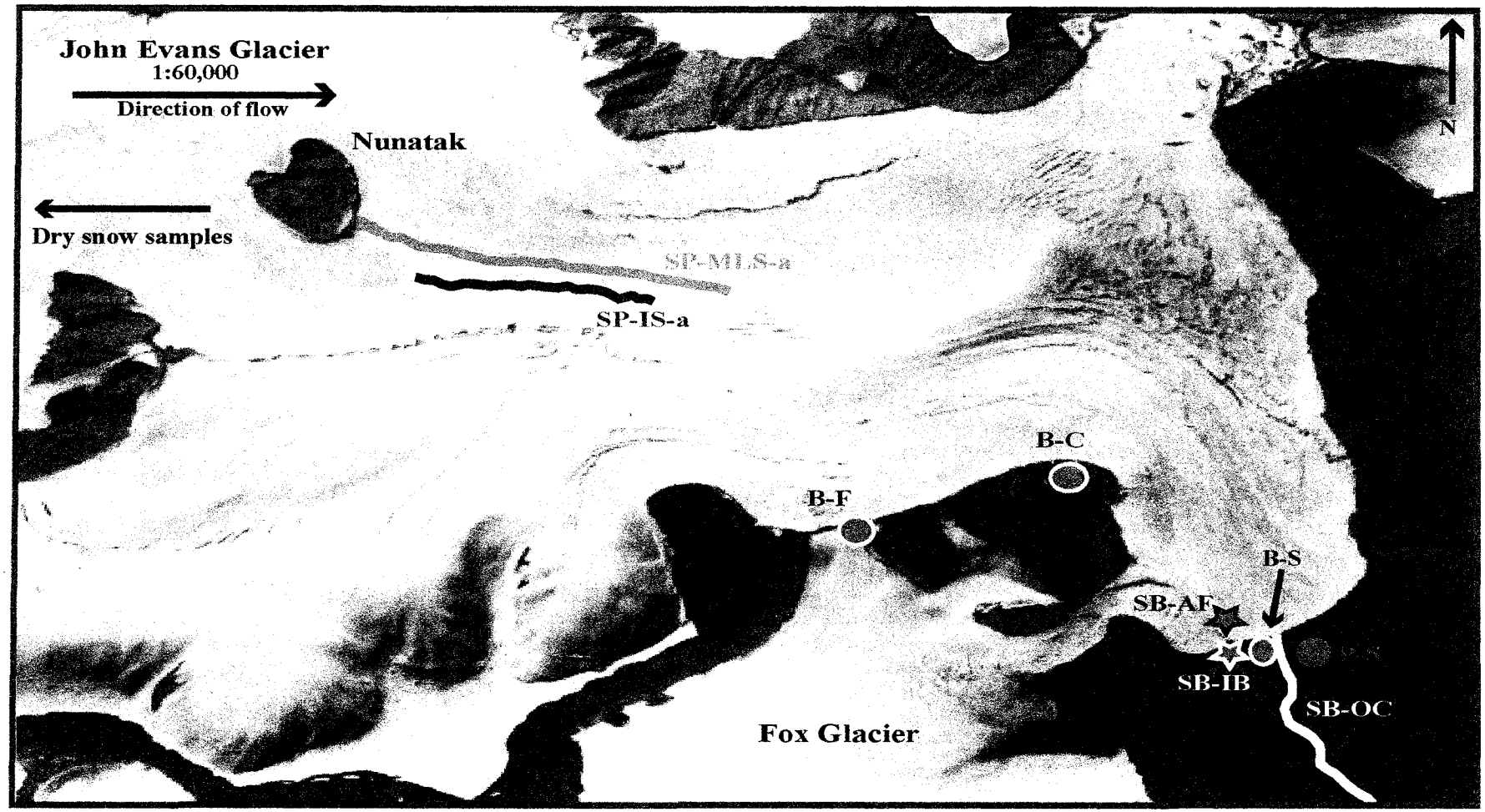

Figure 2.1. Aerial photo of JEG illustrating the subglacial, supraglacial, and proglacial sites from which samples were taken for T-RFLP analysis. The supraglacial sites were the dry snow samples collected at the upper part of the glacier, the marginal lake stream A (SP-MLS-a), which drained a meltwater lake containing sediment from an exposed nunatak, and the ice stream A (SP-IS-a). The subglacial sites comprised two different sub-environments, basal ice and subglacial waters. The basal ice sites are at the junction with Fox glacier (B-F) and in an ice cave at the west margin (B-C), and at the terminus (snout) of the glacier (B-S). The subglacial waters comprised the initial burst (SB-IB) at the glacier front, the artesian fountain (SB-AF) on the glacier surface, and the outburst channel (SB-OC) from the glacier front in the proglacial area. The proglacial sites were the rock polygons (P-R) located in the rock area adjacent to the glacier, and the sediment samples (P-S) located in stream bank cuts directly in front of the glacier terminus. Air photo is from the National Air Photo Library, Ottawa, Ontario.

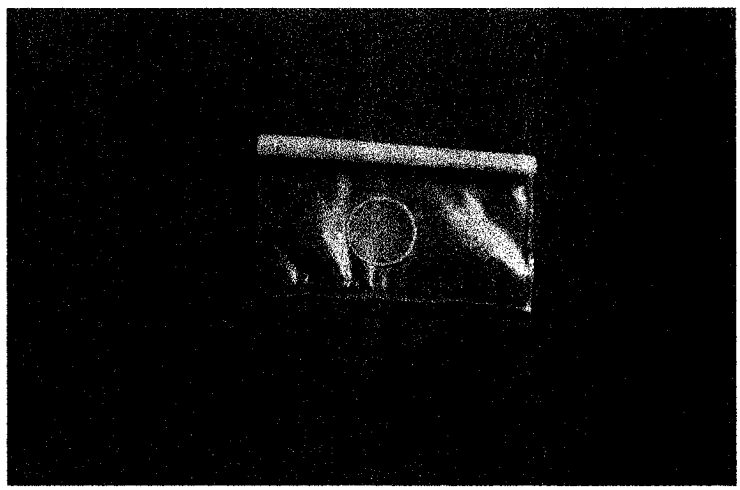

Figure 2.2. Dry snow sample environment. Panel A shows the snow pit from which the samples were collected. Panel B shows the filtering set-up and apparatus at JEG. Panel C shows the filter membrane through which ~ 5 L of melted dry snow was filtered.

Figure 2.3. The supraglacial ice stream A (SP-IS-a) drained a catchment composed entirely of glacier ice.

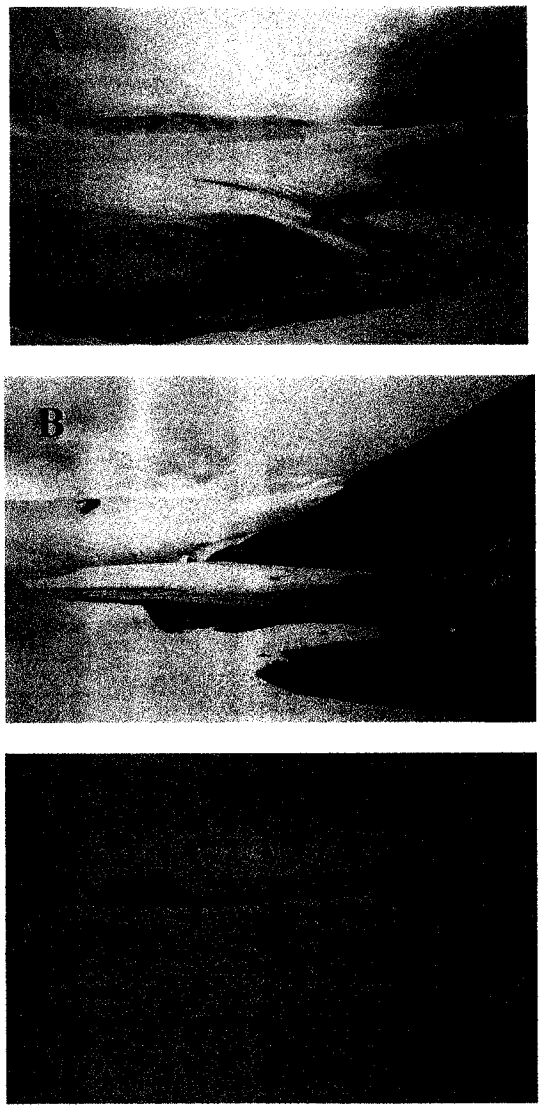

Figure 2.4. The supraglacial marginal lake fed stream A (SP-MLS-a) drained a meltwater lake (panel A) fed by two ice marginal channels that transported sediment from an exposed nunatak (panel B) into the SP-MLS-a (panel C).

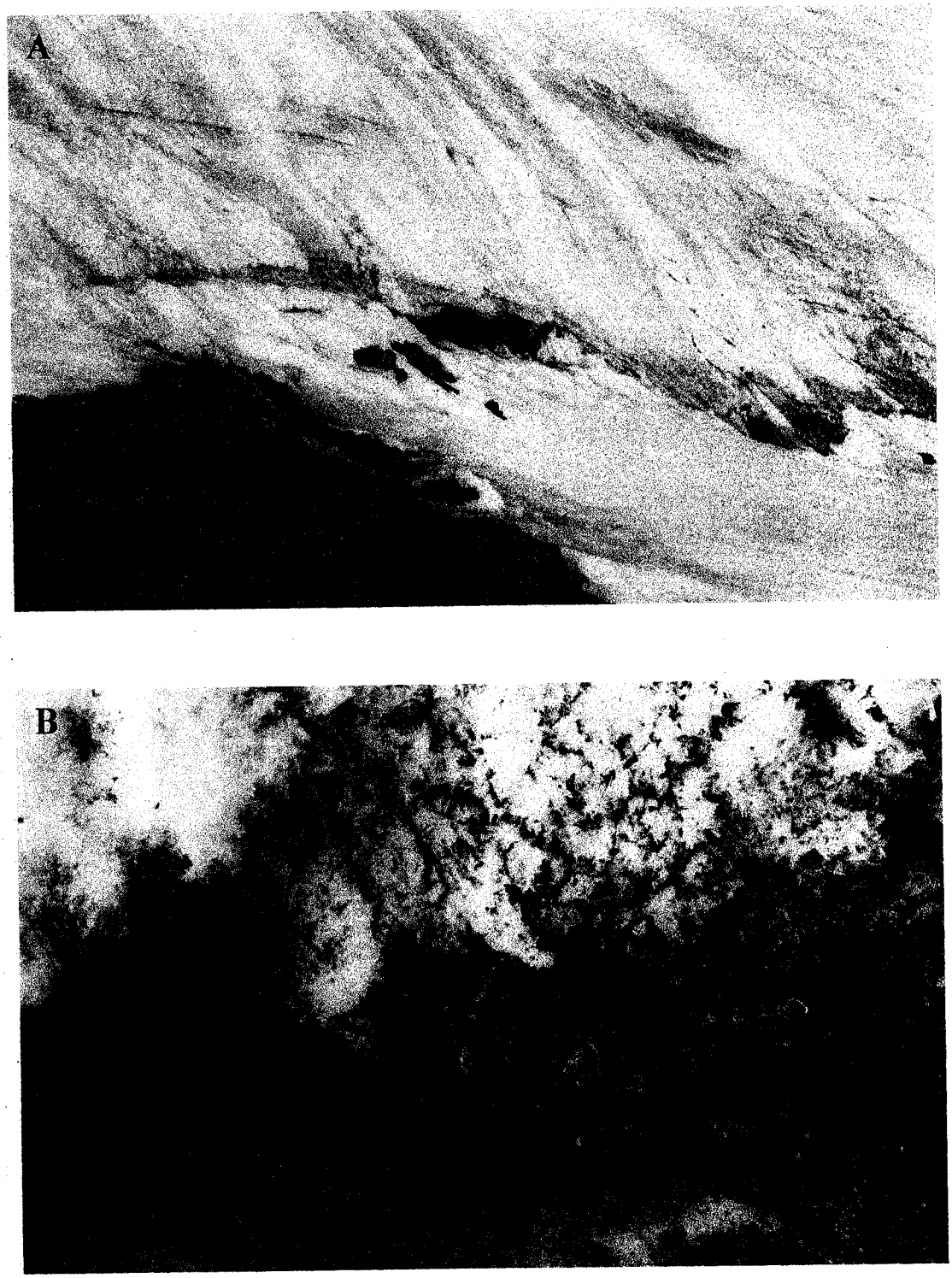

Figure 2.5. The basal ice cave (B-C) located in an ice cave (panel A) at the glacier's west margin, which was exposed as a result of a stream cutting into the glacier bed. Panel B is a close-up picture of the basal ice within the cave.

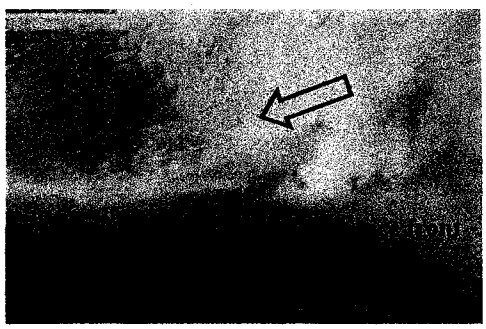

Figure 2.6. The subglacial initial burst (SB-IB) waters on June 30, 2002 (19:00 h) at the glacier terminus from the ice front in a pressurized horizontal flow. The arrow indicates the water burst. This burst contained water that had been stored in the subglacial environment over-winter.

Figure 2.7. The subglacial artesian fountain (SB-AF) on July 1, 2002 on the glacier surface, contained water that had been stored in the subglacial environment over-winter.

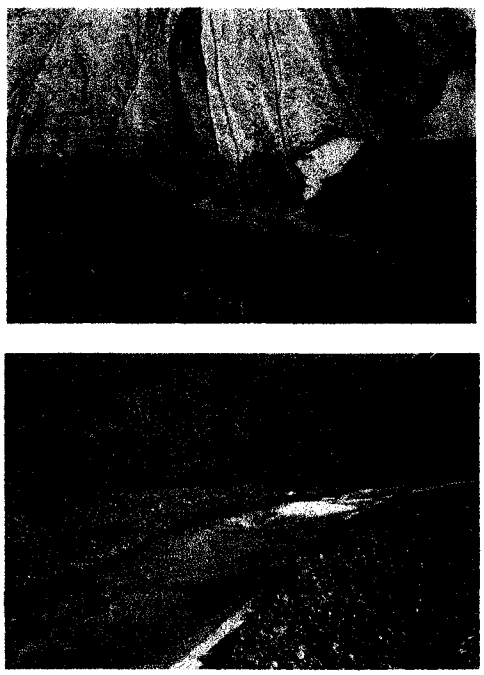

Figure 2.8. The subglacial outburst channel (SB-OC) on July 4, 2002 at the glacier terminus, which contained a mixture of subglacial waters stored at the bed over-winter and fresh supraglacial inflow. Panel A shows the flow from the ice front, and panel B shows the channel flowing into the proglacial area.

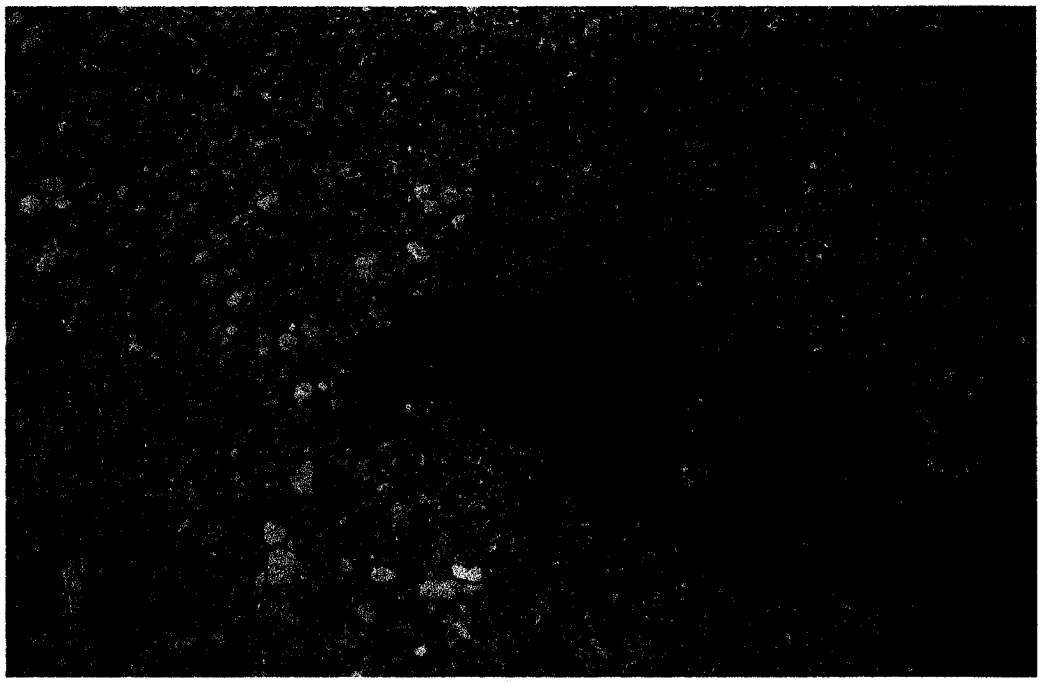

Figure 2.9. The proglacial sediment samples collected from fine gravels exposed in stream bank cuts directly in front of the glacier terminus (P-S). The brown staining represented plant growth.

Figure 2.10. The proglacial sorted rock polygons adjacent to the glacier (P-R).

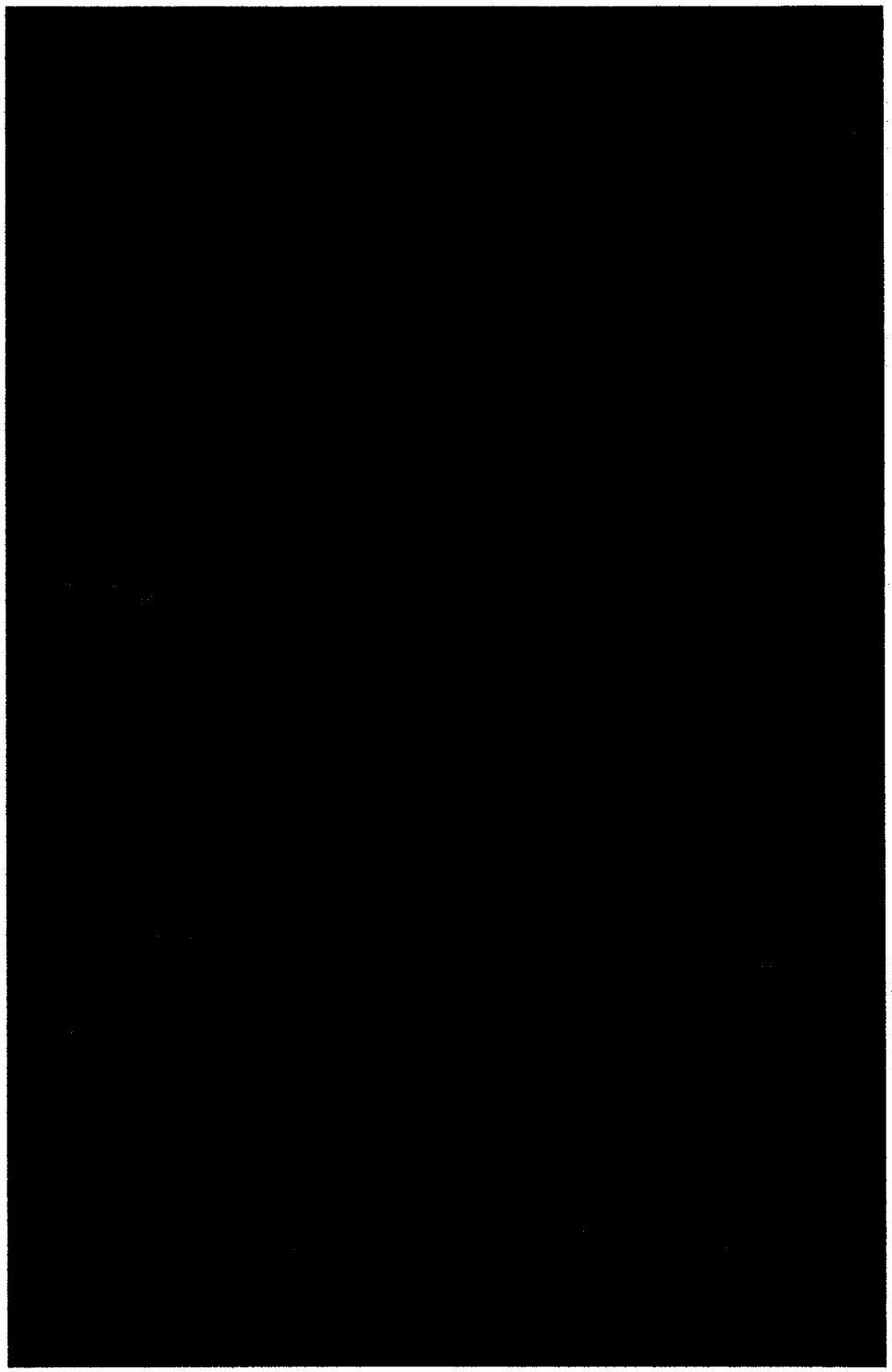

Figure 2.11. An example of a polyacrylamide gel on which JEG samples were analyzed using T-RFLP. The blue represents the sample DNA, and the red represents the size standard (TAMRA 2500). Each lane contains a separate sample, and each fragment is a unique T-RF in the community.

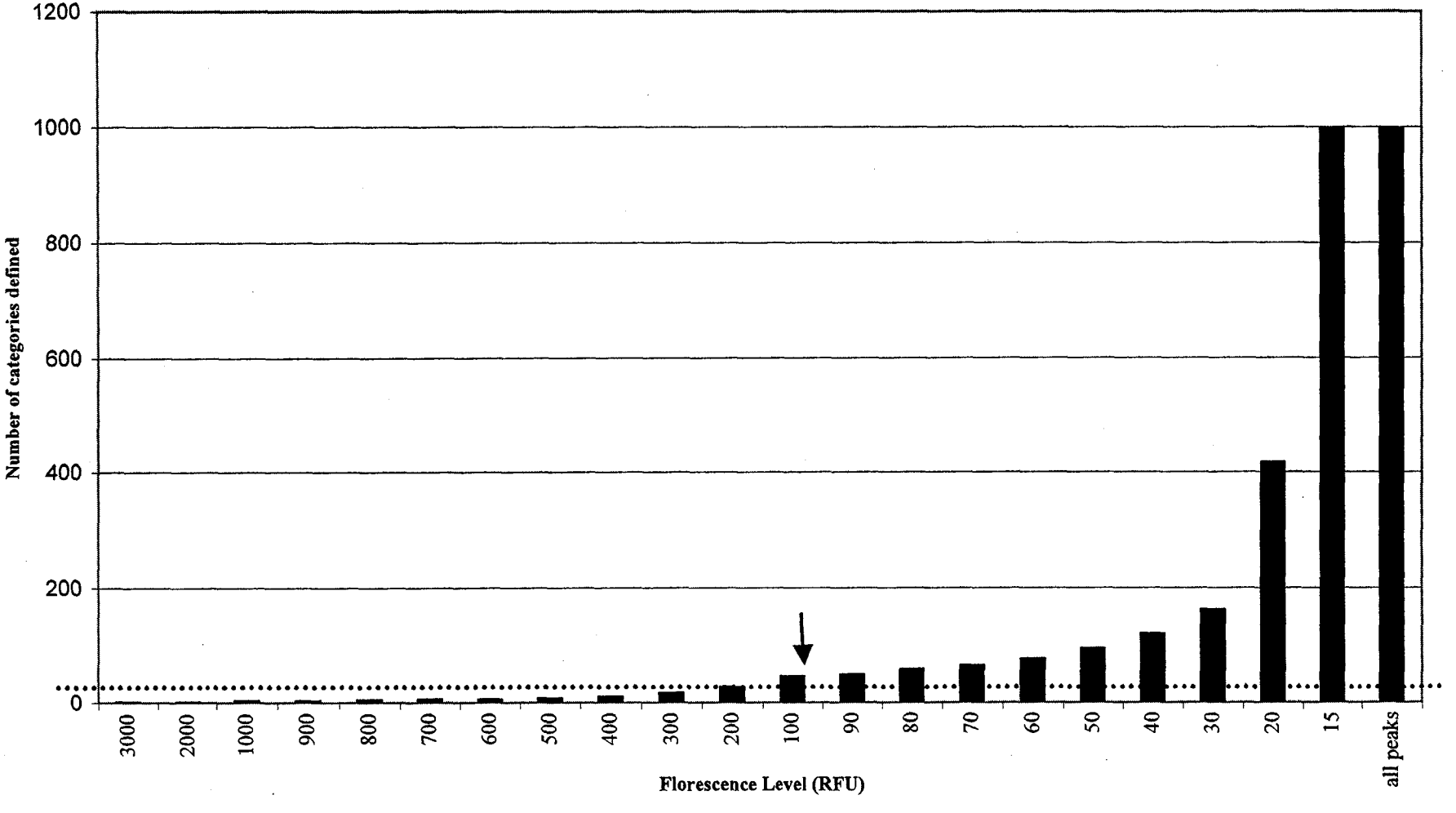

Figure 2.12. Relationship between the number of unique base pair (bp) categories defined and the threshold values of relative fluorescence units (RFU) for all T-RFs ranging from 94 to 1181 bp on gel PAGE 2. The dotted line represents the absolute minimum RFU fluorescence threshold, set at 100 RFU, above which all peaks were considered valid.

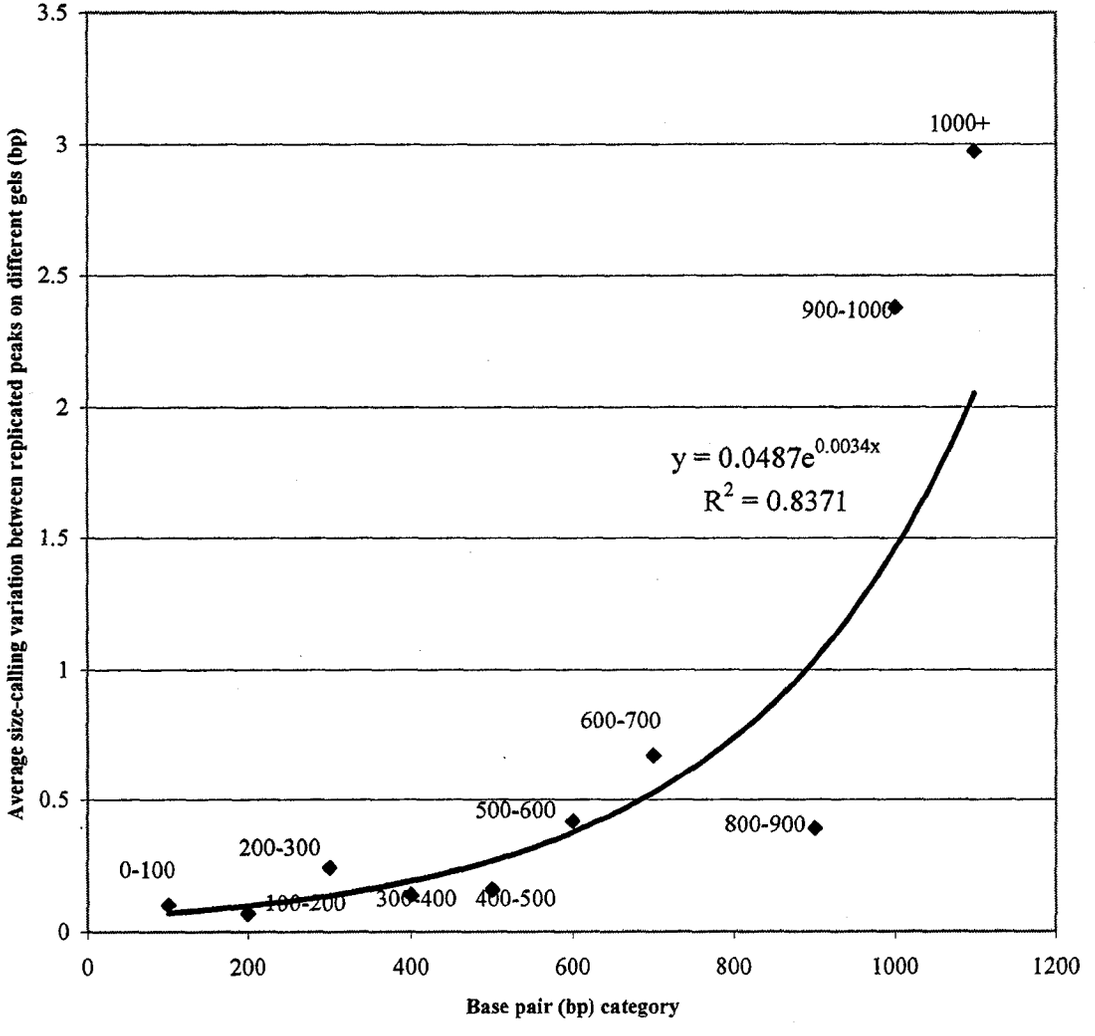

Figure 2.13. The average size-calling margin of error (variation) among 341 replicated peaks from 150 replicated samples on six different gels from identical samples (same extraction, amplification, and digestion) per 100 bp range. A function was fit to the resulting logarithmic curve and the category tolreances per base pair range were calculated using this function.

Chapter 3. Results

Three primary environments were defined at JEG based on their differing physical and chemical properties: the subglacial, supraglacial, and proglacial environments. T-RFLP analysis of 141 samples digested with the *Hae*III enzyme (Appendix 5) and 126 samples digested with the *Hha*I enzyme (Appendix 6) resolved a total of 142 and 102 different T-RFs, respectively. The sizes of the T-RFs are listed in Appendix 7. Based on statistical analyses of the T-RFLP patterns, the subglacial, supraglacial, and proglacial Bacterial communities appear to be distinct, although there are sub-groups of common samples among the primary environments. Differences at the inter-environmental level are due to the presence of distinct characteristic "core groups" of T-RFs that define each primary environment. At the intra-environmental level, differences between sub-groups are defined by the presence in specific samples of additional T-RFs that are not found in the other sample sites in the same primary environment. Similar results were obtained for the samples digested with the *Hae*III and *Hha*I enzymes, so the restriction enzyme used did not appear to influence the overall conclusions of this study. Since the results of the multivariate analysis of the *Hha*I dataset were very similar to those derived from analysis of the *Hae*III dataset and more samples were analyzed with the *Hae*III enzyme, only the *Hae*III results are discussed in detail.

3.1. Controls and Replicates

All of the extraction and PCR water controls were negative (i.e. they did not reveal any DNA bands) on an agarose gel. When resolved on polyacrylamide gels, which have a much higher resolving power than agarose gels, the extraction and water controls generally contained peaks with fluorescence levels below the baseline, and were thus excluded from analysis. Some of the controls had a few peaks above the minimum RFU for import to the GenoTyper™ software (50 RFU) (see 2.3.5). These peaks, and the categories they represented, were eliminated from the

master consolidated category list. Thus any contamination derived from laboratory procedures was identified and eliminated from subsequent analysis. The most convincing evidence that the conclusions in this study were not overtly influenced by errant methodology is the fact that the different replicates all grouped together, whereas, when analyzed with PCA and cluster analysis, samples from different environments did not group together. This confirms that the environmental differences observed between and within the three primary environments at JEG were not attributable to the inherent laboratory biases.

3.2. Hydrochemistry

Hydrochemical analyses were conducted to characterize the subglacial and supraglacial samples and assist in differentiation between the environments. Variations in water chemistry offer insight into the nature of the environments that the waters have passed through prior to sampling. Specifically, the stream hydrochemistry provides information about whether the waters have had contact with rock material, whether that contact was prolonged or short-lived, and possibly whether it occurred in an oxic or anoxic environment. Comparison of the water chemistry of supraglacial input and subglacial output waters may also provide evidence of nutrient depletion or contact with sources of organic C during passage through the glacier. Finally, hydrochemical analyses of basal ice samples also provide information about the degree of contact between source waters, rock material, and sources of organic C prior to formation of the basal ice layer, which is presumed to occur by refreezing of subglacial waters (Skidmore *et al.*, 2000).

3.2.1. EC

EC is a measure of total dissolved solutes in a water sample. When produced from melted snow and/or ice, glacial meltwaters typically contain small amounts of primarily atmospherically derived solute. The solute content of these waters is increased as a result of

weathering reactions that occur when meltwaters come into contact with rock material, either on the glacier surface or, particularly, at the glacier bed. EC can therefore be used as an index of the extent and duration of water:rock contact. The EC of the subglacial samples (range: 62 – 694 μS/cm) was higher than that of the supraglacial samples (range: 3 – 49 μS/cm) (Figure 3.1, Appendix 8). Among the supraglacial samples, the SP-MLS-a samples had the highest EC (range: 8 – 49 μS/cm). This is consistent with the fact that these samples may have had contact with rock material in ice marginal areas upstream of the ice marginal lake from which this stream is derived (see 2.1.1 for field site description). The EC of the subglacial water samples (range: 185 – 694 μS/cm) was generally much higher than that of basal ice samples (range: 62 – 235 μS/cm). This is expected because solutes are rejected from ice as it forms from water. The SB-IB samples, which were the first waters to drain from the glacier at the start of the melt season, were the most solute rich (range: 508 – 694 μS/cm). This suggests that these waters may have been stored over winter at the glacier bed. Dilution of subglacial water samples as the melt season progressed likely reflects the penetration of supraglacial meltwater produced during the current melt season to the glacier bed.

3.2.2. Sulfate Concentrations

Subglacial water samples had much higher sulfate concentrations (range: 1339 – 6674 μeq/L) than the supraglacial snow (range: 0.6 – 3 μeq/L) and water (range: 2 – 9 μeq/L) samples (Figure 3.1, Appendix 9). Sulfate values for the basal ice samples were more variable between sites (range: 6 – 1343 μeq/L). The B-C samples had the highest sulfate contents (1308 and 1343 μeq/L) among the basal ice samples, most closely resembling the subglacial water sulfate values (Figure 3.1). The B-S sample had a sulfate concentration (197 μeq/L) intermediate between the subglacial and supraglacial water values, whereas the B-F samples had low sulfate concentrations (6 and 9 μeq/L), similar to the supraglacial water samples. Analyses of the $\delta^{34}S$ and $\delta^{18}O$ of the

sulfate in the subglacial waters suggest that it is derived primarily from the dissolution of gypsum and/or anhydrite, which are known to outcrop beneath the glacier (Skidmore, 2001).

3.2.3. Nitrate Concentrations

In general, in glacial systems nitrate is atmospherically derived and incorporated into meltwater at the time of melting. Thus, if nitrate concentrations in the out-flowing subglacial waters are less than in surface waters, this implies some utilization of nitrate during transit, either by biological uptake or nitrate reduction or denitrification. Analysis of the nitrate content of subglacial waters revealed two groups, which were, to some extent, temporally separated. Generally, the early season subglacial waters (collected from June 30, 19:00 h to July 1, 2:30 h) were nitrate-depleted (0.1 – 0.5 μeq/L) relative to the later season subglacial waters (collected from June 30, 23:00 h to July 23, 17:00 h) (0.4 – 4 μeq/L) (Figure 3.2, Appendix 9). Nitrate concentrations in later season subglacial waters were similar to those in supraglacial waters (0.2 – 2 μeq/L). This suggests that microbial processes may influence the nitrate content of waters stored at the bed over winter, but do not appear to affect the chemistry of later season waters which pass quickly through the subglacial environment.

Nitrate concentrations in basal ice were more variable (Figure 3.2, Appendix 9). B-C (bag 1) had no nitrate whereas, B-C (bag 2) contained 1 μeq/L, a concentration typical of supraglacial and later season subglacial water samples. Similarly, B-F (bag 1) also contained no nitrate, but B-F (bag 2) was comparatively nitrate-enriched (0.8 μeq/L). The B-S sample contained no nitrate. The variation in nitrate concentrations among the different basal ice sites might indicate the presence of anoxic microenvironments, either within the basal ice layer of the glacier or in those parts of the subglacial drainage system that supply the water that freezes to form basal ice.

3.2.4. DOC concentrations

Generally, the DOC concentrations (DOC) in both subglacial and supraglacial water samples were very low (Figure 3.3, Appendix 10). Supraglacial snow samples had the lowest average DOC concentration (0.96 ppm), followed by supraglacial waters (1.21 ppm), and subglacial waters (1.23 ppm). DOC concentrations in basal ice were much higher (61.9 ppm) on average, but highly variable. B-S (bag 1) had a concentration of 0.55 ppm, B-F (bag 1) contained 1.17 ppm of DOC, B-F (bag 2) had slightly lower concentrations at 0.76 ppm, B-C (bag 1) had a much higher concentration of 62.9 ppm, and B-C (bag 2) contained even more DOC at 244 ppm (Appendix 10). The variability in the DOC content of basal ice samples suggests that the distribution of organic carbon in the subglacial environment at JEG may be heterogeneous and highly localized. However, the fact that there were no differences in DOC concentration between the subglacial and supraglacial waters implies that the subglacial waters sampled did not have access to subglacial OC sources in 2002.

Finally, it should be noted that there was no discernable correlation of pH with sample environment, as all the samples were neutral to alkaline (6.4 – 8.7) (Appendix 8). The results from the hydrochemical analyses illustrate that waters from the subglacial and supraglacial environments have different chemical properties, and that these properties vary both spatially and temporally.

3.3. Multivariate Statistical Analysis of the *Hae*III dataset

Community composition appears to be influenced by environmental location because inter- and intra-environmental differences were observed between and within the subglacial, supraglacial, and proglacial communities. Multivariate statistical analyses (PCA and cluster analysis) were used to identify groups of samples that contained similar assemblages of T-RFs. The results revealed that there were distinct groupings of samples based on environmental

location. It should be noted that attempts to extract DNA from the dry snow and B-S samples were unsuccessful, and thus these samples were not included in subsequent analyses.

PCA identified 15 factors that explained a total of 79% of the variance in the entire *Hae*III dataset. These factors represented groups of samples with a common complement of T-RFs. The groups of samples associated with each factor were identified by their strong loadings (>0.50) on the factor and are listed in Table 3.1. The subglacial samples load strongly on factors 1, 3, 5, 6, 7, 8, and 10. The supraglacial samples load strongly on factors 2, 9, 11, and 12. The proglacial samples load strongly on factors 4, 9, and 15. The factor loadings matrix was then used as input to the cluster analysis. The groups identified by the cluster analysis are listed in Table 3.2. Since the cluster analysis was based on the PCA factor loadings, there is (not surprisingly) close correspondence between the sample groupings derived by the two methods. The results of the cluster analysis on the entire *Hae*III dataset are displayed as a dendrogram (Figure 3.4). It is evident from Figure 3.4 that there is clear separation between the subglacial, supraglacial, and proglacial samples. Scatter plots show that the two supraglacial samples (SP-IS-a and SP-MLS-a) are distinct from each type of proglacial (P-S, P-R) (Figure 3.5) and subglacial sample (B-F, subglacial waters, B-C) (Figure 3.6). The proglacial samples are also distinct from each type of subglacial sample (Figure 3.7). Therefore, the communities in all three primary environments appear to be different. Thus, inter-environmental distinction between the three primary environments occurs because the T-RF composition of each sample is more similar to that of other samples from the same primary environment than to that of samples from the other two environments.

Cluster analysis revealed a secondary level of distinction within each primary environment (intra-environmental distinction) because the samples from the different sites within each primary environment were associated with different factors (Figure 3.8). Accordingly, as shown in Figure 3.8, the samples tended to cluster initially according to specific sample locations, and then by environment. Within the supraglacial environment the SP-IS-a and SP-MLS-a

samples formed distinct clusters (Figures 3.9 and 3.10). The proglacial samples were divided into four clusters, with samples from location P-R forming a single cluster (Figures 3.11 and 3.12). Within the subglacial environment, the B-C, B-F, subglacial waters, and M-N samples also generally clustered into separate groups (Figure 3.13). Figure 3.14 illustrates that the subglacial water samples are distinct from both types of basal ice samples, in terms of factors 1, 3, and 5. Some degree of separation was also evident between the chemically different subglacial water samples, in terms of factors 3 and 7 (Figure 3.15). As shown in Figure 3.15, the later season nitrate-enriched subglacial waters (SB-AF, SB-OC, and SB-IB 23:00 h) grouped separately from the principal clusters of early season nitrate-depleted waters (SB-IB 19:00 h). The basal ice samples were almost entirely separated according to their sample locations, B-C and B-F (Figure 3.16).

The specific properties of the T-RF dataset that resulted in the observed inter- and intra-environmental distinction at JEG, revealed by multivariate statistics, are discussed in the following section.

3.4. Comparison of T-RFLP patterns

Inter-environmental differences result from the presence of different characteristic core groups of T-RFs that define each primary environment; intra-environmental differences result from the presence of additional T-RFs in samples from specific sites, which are not found in samples from other sites in the same primary environment.

3.4.1. Inter-environmental community differences

Comparison of the T-RF patterns associated with the three primary environments provides insights into the specific properties of the dataset that cause the observed community differences. First, each T-RF was characterized in terms of its environmental preference according to its frequency of occurrence in samples from each environment (Table 3.3). The T-

RFs present in each sample were identified, and the percent of samples from each primary environment in which each T-RF occurred was determined. Table 3.3 lists the T-RFs identified and the environment(s) they were associated with. Second, each sample was characterized in terms of the predominant environmental preference of the T-RFs found within it. A list of the T-RFs present in each sample was compiled, along with data on the proportion of samples from each environment in which each T-RF was found. For each sample, the percentage occurrence of all T-RFs present in samples from each primary environment were summed, and divided by the total number of T-RFs present in the sample (Appendix 11). This provides an index of environmental affinities of the assemblage of T-RFs in each sample. The index consists of three numbers, representing the average proportion of samples from each primary environment in which the T-RFs found in a particular sample occur. High average occurrence in any of the three environments implies a strong association with that environment. In this way, each sample was characterized by its T-RF composition. Table 3.2 shows the environmental affinities of samples in each of the major clusters derived from the entire *Hae*III dataset. Finally, this summary information about each sample was used to characterize the environments in terms of their T-RF content (Table 3.4). By characterizing the T-RFs, samples, and environments in this three-step manner, it became clear that the subglacial, supraglacial, and proglacial environments at JEG had different T-RF community compositions.

While some T-RFs were common to all three environments (6%) or two environments (28%), most (67%) were unique to a single environment (Table 3.3). Each environment contained a group of "unique" T-RFs (28 – 58% of the total number of T-RFs found). Each environment also contained a group of "widespread" T-RFs that occurred in more than 10% of the samples from that environment (24 – 53% of all T-RFs). The proportion of unique T-RFs that occurred widely in an environment was, however, relatively low, ranging from 5.7% in the subglacial environment to 20% in the proglacial environment (Table 3.4). In general, however, the index of environmental affinity showed that most samples from a given environment were

dominated by T-RFs that showed a strong affinity for that environment (Table 3.2). Some subglacial water and basal ice samples also contained T-RFs that showed some affinity for the supraglacial and/or proglacial environments (Table 3.2, clusters 12, 21, 23, 25, and 27). Supraglacial and proglacial samples typically contained some T-RFs with an affinity for the subglacial environment, but virtually no supraglacial samples contained T-RFs with a proglacial affinity, and vice versa (Table 3.2, clusters 3 and 32). Overall, therefore, the supraglacial and proglacial communities were dominated by T-RFs that showed a strong preference for the environment from which samples were collected. The subglacial communities, on the other hand, tended to include T-RFs that were most commonly associated with either the supraglacial or proglacial environment, as well as T-RFs with a clear preference for the subglacial environment.

Distinct subglacial sample clusters were evident (Figure 3.4, dark grey regions) due to the presence of combinations of specific T-RFs (46, 202, 72, 74, 48, 172, 84, 131, 82, 171, 42, 47, 174, 43, 73, 75, 132, and 50) (Table 3.2), which were widespread in both types of subglacial samples (basal ice and subglacial waters). All of the B-C samples and 97% of the subglacial water and B-F samples contained notable average proportions (>10%) of T-RFs occurring in the subglacial dataset. The majority of the T-RFs occurred in the subglacial environment (73%) and the majority of these were unique to this environment (Table 3.4). However, most (87%) of the uniquely subglacial T-RFs occurred in only a small number (≤3%) of the subglacial samples, and only 10% of the unique T-RFs were widely distributed (occurred in >10% of samples) in the subglacial dataset. Overall, only 24% of the total subglacial T-RFs were widespread in the subglacial dataset. Thus although the majority of the T-RFs found were present in the subglacial environment, most were present only sparsely (Table 3.3, group E).

Conversely, though only 30% of the total T-RFs were found in the supraglacial environment, 54% of these T-RFs were widespread throughout the supraglacial dataset. Only 28% of the total supraglacial T-RFs were unique to that environment, but 42% of these unique T-RFs were widespread (Tables 3.3 and 3.4). A distinct supraglacial sample cluster was evident

due to the presence of combinations of specific T-RFs (no. 29, 83, 166, 39, 96, 135, 171, 130, 219, 127, 30, 41, 109, 164, and 192) (Table 3.2), which were widespread throughout the SP-IS-a samples that comprised the majority of the supraglacial dataset, and they displayed a stronger association with the supraglacial environment than with either the subglacial or proglacial environments.

The proglacial samples also contained a large array of T-RFs that were widespread throughout the sample set and exhibited a strong preference for this environment. Thus, though only 35% of the total T-RFs found were present in the proglacial environment, 46% of these were widespread throughout the proglacial dataset. The proglacial environment also had a large proportion of unique T-RFs (46% of the total proglacial T-RFs), many of which (44%) were widespread throughout the proglacial dataset (Tables 3.3 and 3.4). A distinct proglacial sample cluster was evident because of the presence of combinations of specific T-RFs (no. 127, 89, 68, 138, 45, 88, 124, 90, 91, 126, and 129) (Table 3.2). These were widespread throughout the P-R samples that comprised the majority of the proglacial dataset, and also had a stronger association with the proglacial environment than with the subglacial or supraglacial environments.

The subglacial environment shared many more T-RFs with the supraglacial and proglacial environments than the latter two environments had in common with each other (Table 3.4). Thus the presence in the supraglacial and proglacial environments of characteristic core groups of T-RFs that are widespread and exhibit a strong preference for these two environments, means that samples from each primary environment are easily differentiated based on their T-RF composition.

3.4.2. Intra-environmental community differences

Although it was expected that different sub-environments and sample sites in the same primary environment will have somewhat different T-RF compositions, some of the intra-environmental variability observed seems to be explicable in terms of obvious physical and/or

chemical differences between the sub-environments and sample sites. This idea is discussed in detail in section 4.2. The following is a presentation of the characteristics that result in the observed intra-environmental variability within the *Hae*III dataset. In conjunction with the core groups of widespread T-RFs, which define the communities in the primary environments, the presence in each sample of additional T-RFs that are not found at the other sample sites in the same primary environment allows intra-environmental distinction (Figure 3.8).

The subglacial dataset displayed several levels of intra-environmental differentiation. Firstly, the subglacial waters and basal ice samples clustered separately. There were nine subglacial water clusters and 13 basal ice clusters (Figure 3.13 and Table 3.2, clusters 9 – 17 and 18 – 20). This is because the subglacial water samples resembled the supraglacial dataset more closely than the proglacial dataset, because the average proportions of T-RFs occurring in the supraglacial environment (average proportion range: 10 – 42%) were generally greater than those T-RFs from the proglacial environment (average proportion range: 10 – 21%) (Table 3.2, clusters 9 – 17).

Secondly, within the subglacial water sub-environment there was T-RF composition variability between the early season nitrate-reduced waters and the late season nitrate-enriched waters. There were six early season water clusters and three late season water clusters (Figure 3.13 and Table 3.2, clusters 9 – 12, 15, 17, and 13, 14, 16). The later season nitrate-enriched subglacial waters generally contained low average proportions (< 30%) of T-RFs found in each environment (Table 3.2, clusters 13, 14, and 16, samples highlighted in blue) indicating that the T-RFs found in these samples did not occur frequently in any of the three environments. This may suggest that the later season subglacial waters access an environment that was not sampled anywhere else in this study. For example, these waters may access and transport glacier ice communities as they pass through englacial channels in the summer.

Thirdly, within the basal ice sub-environment the two different sample sites (B-F and B-C) also grouped into distinct clusters. There were four main clusters of B-C samples, and two

main clusters of B-F samples (Figure 3.13 and Table 3.2, clusters 18, 21, 35, 30 and 19, 23). The T-RF composition of the B-F samples resembled the proglacial dataset more closely than the supraglacial dataset, because a greater percentage of the B-F samples (74%) contained notable average proportions of proglacial T-RFs occurrences than supraglacial occurrences (40%). Also, the average proportions of T-RFs occurring in the proglacial environment (average proportion range: 10 – 27%) in the B-F samples were higher than the average proportions of T-RFs occurring in the supraglacial environment (average proportion range: 10 – 15%) (Table 3.2, clusters 19, 22, 23, 26, and 27). The B-C samples were not more evidently associated with either the supraglacial or proglacial dataset, as the T-RFs comprising the B-C samples occurred in approximately equal average proportions in both the supraglacial (average proportion range: 12 – 24%) and proglacial (average proportion range: 10 – 24%) datasets (Table 3.2, clusters 18, 20, 21, 24, 25, 27, 29, and 30). However, the B-C samples were more similar to the B-F samples than the subglacial waters because they contained a complement of T-RFs widespread throughout the basal ice sub-environment (T-RFs 220, 116, 230, 135, and 85), which were not found in the subglacial waters. The difference between the B-C and B-F samples was the result of the presence of additional T-RFs in the B-C sample site (T-RFs 83, 114, 86, 115, 125, 206, 111, 126, 130, and 164), which were not found in the B-F samples.

It should be noted that the M-N samples also had higher average proportions of subglacial and proglacial T-RFs than supraglacial T-RFs. Factor 5 of the *Hae*III PCA analysis (Table 3.1, factor 5) is strongly associated with only basal ice cave samples and the two M-N samples, thus indicating a possible close relationship between the T-RFs found in these two sample sites. However, additional M-N samples would have to be analyzed to confirm this hypothesis.

Since the supraglacial and proglacial datasets were both dominated by samples from a single site (the SP-IS-a and P-R sites, respectively) it is not possible to gain a complete understanding of the degree of intra-environmental variability within these two primary

environments. However, the few samples from the SP-MLS-a and P-S sites that were analyzed clustered separately from the remainder of their respective datasets, indicating that these two sites differed from the other site in the same primary environment. The SP-IS-a and SP-MLS-a samples shared a few T-RFs that were widespread throughout the supraglacial dataset (T-RFs 131, 201, 108, 132, 43 and 172), but the SP-MLS-a samples contained additional T-RFs present in both the SP-MLS-a samples (T-RFs 77, 98, 46, 81, 104, 129, 136, and 165). These were not found in the SP-IS-a samples that comprised the bulk of the supraglacial dataset. The differentiation among the communities from the two proglacial sample sites resulted from the P-R and P-S samples containing almost entirely different sets of T-RFs. The P-R and P-S samples shared only three common T-RFs (no. 59, 72, and 73), but these were widespread throughout the proglacial dataset. The P-S dataset contained additional T-RFs (no. 9, 16, 18, 37, 54, 66, 84, and 137), which were widespread throughout the P-S samples, but not present in the P-R samples.

Table 3.1. Sample loadings on fifteen factors identified by principal component analysis (PCA) as new variables that explained a total of 79% of the variance observed in the *Hae* III dataset. The percent of the total variance explained by each factor is shown in parentheses. The groups of samples which loaded strongly on each factor are listed. A strong loading was 0.50 or higher. Samples with an asterisk loaded slightly lower than 0.50 but were included. Cross reference the *Hae* III sample key number with the *Hae* III sample key (Appendix 6) for an explanation of the sample.

Factor	*Hae* III sample key no.	Sample name	No. of T-RFs in each sample
1 (24%)	6	B-C	11
	13	B-C	17
	18	B-C	17
	32	SB-IB3-19:00 h	13
	66	B-F	14
	67	B-F	12
	68	B-F	4
	69	B-F	4
	71	B-F	15
	72	B-F	13
	73	B-F	12
	74	B-F	10
	75	B-F	10
	76	B-F	7
	77	B-F	15
	78	B-F	13
	79	B-F	9
	80	B-F	13
	82	B-F	4
	83	B-F2	6
	84	B-F2	7
	91	B-F2	8
	92	B-F2	13
	95	B-F2	8
	96	B-F2	9
2 (10.7%)	104	SP-IS-a	12
	105	SP-IS-a	11
	106	SP-IS-a	10
	107	SP-IS-a	9
	108	SP-IS-a	12
	109	SP-IS-a	12
	110	SP-IS-a	19
	111	SP-IS-a	19
	112	SP-IS-a	6
	113	SP-IS-a	12
	114	SP-IS-a	9
	115	SP-IS-a	11
	116	SP-IS-a	9
	117	SP-IS-a	10
	119	SP-IS-a	10
	120	SP-IS-a	10
	121	SP-IS-a	9
3 (7.8%)	29	SB-IB2-19:00 h	2
	31	SB-IB2-19:00 h	1
	41	SB-IB3-19:00 h	1
	42	SB-IB3-19:00 h	2
	44	SB-IB3-19:00 h	1
	45	SB-IB3-19:00 h	1
	46	SB-IB3-19:00 h	1
	47	SB-IB3-19:00 h	2
	53	SB-IB3-19:00 h	1
	54	SB-IB3-19:00 h	1
	55	SB-IB3-19:00 h	1
	56	SB-IB4-19:00 h	1
4 (6.3%)	130	P-R1	3
	131	P-R1	4
	132	P-R1	12
	133	P-R1	11
	134	P-R1	8
	135	P-R1	12
	136	P-R1	6
	137	P-R1	4
	138	P-R1	12
	139	P-R1	10
	140	P-R1	14
	141	P-R1	15
5 (5.4%)	5	B-C	17
	6	B-C	11
	7	B-C	15
	8	B-C	13

Factor	*Hae* III sample key no.	Sample name	No. of T-RFs in each sample
5 (5.4%)	9	B-C	9
continued	10	B-C	9
	11	B-C	4
	12	B-C	13
	13	B-C	17
	16	B-C	4
	19	B-C	15
	20	B-C	12
	21	B-C	5
	22	B-C	10
	23	B-C	8
	24	B-C	13
	99*	M-N	5
	100	M-N	6
6 (4.6%)	12	B-C	13
	17	B-C	13
	33	SB-IB3-19:00 h	12
	34	SB-IB3-19:00 h	5
	35	SB-IB3-19:00 h	7
	36	SB-IB3-19:00 h	7
	37	SB-IB3-19:00 h	4
	38	SB-IB3-19:00 h	10
	39	SB-IB3-19:00 h	9
	40	SB-IB3-19:00 h	8
	48	SB-IB3-19:00 h	4
	50	SB-IB3-19:00 h	5
	51	SB-IB3-19:00 h	4
	52	SB-IB3-19:00 h	4
7 (3.6%)	1	B-C	4
	2	B-C	7
	3	B-C	8
	4	B-C	18
	27	SB-IB2-19:00 h	8
	28	SB-IB3-19:00 h	1
	30	SB-IB4-19:00 h	7
	49	SB-IB3-19:00 h	3
	57	SB-IB4-19:00 h	11
	60*	SB-OC	27
	61	SB-AF	12
	64	B-F	10
8 (3.5%)	14	B-C	10
	15	B-C	8
	87	B-F2	8
	88	B-F2	6
	93	B-F2	9
	94	B-F2	7
9 (2.4%)	101	SP-IS-a	7
	102	SP-IS-a	13
	103	SP-IS-a	7
	126*	P-S	6
	127	P-S	2
10 (2.2%)	43	SB-IB3-19:00 h	5
	65	B-F	1
	81	B-F	1
	85	B-F2	2
	86	B-F2	2
	89	B-F2	4
	90	B-F2	3
	98	B-F2	1
11 (1.9%)	25	B-C2	1
	26	B-C2	1
	124	SP-MLS-a	
12 (1.8%)	59	SB-IB-19:00 h	6
	63*	SB-AF	16
	122	SP-MLS-a	11
	123	SP-MLS-a	4
13 (1.7%)	58*	SB-IB4-19:00 h	24
	62	SB-AF	22
14 (1.6%)	NO SAMPLES LOADED STRONGLY		
15 (1.5%)	128	P-S	7
	129	P-S	7

Table 3.2. Groups of samples identified by cluster analysis based on the PCA factor loadings for the *Hae* III dataset. The specific T-RFs present in each sample and the three number index , representing the average proportion of samples from each primary enviornment in which the T-RFs found in a particular sample occur are also presented. The three number index highlighted in yellow represents the average proportion of samples in each environment in which T-RFs found in the entire cluster occur. The overall environmental presence of the T-RFs found in each sample and cluster (highlighted in yellow) are also listed. "All" signifies that at least one T-RF in the sample or cluster was found in all three primary environments. "SB" signifies that at least one T-RF in the sample or cluster was found in the subglacial environment. "SP" signifies that at least one T-RF in the sample or cluster was found in the supraglacial environment. "P" signifies that at least one T-RF in the sample or cluster was found in the proglacial environment. "Bold face" indicates that the T-RFs in the sample or cluster were found in proportions > 10% in any one environment. The basal ice samples (B-C and B-F) are listed in black, the subglacial water samples in grey, the M-N samples in green, the SP-IS-a supraglacial samples in dark blue, the SP-MLS-a supraglacial samples in light blue, the P-R proglacial samples in red, and the P-S proglacial samples in orange. Samples highlighted in light blue represent the late season nitrate-enriched subglacial waters. Cross reference the HaeIII sample key number with the HaeIII sample key (Appendix 6) for a description of the sample. Cross reference T-RF numbers with Appendix 9.

Cluster No.	Environment cluster type	Samples in cluster	Sample name	T-RFs in samples (listed by number designations)	Average proportion of samples in each environment in which T-RFs found in a particular sample/cluster occur			
					Subglacial	Supraglacial	Proglacial	Environmental Presence
1	**Supraglacial Cluster**	102	SP-IS-a	30, 41, 43, 83, 84, 99, 109, 130, 131, 134, 164, 170, 171	9	**26**	2	ALL
		103	SP-IS-a	30, 41, 84, 109, 130, 131, 164	8	**28**	3	ALL
		101	SP-IS-a	30, 41, 84, 109, 130, 131, 164	8	**28**	3	ALL
					8	**27**	2	ALL
2	**Supraglacial Cluster**	118	SP-IS-a	29, 72, 75, 84, 131, 132, 166, 198	**17**	**41**	**12**	ALL
3	**Supraglacial Cluster**	111	SP-IS-a	28, 29, 39, 43, 82, 83, 96, 108, 122, 127, 130, 131, 132,	**11**	**45**	5	ALL
		110	SP-IS-a	29, 39, 43, 82, 83, 96, 108, 122, 127, 130, 131, 135, 166,	**11**	**43**	5	ALL
		119	SP-IS-a	29, 39, 74, 83, 96, 108, 131, 132, 166, 201	**12**	**65**	5	ALL
		112	SP-IS-a	29, 83, 131, 132, 166, 201	**12**	**76**	0	**SBSP**
		120	SP-IS-a	29, 39, 83, 96, 108, 127, 131, 132, 166, 201	8	**66**	8	ALL
		117	SP-IS-a	29, 39, 83, 96, 108, 130, 131, 132, 166, 201	7	**68**	1	ALL
		121	SP-IS-a	29, 39, 83, 96, 108, 131, 132, 166, 201	8	**71**	1	ALL
		116	SP-IS-a	29, 39, 83, 96, 108, 131, 132, 166, 201	8	**71**	1	ALL
		107	SP-IS-a	29, 39, 83, 96, 131, 132, 135, 166, 201	**10**	**69**	1	ALL
		106	SP-IS-a	29, 39, 83, 131, 132, 135, 166, 201, 213, 214	9	**57**	1	ALL
		113	SP-IS-a	29, 39, 82, 83, 96, 130, 131, 132, 135, 166, 171, 201	**11**	**60**	1	ALL
		109	SP-IS-a	29, 39, 83, 96, 108, 127, 130, 131, 135, 166, 171, 201	9	**60**	7	ALL
		114	SP-IS-a	29, 39, 83, 96, 108, 131, 166, 171, 201	9	**69**	1	ALL
		108	SP-IS-a	29, 39, 83, 96, 108, 130, 131, 135, 166, 171, 192, 201	8	**60**	1	ALL
		115	SP-IS-a	29, 39, 83, 96, 108, 131, 135, 166, 171, 201, 219	9	**63**	1	ALL
		105	SP-IS-a	29, 39, 83, 96, 108, 131, 135, 166, 171, 201, 219	9	**63**	1	ALL
		104	SP-IS-a	29, 39, 83, 96, 108, 131, 135, 166, 171, 192, 201, 219	9	**58**	1	ALL
					9	**63**	2	ALL
4	**Supraglacial Cluster**	123	SP-MLS-a	77, 98, 132, 201	5	**39**	0	SBSP
		122	SP-MLS-a	43, 46, 77, 98, 108, 129, 132, 136, 165, 172, 201	**13**	**23**	2	ALL
					9	**31**	1	ALL
5	**Mixed Clusters Supraglacial -Sub Ice**	124	SP-MLS-a	81, 104, 131, 132	**12**	**40**	0	**SBSP**
		26	B-C2	131	**27**	**92**	0	**SBSP**
		25	B-C2	131	**27**	**92**	0	**SBSP**
					22	**74**	0	**SBSP**
6	**Proglacial - Sub Ice**	126	P-S	37, 49, 41, 59, 72, 84	**14**	**17**	**33**	ALL
		127	P-S	37, 84	**15**	**8**	**12**	ALL
		97	B-F2	58, 59, 84, 135, 177	**10**	**12**	**19**	ALL
					13	**12**	**21**	ALL

CONTINUED

Cluster No.	Environment cluster type	Samples in cluster	Sample name	T-RFs in samples (listed by number designations)	Average proportion of samples in each environment in which T-RFs found in a particular sample/cluster occur			
					Subglacial	Supraglacial	Proglacial	Environmental Presence
7	*Proglacial - Nunatak Mud*	125	P-S	3, 5, 6, 7, 31, 34, 36, 38, 40, 43, 47, 59, 60, 69, 70, 72, 73, 82, 85, 86, 87, 116, 171	8	3	14	ALL
		99	M-N	73, 82, 85, 120, 160	11	3	8	ALL
					9	3	11	ALL
8	Basal Ice - Subglacial Waters	64	B-F	43, 47, 50, 73, 75, 134, 135, 168, 171, 172	15	12	5	ALL
		30	SB-IB2-19:00 h	47, 75, 81, 120, 158, 169, 171	9	7	2	ALL
		27	SB-IB2-19:00 h	47, 73, 75, 81, 120, 158, 169, 171	10	6	5	ALL
					11	8	4	ALL
9	Subglacial Waters Cluster	42	SB-IB3-19:00 h	46, 201	37	42	0	SBSP
		56	SB-IB4-19:00 h	46	66	4	0	SBSP
		55	SB-IB3-19:00 h	46	66	4	0	SBSP
		54	SB-IB3-19:00 h	46	66	4	0	SBSP
		53	SB-IB3-19:00 h	46	66	4	0	SBSP
		46	SB-IB3-19:00 h	46	66	4	0	SBSP
		45	SB-IB3-19:00 h	46	66	4	0	SBSP
		44	SB-IB3-19:00 h	46	66	4	0	SBSP
		41	SB-IB3-19:00 h	46	66	4	0	SBSP
		31	SB-IB2-19:00 h	46	66	4	0	SBSP
					63	8	0	SBSP
10	Subglacial Waters Cluster	47	SB-IB3-19:00 h	46, 172	25	4	0	SBSP
		43	SB-IB3-19:00 h	46, 59, 84, 202, 212	32	4	19	ALL
					29	4	9	ALL
11	Subglacial Waters Cluster	29	SB-IB2-19:00 h	46, 74	55	4	21	ALL
12	Subglacial Waters Cluster	52	SB-IB3-19:00 h	46, 48, 74, 172	46	5	10	ALL
		51	SB-IB3-19:00 h	46, 48, 74, 172	46	5	10	ALL
		48	SB-IB3-19:00 h	46, 48, 74, 172	46	5	10	ALL
		50	SB-IB3-19:00 h	46, 48, 74, 131, 172	42	23	8	ALL
		37	SB-IB3-19:00 h	46, 48, 74, 131	44	25	10	ALL
		40	SB-IB3-19:00 h	46, 48, 72, 74, 131, 166, 172, 201	34	34	15	ALL
		34	SB-IB3-19:00 h	46, 48, 131, 172, 202	45	22	0	SBSP
		36	SB-IB3-19:00 h	46, 48, 74, 131, 166, 172, 202	40	27	6	ALL
		39	SB-IB3-19:00 h	43, 46, 48, 72, 74, 131, 166, 172, 202	38	23	14	ALL
		35	SB-IB3-19:00 h	46, 48, 72, 74, 131, 172, 202	45	17	18	ALL
		38	SB-IB3-19:00 h	43, 46, 48, 72, 74, 131, 132, 166, 172, 202	35	27	13	ALL
		33	SB-IB3-19:00 h	43, 46, 48, 72, 131, 132, 166, 171, 172, 201, 202	28	32	8	ALL
		32	SB-IB3-19:00 h	42, 46, 48, 72, 74, 81, 131, 166, 171, 172, 174, 202	33	20	12	ALL
					40	20	10	ALL
13	Subglacial Waters Cluster	59	SB-IB-23:00 h	47, 74, 132, 172, 201, 202	29	26	8	ALL
		63	S-AF(7/1)11:00	43, 45, 47, 48, 53, 73, 74, 75, 76, 122, 132, 153, 155, 165, 201, 202	15	11	8	ALL
		62	S-AF(7/1)11:00	33, 40, 42, 45, 47, 48, 53, 71, 73, 74, 75, 76, 82, 100, 122, 132, 153, 155, 165, 170, 171, 201	11	10	7	ALL
13	Subglacial Waters Cluster continued	58	SB-IB4-19:00 h	9, 40, 46, 47, 48, 50, 53, 62, 73, 74, 75, 76, 82, 98, 108, 122, 124, 132, 136, 148, 165, 170, 171, 202	14	9	6	ALL
					17	14	7	ALL
14	Subglacial Waters Cluster	61	S-AF(7/1)11:00	26, 44, 46, 47, 50, 55, 72, 73, 74, 75, 123, 133	18	1	14	ALL
		57	SB-IB4-19:00 h	26, 44, 46, 47, 50, 72, 73, 74, 75, 133, 205	20	2	14	ALL
					19	1	14	ALL
15	Subglacial Waters Cluster	49	SB-IB3-19:00 h	47, 172, 197	19	4	2	ALL
		28	SB-IB2-19:00 h	47	17	0	6	SBP

CONTINUED

Cluster No.	Environment cluster type	Samples in cluster	Sample name	T-RFs in samples (listed by number designations)	Average proportion of samples in each environment in which T-RFs found in a particular sample/cluster occur			
					Subglacial	Supraglacial	Proglacial	Environmental Presence
15	Subglacial Waters Cluster							
16	Subglacial Waters Cluster	60	S-OC1-7/4-12:45	32, 43, 46, 47, 50, 67, 72, 73, 75, 79, 81, 82, 92, 93, 97, 101, 105, 106, 123, 133, 137, 167, 171, 172, 173, 202, 203	13	4	5	ALL
17	Subglacial Waters Cluster	30	SB-IB2-19:00 h	47, 75, 81, 120, 158, 169, 171	9	7	2	ALL
		27	SB-IB2-19:00 h	47, 73, 75, 81, 120, 158, 169, 171	10	6	5	ALL
					10	7	3	ALL
18	Basal Ice Cluster	16	B-C	72, 83, 84, 202	38	24	24	ALL
		11	B-C	72, 83, 84, 202	38	24	24	ALL
		9	B-C	47, 72, 83, 84, 85, 116, 202, 206, 220	26	11	12	ALL
					34	20	20	ALL
19	Basal Ice Cluster	89	B-F2	84, 202, 220, 230	36	5	3	ALL
		90	B-F2	74, 202, 220	45	1	14	ALL
		86	B-F2	202, 220	46	0	0	SB
		85	B-F2	202, 220	46	0	0	SB
		98	B-F2	202	58	0	0	SB
		81	B-F	202	58	0	0	SB
		65	B-F	202	58	0	0	SB
					50	1	2	ALL
20	Basal Ice Cluster	21	B-C2	46, 82, 84, 85, 202	38	7	5	ALL
21	Basal Ice Cluster	23	B-C2	46, 72, 82, 84, 85, 131, 132, 202	35	23	13	ALL
		24	B-C2	46, 72, 83, 82, 84, 85, 114, 116, 131, 132, 172, 202, 220	30	21	9	ALL
		22	B-C2	46, 72, 82, 84, 85, 116, 131, 132, 202, 220	33	19	11	ALL
		20	B-C2	46, 72, 82, 83, 84, 85, 116, 131, 132, 202, 203, 220	29	24	9	ALL
		19	B-C2	46, 72, 74, 81, 82, 84, 85, 116, 131, 132, 166, 197, 202, 205, 220	27	18	10	ALL
					31	21	11	ALL
22	Basal Ice Cluster	71	B-F	35, 37, 42, 43, 46, 72, 74, 82, 84, 85, 135, 171, 172, 174, 202	27	10	12	ALL
23	Basal Ice Cluster	82	B-F	46, 72, 202, 220	52	2	21	ALL
		69	B-F	46, 72, 202, 220	52	2	21	ALL
		68	B-F	46, 72, 202, 220	52	2	21	ALL
		91	B-F2	46, 46, 48, 72, 74, 202, 220, 230	41	2	15	ALL
		96	B-F2	43, 46, 50, 72, 74, 197, 202, 220, 230	33	4	14	ALL
		95	B-F2	43, 46, 72, 74, 202, 205, 220, 230	37	4	16	ALL
		84	B-F2	42, 46, 72, 74, 202, 220, 230	41	2	18	ALL
		83	B-F2	46, 72, 74, 202, 220, 230	45	3	21	ALL
		75	B-F	42, 46, 48, 72, 94, 95, 135, 201, 202, 207	26	13	8	ALL
		79	B-F	42, 46, 48, 72, 135, 201, 202, 220, 230	34	15	9	ALL
		76	B-F	42, 46, 48, 72, 135,, 202, 220	40	7	12	ALL
		74	B-F	42, 46, 48, 72, 135, 171, 174, 202, 220, 230	34	10	10	ALL
		92	B-F2	42, 43, 46, 48, 72, 74, 131, 172, 202, 205, 220, 230	32	11	10	ALL
		77	B-F	42, 43, 46, 48, 72, 74, 131, 135, 171, 172, 174, 202, 205, 220, 230	31	15	10	ALL
		67	B-F	42, 43, 46, 48, 72, 74, 135, 171, 172, 174, 202, 220	34	10	12	ALL
		73	B-F	42, 46, 48. 72, 74, 135, 171, 172, 174, 202, 220, 230	35	9	12	ALL
		80	B-F	42, 43, 46, 48, 72, 74, 135, 171, 172, 174, 202, 220, 230	33	10	11	ALL
		78	B-F	42, 43, 46, 48, 72, 74, 135, 171, 172, 174, 202, 220, 230	33	10	11	ALL
		72	B-F	42, 43, 46, 48, 72, 74, 135, 171, 172, 174, 202, 220, 230	33	10	11	ALL
		66	B-F	42, 43, 46, 48, 72, 74, 135, 171, 172, 174, 202, 205, 220, 230	31	9	11	ALL
					37	7	14	ALL
24	Basal Ice Cluster	10	B-C	46, 48, 72, 82, 83, 84, 114, 116, 202	34	13	12	ALL

CONTINUED

Cluster No.	Environment cluster type	Samples in cluster	Sample name	T-RFs in samples (listed by number designations)	Average proportion of samples in each environment in which T-RFs found in a particular sample/cluster occur			
					Subglacial	Supraglacial	Proglacial	Environmental Presence
25	Basal Ice Cluster	17	B-C	46, 48, 72, 74, 82, 83, 84, 114, 131, 171, 172, 174, 202	33	20	12	ALL
		12	B-C	46, 48, 72, 74, 82, 83, 84, 114, 116, 131, 171, 172, 202	34	20	12	ALL
		6	B-C	46, 48, 72, 74, 82, 83, 114, 116, 202, 220, 230	35	9	12	ALL
		18	B-C	46, 48, 72, 74, 82, 84, 86, 114, 116, 131, 166, 171, 172, 174, 202, 220, 230	30	16	10	ALL
		13	B-C	46, 48, 72, 74, 82, 83, 84, 114, 116, 131, 166, 171, 172, 174, 202, 220, 230	31	20	10	ALL
		8	B-C	46, 48, 59, 72, 74, 82, 83, 114, 116, 131, 202, 220, 230	32	15	17	ALL
		7	B-C	46, 48, 59, 72, 74, 82, 83, 114, 116, 131, 172, 197, 202, 220, 230	30	14	15	ALL
		5	B-C	46, 48, 72, 74, 82, 83, 84, 93, 94, 114, 116, 127, 131, 172, 202, 220, 230	28	14	13	ALL
					32	16	13	ALL
26	Basal Ice Cluster	70	B-F	59, 200, 204	2	0	27	SBP
27	Basal Ice Cluster	88	B-F2	82, 84, 113, 116, 117, 127	14	8	16	ALL
		87	B-F2	64, 78, 80, 82, 84, 110, 116, 127	11	6	12	ALL
		15	B-C	82, 84, 113, 116, 125, 127, 172, 174	17	7	13	ALL
		93	B-F2	81, 82, 84, 112, 116, 127, 135, 174, 222	14	10	12	ALL
		94	B-F2	81, 84, 112, 116, 127, 135, 174	15	11	14	ALL
		14	B-C	78, 80, 84, 110, 111, 116, 127, 135, 174, 206	10	8	10	ALL
					14	8	13	ALL
28	Basal Ice Cluster	100	M-N	72, 74, 82, 85, 121, 162	22	3	23	ALL
29	Basal Ice Cluster	4	B-C	47, 50, 73, 75, 81, 83, 84,115, 116, 125, 126, 127, 130, 131, 164, 168, 171, 172	13	17	8	ALL
30	Basal Ice Cluster	1	B-C	47, 50, 84, 85	17	4	6	ALL
		2	B-C	47, 50, 73, 83, 84, 85, 86	14	13	8	ALL
		3	B-C	47, 50, 73, 75, 83, 84, 115, 116	15	12	7	ALL
					15	10	7	ALL
31	Proglacial Clusters	129	P-S	9, 16, 18, 54, 66, 174, 175	3	0	11	SBP
		128	P-S	9, 16, 18, 52, 54, 66, 174	3	0	11	SBP
					3	0	11	SBP
32	Proglacial Clusters	139	P-R1	45, 59, 68, 72, 74, 88, 89, 126, 127, 138	11	3	55	ALL
		135	P-R1	45, 59, 68, 72, 74, 88, 89, 91, 122, 124, 127, 138	9	3	50	ALL
		133	P-R1	45, 59, 68, 72, 74, 88, 89, 90, 124, 127, 138	10	2	54	ALL
		141	P-R1	45, 59, 68, 72, 73, 74, 88, 89, 91, 93, 123, 124, 126, 127, 138	11	4	48	ALL
		140	P-R1	45, 59, 68, 72, 73, 74, 88, 89, 90, 91, 124, 127, 129, 138	9	2	47	ALL
		138	P-R1	45, 59, 68, 72, 73, 74, 88, 89, 90, 124, 127, 138	10	2	52	ALL
		132	P-R1	45, 59, 68, 72, 73, 74, 88, 89, 90, 124, 127, 138	10	2	52	SBP
		134	P-R1	45, 59, 68, 72, 88, 89, 127, 138	8	3	62	ALL
		136	P-R1	59, 68, 72, 127, 129, 138	10	4	59	ALL
		137	P-R1	59, 72, 89, 127	15	5	74	ALL
		131	P-R1	59, 72, 89, 127	15	5	74	ALL
		130	P-R1	59, 72, 127	20	7	78	ALL
					12	4	59	ALL

Table 3.3. Compilation of all T-RFs successfully resolved with the *Hae* III enzyme, and the percent occurrence of each T-RF in each primary environment. Percent occurrences which are greater than 10% in any environment are in boldface. The environmental presence of each T-RF is also summarized by group number.

Group No.	Environmental Presence	T-RF No.	T-RF Name	% occurrence in subglacial samples	% occurrence in supraglacial samples	% occurrence in proglacial samples
A	All environments	**72**	**H(1)27-D(1)21**	**48**	**4**	**82**
	(8 total)	**74**	**M(01)16-I(1)20**	**44**	**4**	**41**
		84	**A(1)62-K(1)09**	**29**	**17**	**12**
		82	**M(01)22-G(1)23**	**25**	**13**	**6**
		171	**H(3)2-D(3)4**	**23**	**42**	**6**
		43	**Q(1)27-D(1)10**	**16**	**17**	**6**
		127	**E(1)39-I(2)1**	**8**	**17**	**71**
		122	D(1)60-Q(01)99	3	8	6
B	Subglacial and Supraglacial	**46**	**Q(1)31-I(1)07**	**66**	**4**	**0**
	(20 total)	**172**	**M(03)2-A(3)4**	**35**	**13**	**0**
		131	**A(2)03-J(2)1**	**27**	**92**	**0**
		230	**D(10)1-2**	**21**	**4**	**0**
		135	**E(2)7-D(2)7**	**17**	**42**	**0**
		83	**A(1)61-J(1)31**	**15**	**75**	**0**
		75	**Q(01)86-A(1)57**	**11**	**4**	**0**
		132	**E(2)5-F(02)4**	**11**	**58**	**0**
		166	**F(03)1-D(3)1**	**9**	**75**	**0**
		81	M(01)21-I(1)21	8	4	0
		201	**Q(5)6-E(5)3**	**8**	**79**	**0**
		165	Q(3)1	3	4	0
		170	A(3)2-Q(3)2	2	4	0
		219	**D(7)1**	2	**21**	**0**
		98	Q(01)92-93	1	8	0
		108	**D(1)48-49**	1	**58**	**0**
		130	**E(2)2-A(2)02**	1	**38**	**0**
		134	A(2)05	1	4	0
		136	Q(2)4	1	4	0
		164	**A(2)10**	1	**13**	**0**
C	Subglacial and Proglacial	**116**	**E(1)34-F(01)40**	**21**	**0**	**6**
	(16 total)	**174**	**H(3)5-Q(3)5**	**17**	**0**	**12**
		47	**K(1)02-C(1)66**	**17**	**0**	**6**
		73	**M(01)13-M(01)15**	**13**	**0**	**29**
		85	**A(1)65-G(1)28**	**12**	**0**	**6**
		59	**A(1)43-A(1)45**	5	**0**	**82**
		123	O(01)47-M(01)29	2	**0**	**6**
		93	O(01)43-D(1)44	2	**0**	**6**
		86	I(1)29	2	**0**	**6**
		45	**Q(01)28-30**	2	**0**	**47**
		40	A(1)31	2	**0**	**6**
		126	**O(1)49-A(1)79**	1	**0**	**12**
		124	**Q(1)100-O(1)48**	1	**0**	**35**
		60	Q(01)70-J(1)28	1	**0**	**6**
		37	**H(1)11-C(1)54**	1	**0**	**12**
		9	**Q(01)3-4**	1	**0**	**12**
D	Supraglacial and Proglacial	**39**	**D(1)05-H(1)12**	**0**	**67**	**6**
	(3 total)	**41**	**A(1)32**	**0**	**13**	**6**
		129	**Q(2)1**	**0**	**4**	**12**
E	Subglacial Only	**202**	**E(5)4-E(5)6**	**58**	**0**	**0**
	(60 total)	**48**	**Q(01)37-G(1)12**	**38**	**0**	**0**
		220	**D(7)2-D(7)3**	**34**	**0**	**0**
		42	**D(1)07-09**	**17**	**0**	**0**
		114	**E(1)33-D(1)55**	**10**	**0**	**0**
		50	**M(01)09-O(01)20**	**10**	**0**	**0**
		205	E(5)7-8	6	**0**	**0**
		197	Q(5)2-F(add1)	4	**0**	**0**
		133	M(02)1	3	**0**	**0**
		120	A(1)77	3	**0**	**0**
		76	Q(01)88-89	3	**0**	**0**
		53	Q(01)46-47	3	**0**	**0**
		206	D(5)5	2	**0**	**0**
		169	A(add6)	2	**0**	**0**
		168	A(3)1	2	**0**	**0**
		158	Q(2)26-A(add2)	2	**0**	**0**
		155	K(2)1-Q(2)24	2	**0**	**0**
		153	Q(add1)	2	**0**	**0**
		125	E(1)38	2	**0**	**0**
		115	A(1)73	2	**0**	**0**
		113	E(1)31-32	2	**0**	**0**
		112	H(1)40-F(01)38	2	**0**	**0**
		110	D(1)50-51	2	**0**	**0**
		94	G(1)29-D(1)47	2	**0**	**0**
		80	D(1)27-29	2	**0**	**0**

CONTINUED

Group No.	Environmental Presence	T-RF No.	T-RF Name	% occurrence in subglacial samples	% occurrence in supraglacial samples	% occurrence in proglacial samples
E (continued)	Subglacial Only (60 total)	78	D(1)25-26	2	0	0
		44	M(01)04-C(1)58	2	0	0
		26	M(01)01	2	0	0
		222	F(08)3	1	0	0
		212	C(add1)	1	0	0
		207	G(5)3	1	0	0
		204	F(add4)	1	0	0
		203	M(05)2	1	0	0
		200	F(add3)	1	0	0
		177	F(03)5	1	0	0
		173	M(03)3	1	0	0
		167	M(03)1	1	0	0
		162	I(2)5	1	0	0
		160	P(2)21-A(2)08	1	0	0
		148	Q(2)9-A(add4)	1	0	0
		137	M(02)2	1	0	0
		121	I(1)35	1	0	0
		117	D(1)59-I(1)33	1	0	0
		111	D(1)52	1	0	0
		106	M(01)28	1	0	0
		105	M(01)27	1	0	0
		101	M(01)26	1	0	0
		100	Q(01)94	1	0	0
		97	M(01)25	1	0	0
		95	G(add1)	1	0	0
		92	M(01)23	1	0	0
		79	M(01)20	1	0	0
		71	A(1)51	1	0	0
		67	M(01)11	1	0	0
		64	A(1)47-Q(01)78	1	0	0
		62	Q(1)75-F(01)19	1	0	0
		55	F(01)08-Q(01)53	1	0	0
		35	H(1)10	1	0	0
		33	Q(01)24	1	0	0
		32	M(01)02	1	0	0
F	Supraglacial Only (12 total)	**29**	**E(1)03-H(1)09**	0	**75**	0
		96	**E(1)30-D(1)47**	0	**63**	0
		30	**A(1)26**	0	**13**	0
		109	**A(1)68**	0	**13**	0
		192	**D(4)1-Q(4)4**	0	**13**	0
		77	Q(01)90	0	8	0
		28	E(1)02	0	4	0
		99	A(1)67	0	4	0
		104	K(1)11	0	4	0
		198	F(add2)-Q(5)5	0	4	0
		213	F(05)11	0	4	0
		214	F(06)3	0	4	0
G	Proglacial Only (23 total)	**89**	**O(01)37-39**	0	0	**59**
		68	**O(01)28-29**	0	0	**53**
		138	**O(2)4-5**	0	0	**53**
		88	**O(01)35-36**	0	0	**47**
		90	**O(01)40-41**	0	0	**24**
		91	**O(01)42-I(1)31**	0	0	**18**
		16	**C(1)11-A(1)21**	0	0	**12**
		18	**Q(01)15**	0	0	**12**
		54	**F(01)07-Q(01)51**	0	0	**12**
		66	**A(1)48-Q(1)81**	0	0	**12**
		3	A(1)05-08	0	0	6
		5	A(1)10	0	0	6
		6	A(1)11	0	0	6
		7	A(1)12	0	0	6
		31	A(1)27	0	0	6
		34	A(1)28	0	0	6
		36	A(1)29	0	0	6
		38	A(1)30	0	0	6
		52	A(1)40-Q(01)45	0	0	6
		69	A(1)49	0	0	6
		70	A(1)50	0	0	6
		87	A(1)66	0	0	6
		175	Q(3)6-8	0	0	6

Table 3.4. Summary of the presence and distribution of 142 *Hae*III T-RFs resolved at JEG by T-RFLP analysis.

T-RF summary information	Subglacial Samples	Supraglacial Samples	Proglacial Samples
No. of T-RFs present	104	43	50
No. of unique T-RFs[a]	60	12	23
No. of widespread T-RFs[b]	25	23	23
No. of unique and widespread T-RFs[c]	6	5	10
No. of T-RFs shared with subglacial only	---[d]	20	16
No. of T-RFs shared with supraglacial only	20	---	3
No. of T-RFs shared with proglacial only	16	3	---

[a] found in only the cognate environment
[b] present in >10% of all samples within that environment
[c] found only in the cognate environment, but in > 10% of the samples in that environment
[d] ---, not applicable

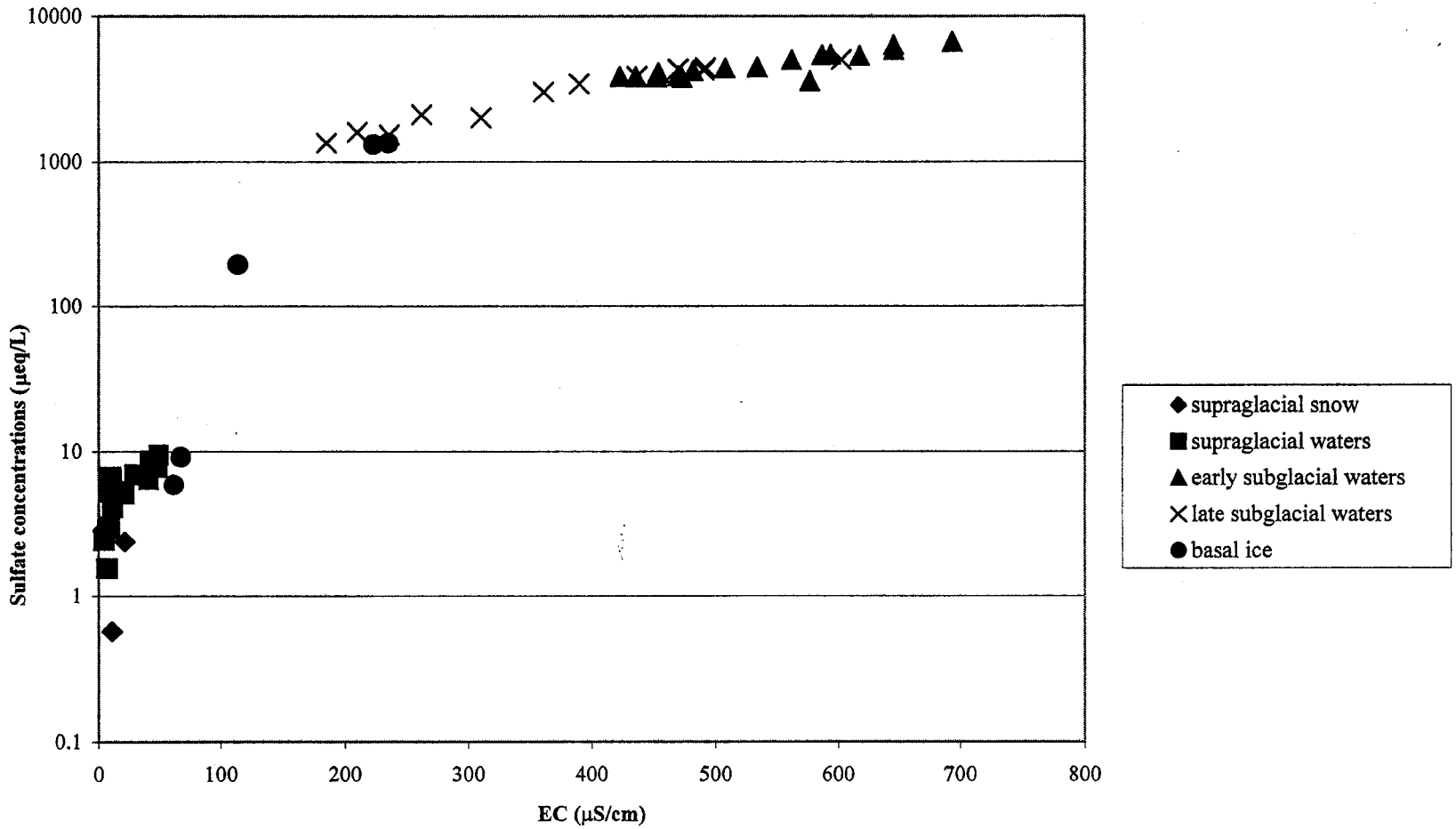

Figure 3.1. Relationship between EC and sulfate values in samples collected at JEG from May - August 2002. Three supraglacial wet snow samples, 16 supraglacial stream (SP-IS-a, SP-MLS-a, SP-ML-a, SP-IS-b, and SP-MLS-b) samples, 17 early subglacial water (SB-IB 6/30/02 19:00 h - 7/1/02 14:30 h, and S-AF 7/1/02 12:30 h and 14:30 h) samples, 13 late subglacial water samples (SB-AF, SB-OC, and SB-IB 6/30/02 23:00 h, 24:00 h), and five basal ice samples (B-S, B-C, and B-F) were analyzed.

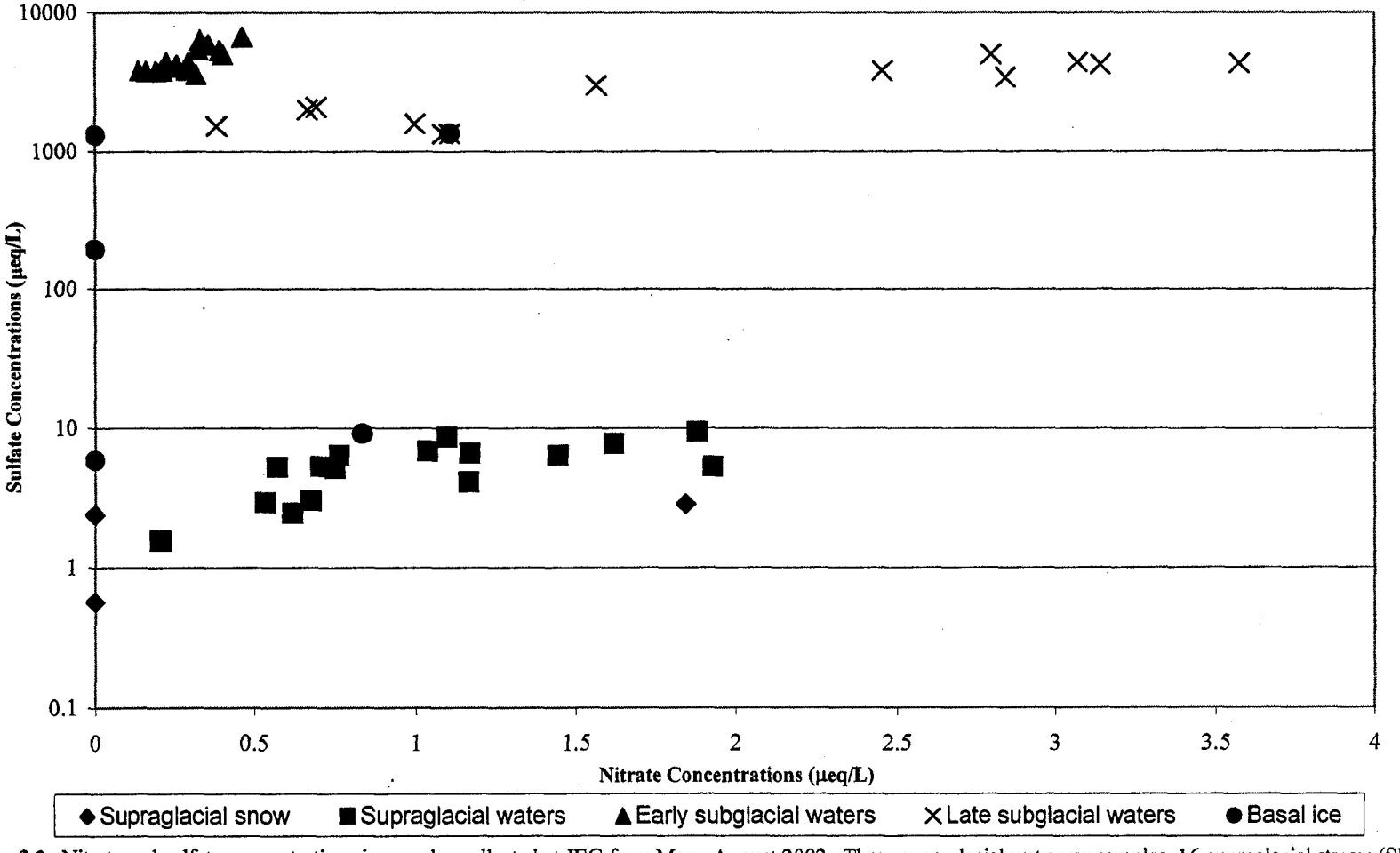

Figure 3.2. Nitrate and sulfate concentrations in samples collected at JEG from May - August 2002. Three supraglacial wet snow samples, 16 supraglacial stream (SP-IS-a, SP-MLS-a, SP-ML-a, SP-IS-b, and SP-MLS-b) samples, 17 early subglacial water (SB-IB 6/30/02 19:00 h - 7/1/02 14:30 h, and S-AF 7/1/02 12:30 h and 14:30 h) samples, 13 late subglacial water samples (SB-AF, SB-OC, and SB-IB 6/30/02 23:00 h, 24:00 h), and five basal ice samples (B-S, B-C, and B-F) were analyzed.

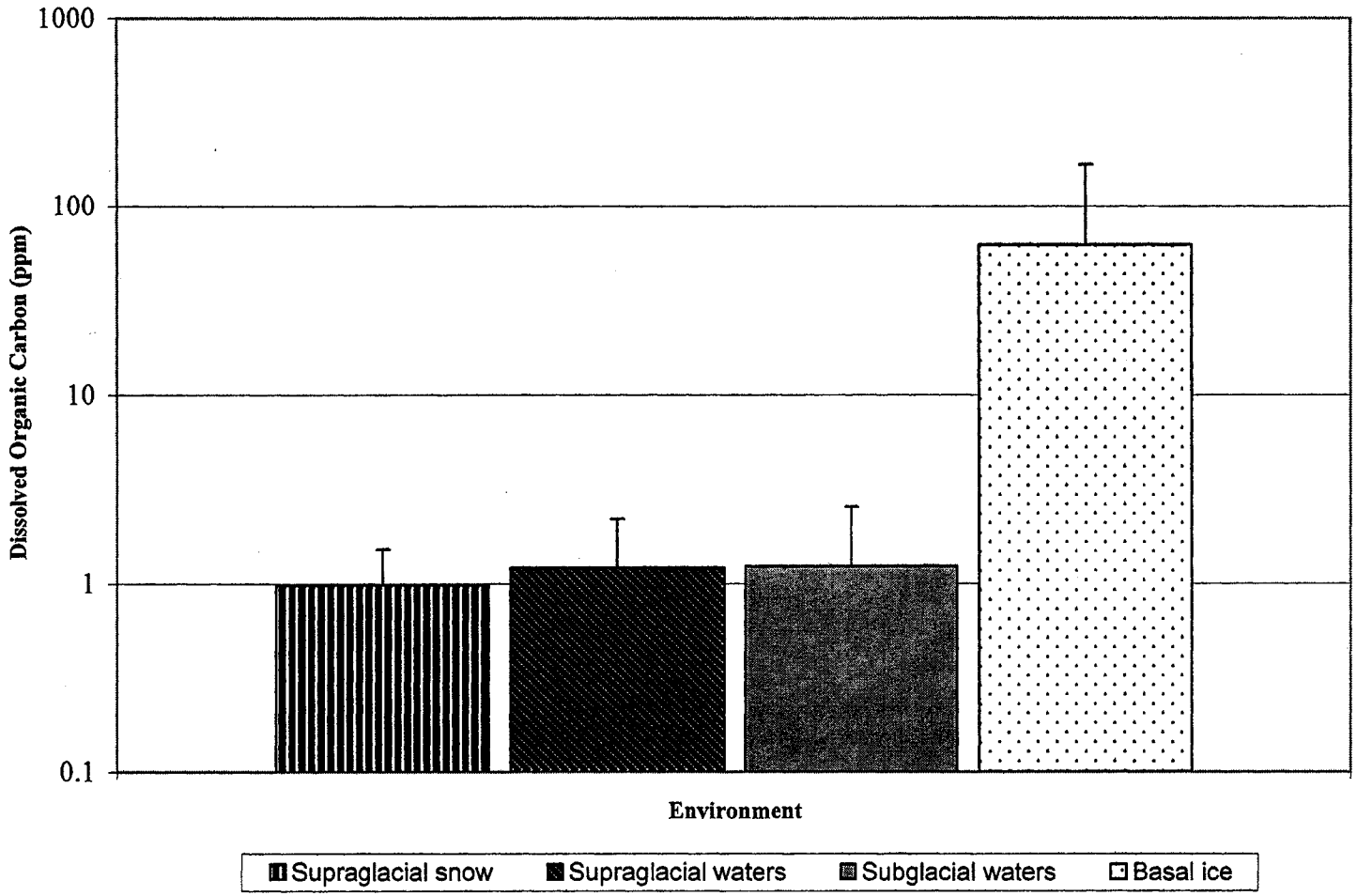

Figure 3.3. DOC concentrations (ppm) in samples collected at JEG from May - August 2002. Three supraglacial wet snow samples, 11 supraglacial stream (SP-IS-a, SP-MLS-a, and SP-MLS-b) samples, nine subglacial water (SB-IB, SB-AF, and SB-OC) samples, and five basal ice (B-S, B-F, and B-C) samples were analyzed.

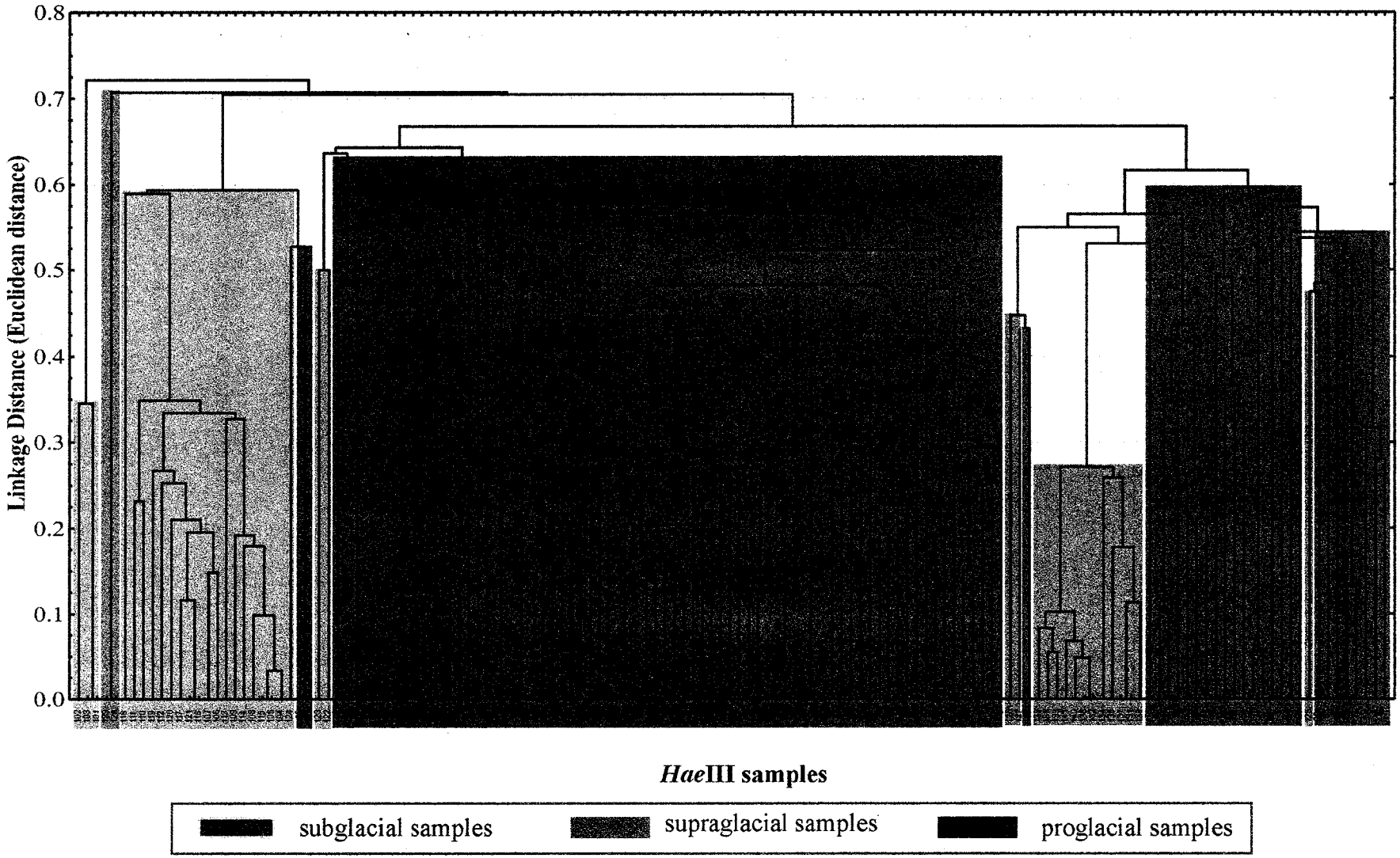

Figure 3.4. Dendrogram illustrating inter-environmental T-RF variability at JEG based on cluster analysis of all subglacial, supraglacial, and proglacial samples digested with the *Hae*III enzyme. Cluster analysis was based on the principal component analysis (PCA) factor loadings of each sample on the new variables defined by PCA.

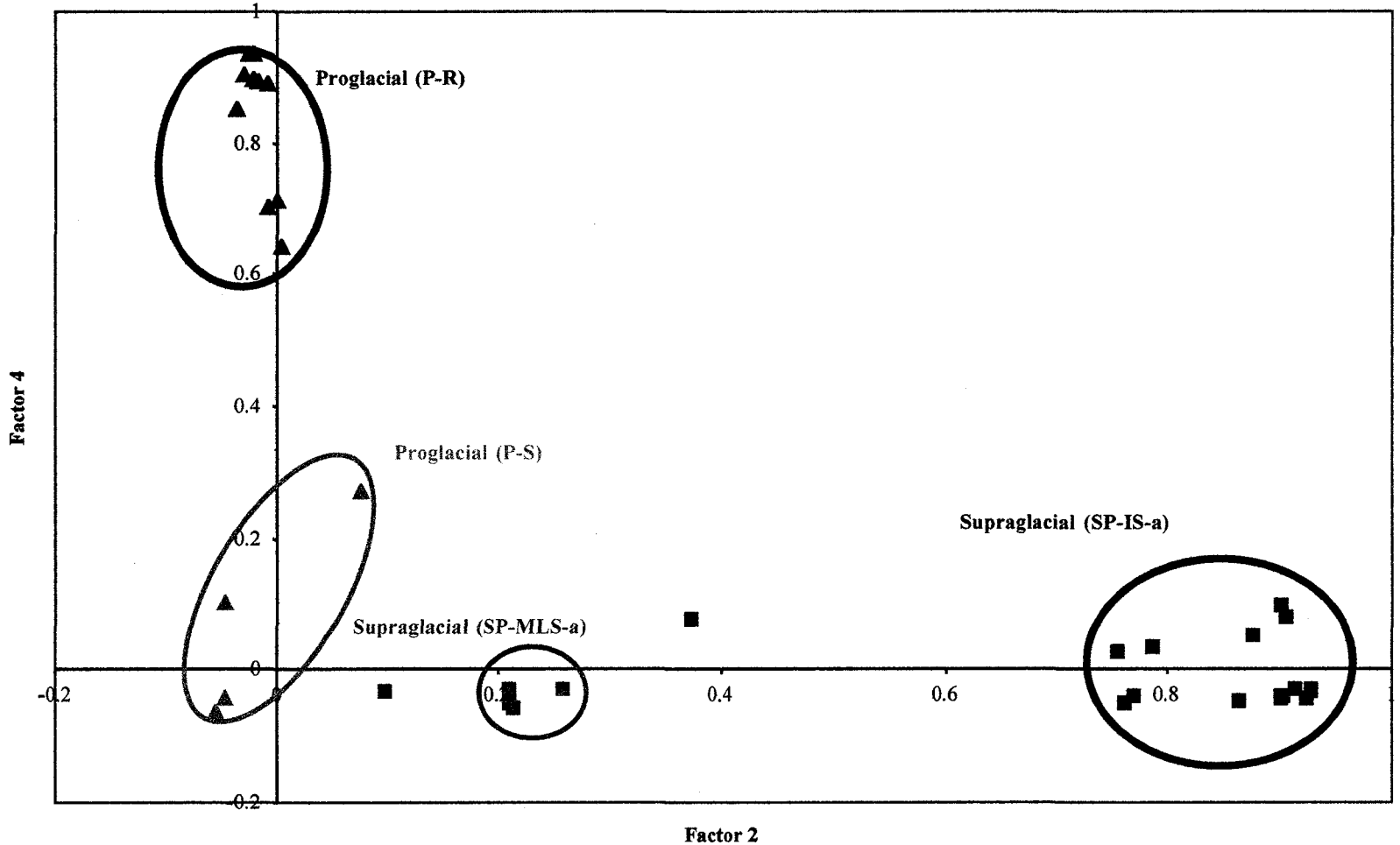

Figure 3.5. Scatter plot of the supraglacial and proglacial sample factor loadings on factors 2 and 4 from PCA analysis, illustrates that each type of supraglacial sample (SP-IS-a and SP-MLS-a) is distinct from each type of proglacial sample (P-R and P-S). Supraglacial samples are presented in dark blue (SP-IS-a) and light blue (SP-MLS-a). Proglacial samples are presented in red (P-R) and orange (P-S).

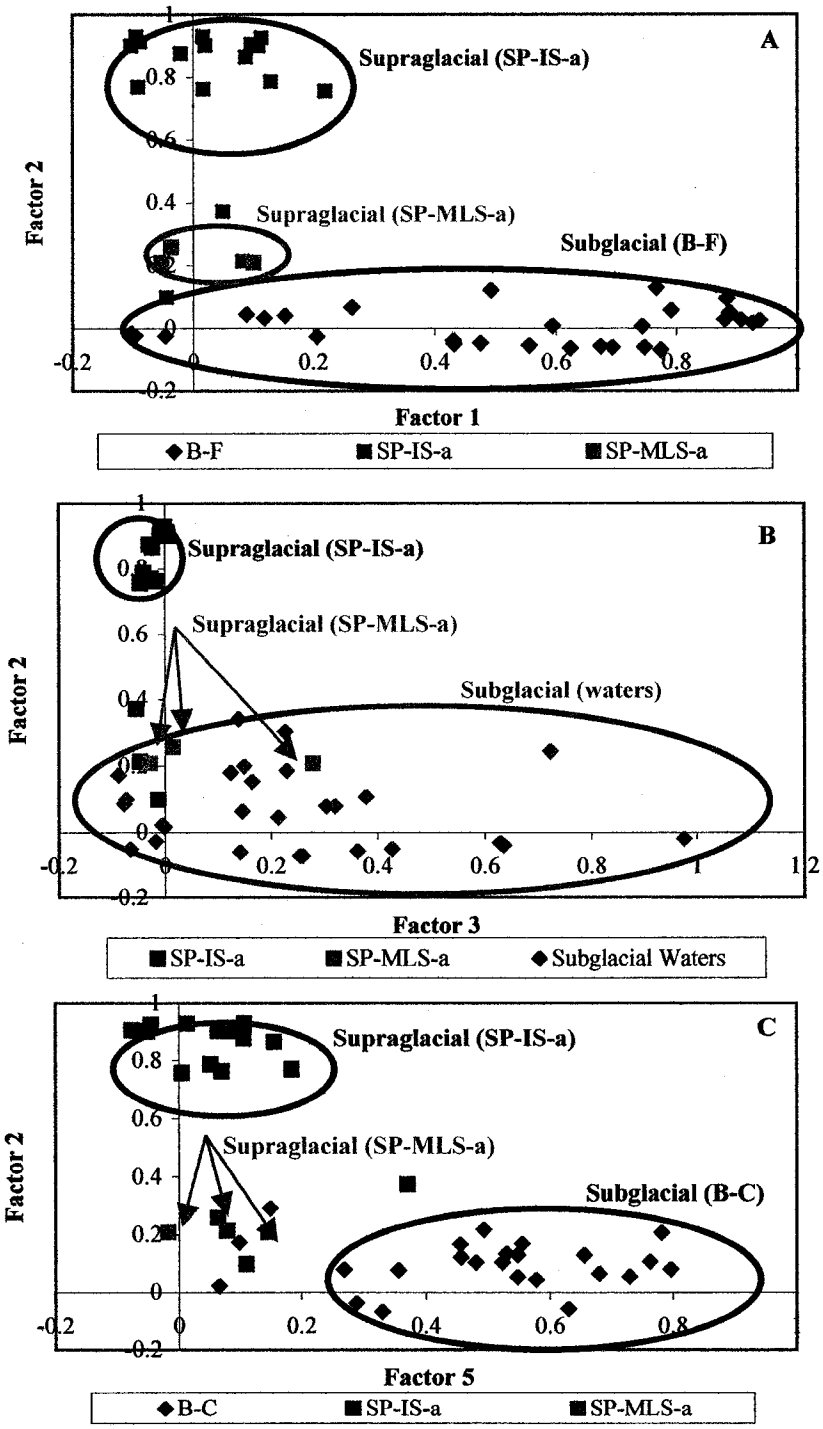

Figure 3.6. Scatter plots of subglacial and supraglacial sample factor loadings from PCA analysis. Panel A, factors 1 and 2, illustrates that the supraglacial samples are distinct from the basal ice Fox Junction (B-F) samples. Panel B, factors 3 and 2, illustrates that the supraglacial samples are distinct from the subglacial water samples. Panel C, factors 5 and 2, illustrates that the supraglacial samples are distinct from the basal ice cave (B-C) samples.

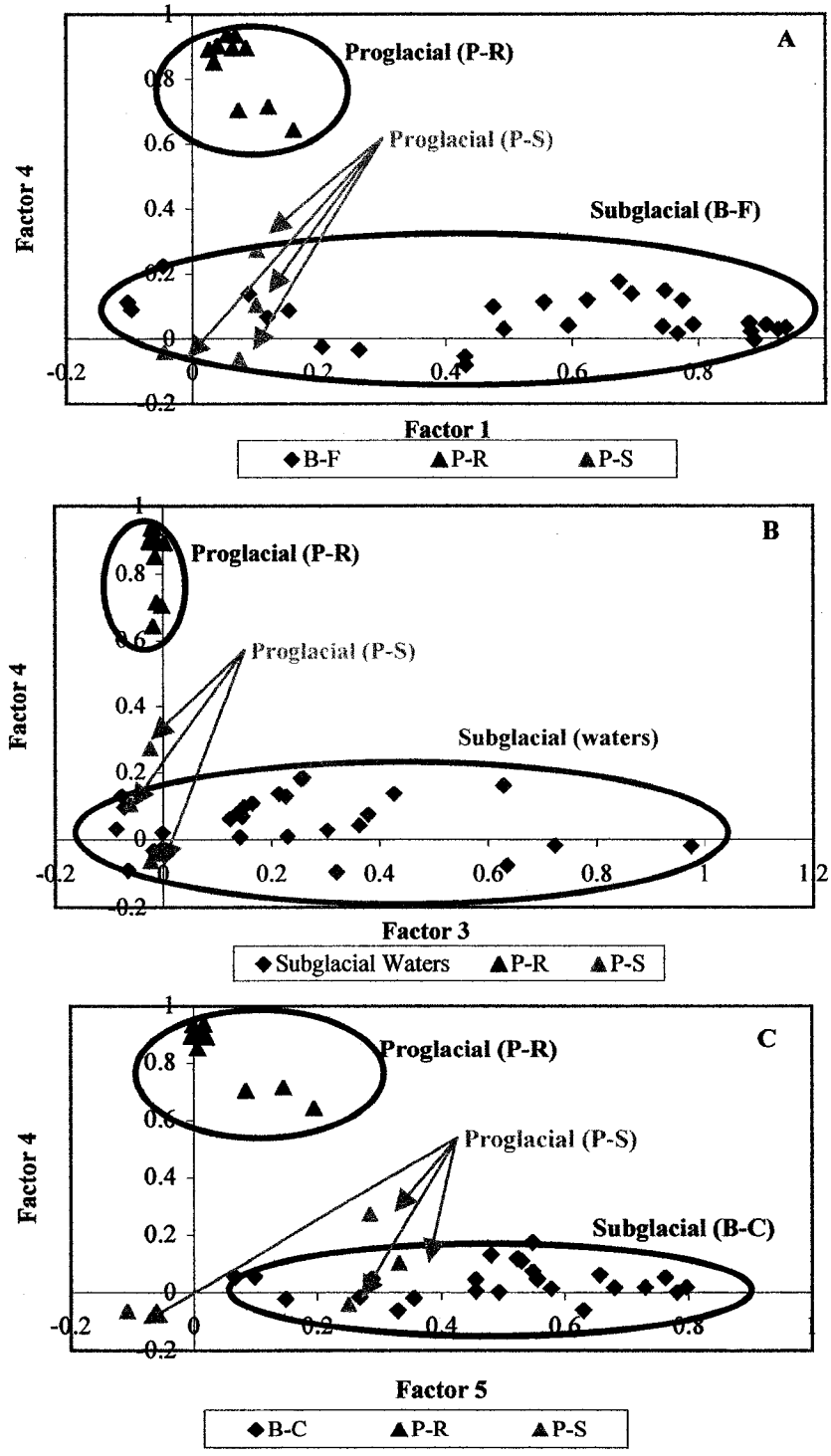

Figure 3.7. Scatter plots of subglacial and proglacial sample factor loadings from PCA analysis. Panel A, factors 1 and 4, illustrates that the proglacial samples are distinct from the basal ice Fox Junction (B-F) samples. Panel B, factors 3 and 4, illustrates that the proglacial samples are distinct from the subglacial water samples. Panel C, factors 5 and 4, illustrates that the proglacial samples are distinct from the basal ice cave (B-C) samples.

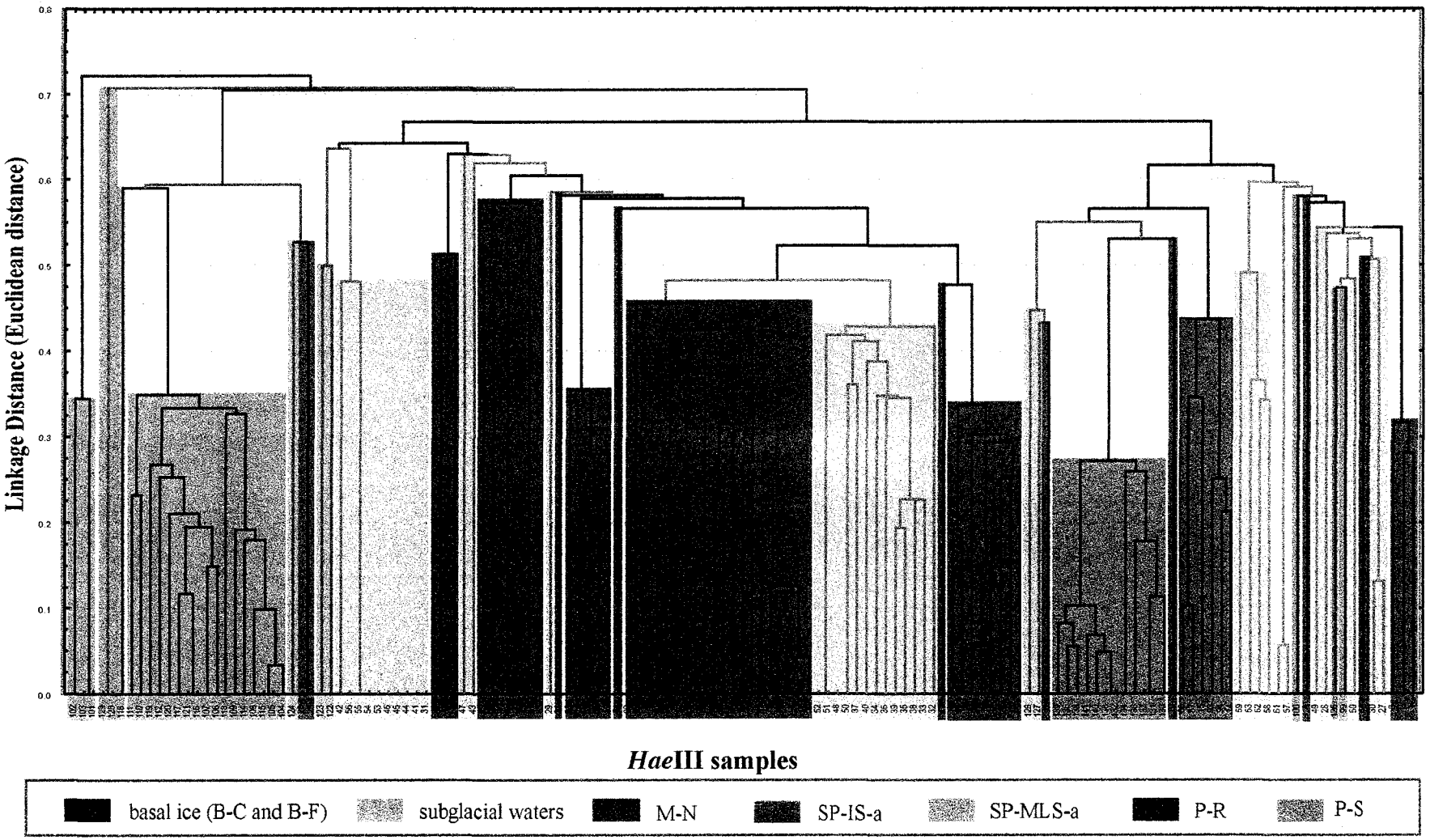

Figure 3.8. Dendrogram illustrating intra-environmental T-RF variability at JEG based on cluster analysis of all subglacial, supraglacial, and proglacial samples digested with the *Hae*III enzyme. Cluster analysis was based on the principal component analysis (PCA) factor loadings of each sample on the new variables defined by PCA. The basal ice, subglacial waters, and M-N samples are from the subglacial environment. The SP-IS-a and SP-MLS-a samples are from the supraglacial environment. The P-R and P-S samples are from the proglacial environment.

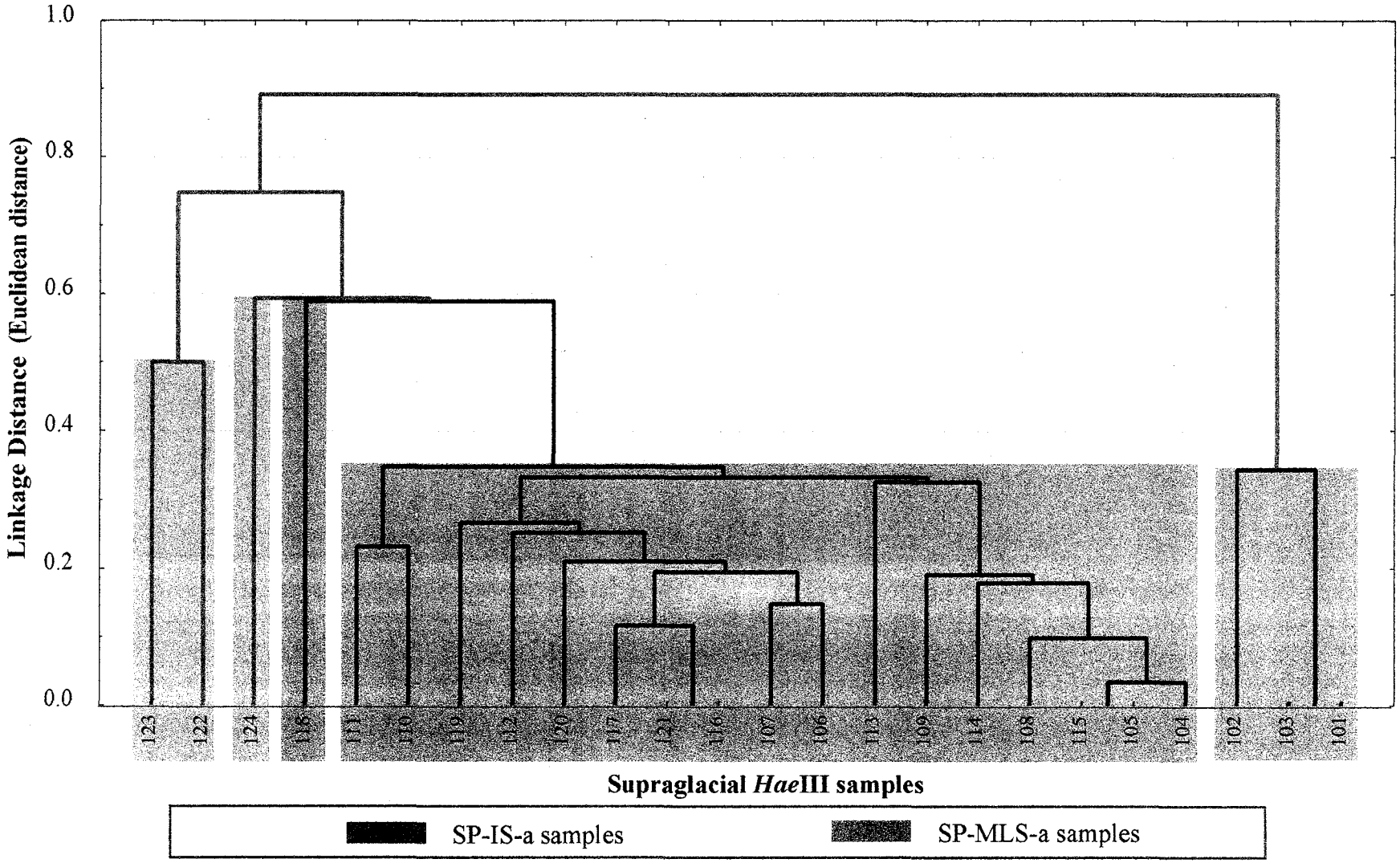

Figure 3.9. Dendrogram illustrating intra-environmental T-RF variability within the supraglacial environment at JEG between the SP-IS-a and SP-MLS-a sample sites. The dendrogram was created using cluster analysis of all subglacial, supraglacial, and proglacial samples digested with the *Hae*III enzyme, but only the supraglacial samples are presented. Cluster analysis was based on the principal component analysis (PCA) factor loadings of each sample on the new variables defined by PCA.

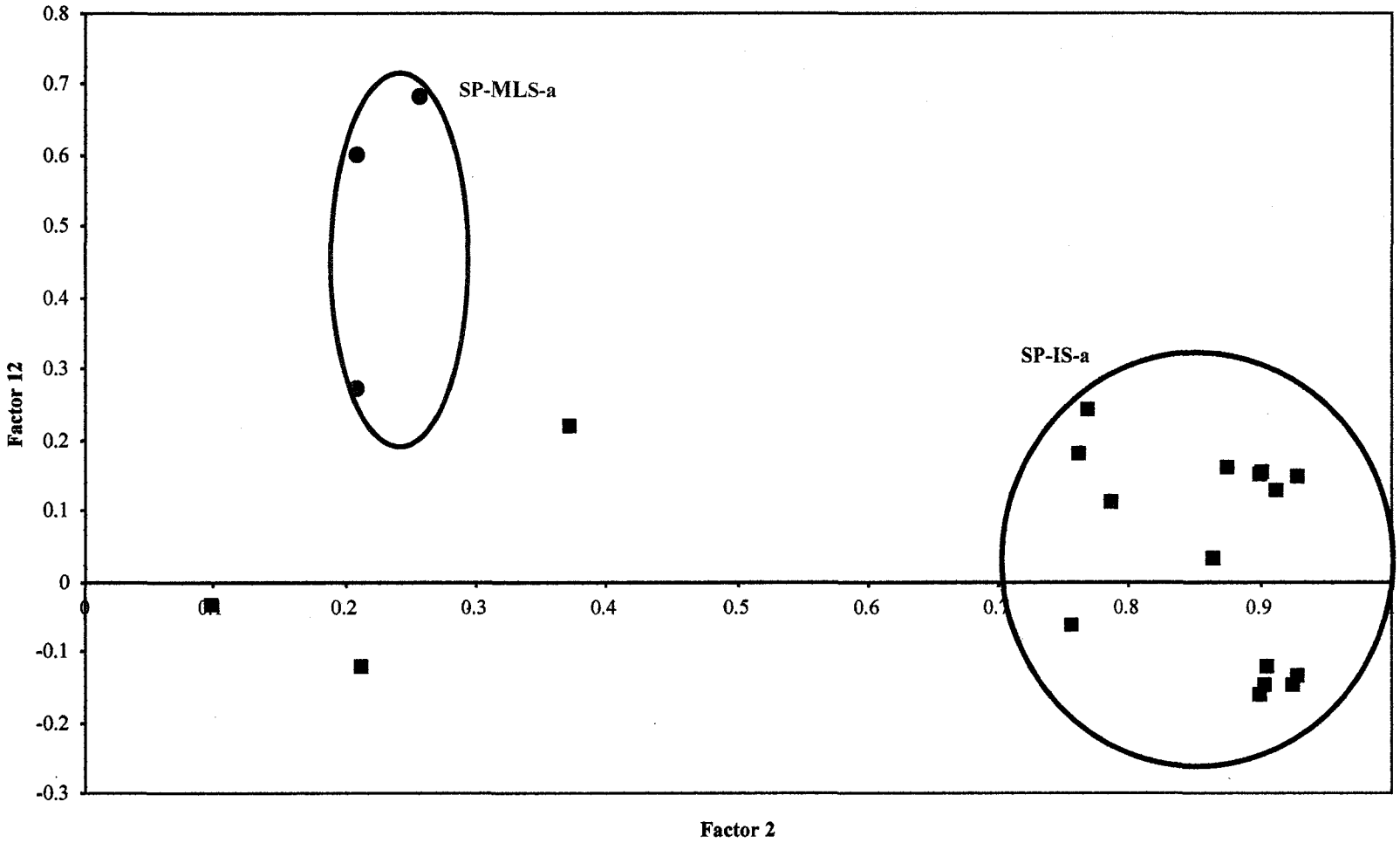

Figure 3.10. Scatter plot of the supraglacial sample factor loadings on factors 2 and 12 from PCA analysis, illustrates that the SP-MLS-a samples and SP-IS-a samples are distinct. The SP-IS-a samples are presented in dark blue, and the SP-MLS-a samples are presented in light blue.

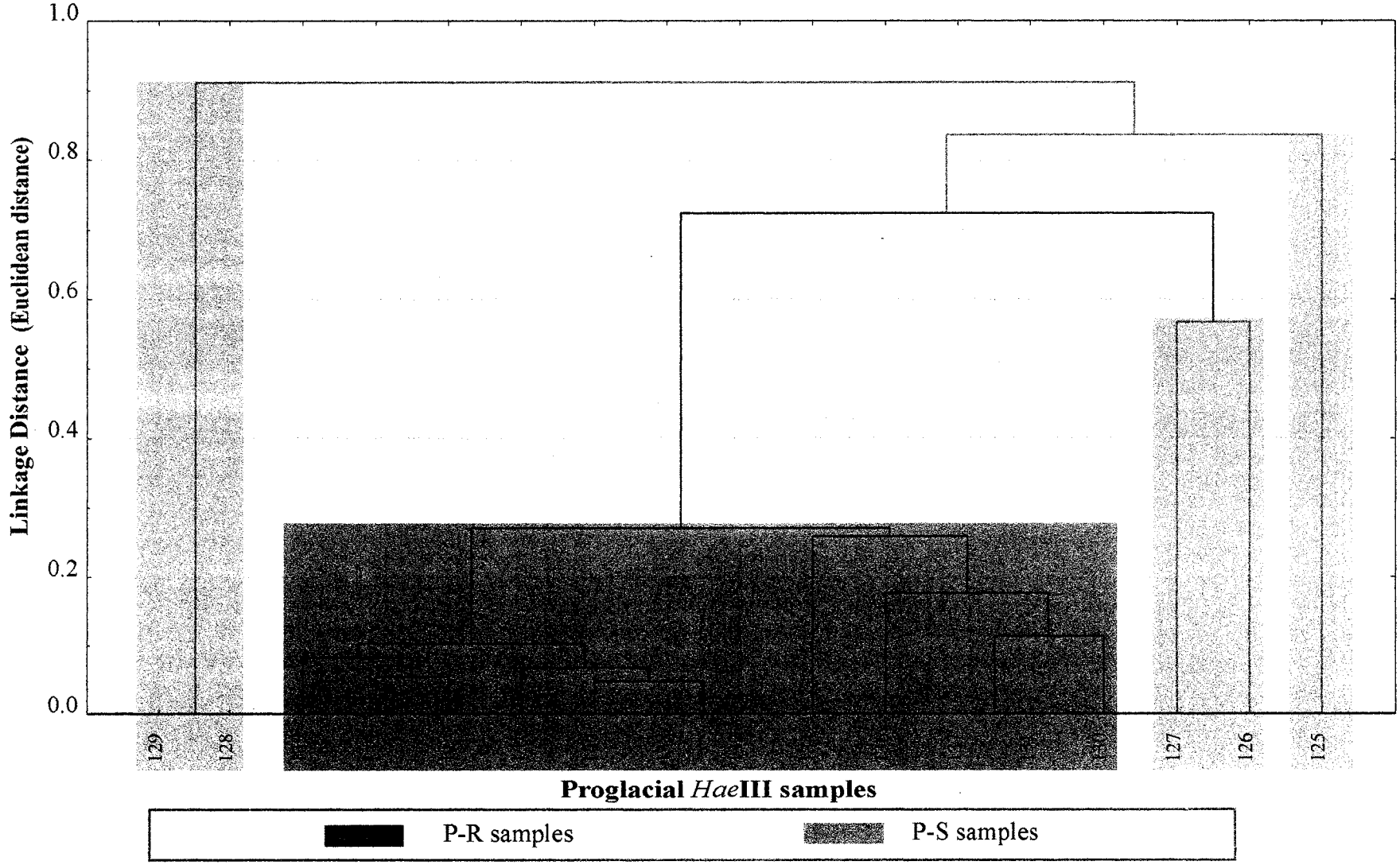

Figure 3.11. Dendrogram illustrating intra-environmental T-RF variability within the proglacial environment at JEG between the P-R and P-S sample sites. The dendrogram was created using cluster analysis of all subglacial, supraglacial, and proglacial samples digested with the *Hae*III enzyme, but only the proglacial samples are presented. Cluster analysis was based on the principal component analysis (PCA) factor loadings of each sample on the new variables defined by PCA.

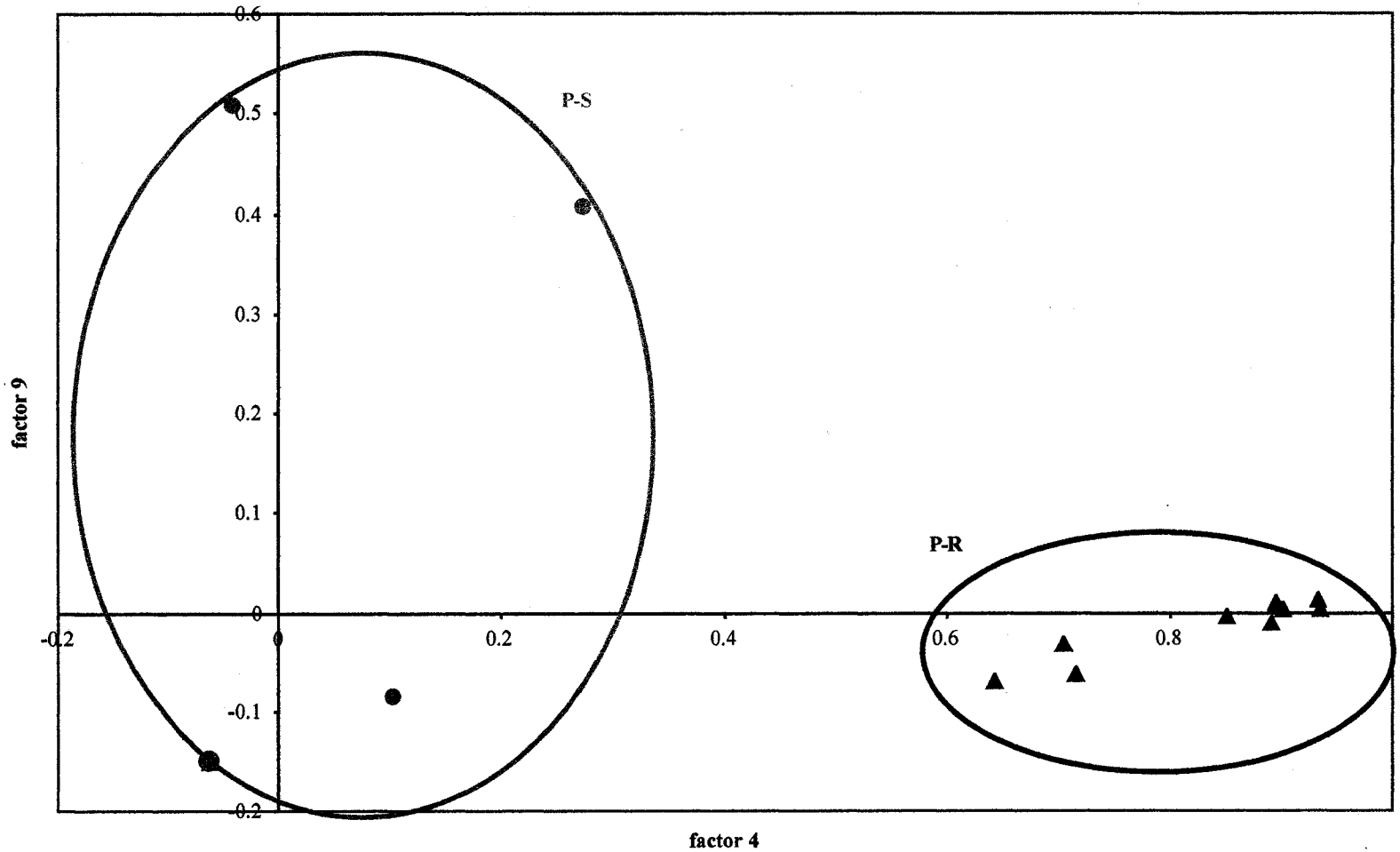

Figure 3.12. Scatter plot of the proglacial sample factor loadings on factors 4 and 9 from PCA analysis, illustrates that the P-R samples and P-S samples are distinct. The P-R samples are presented in red and the P-S samples are presented in orange.

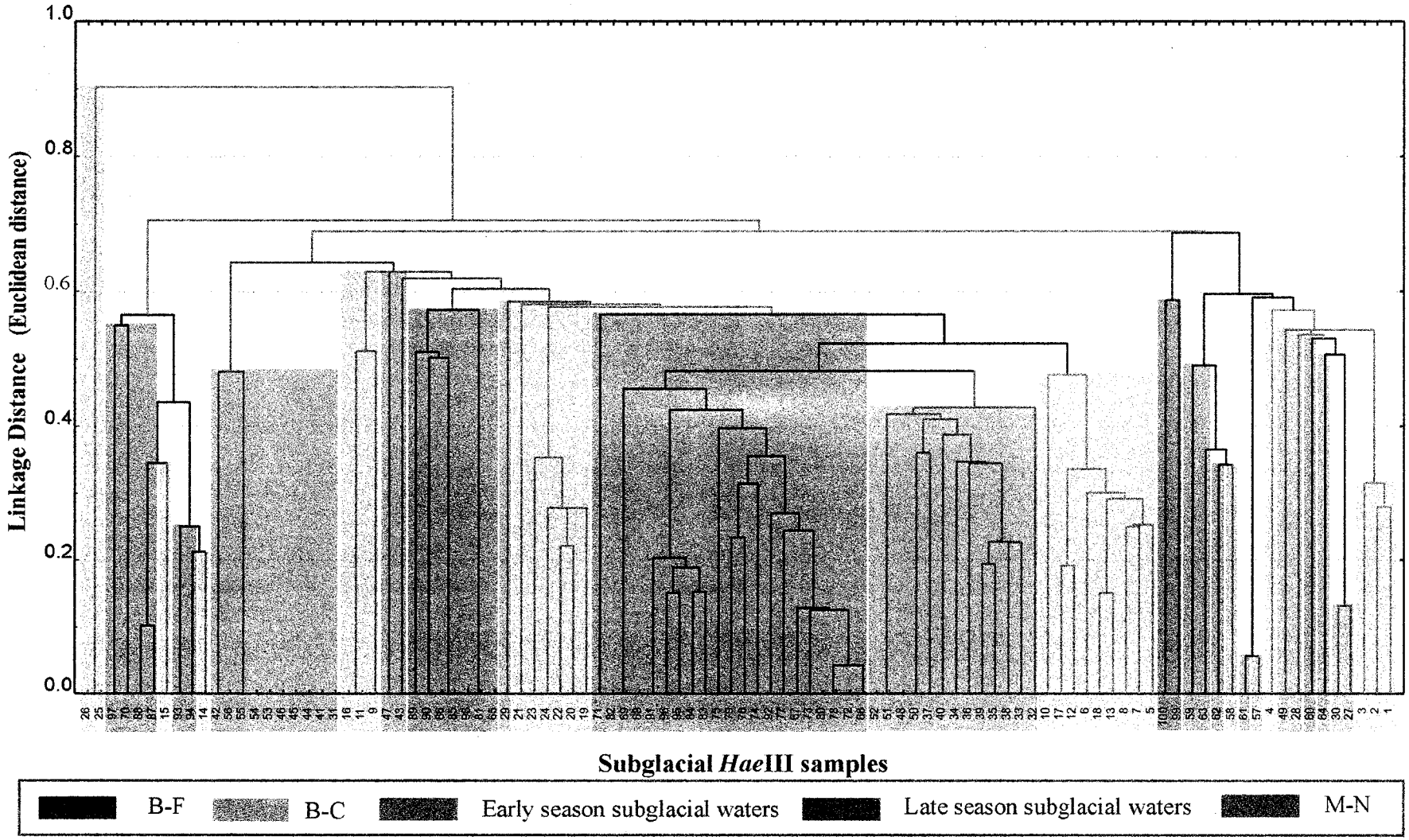

Figure 3.13. Dendrogram illustrating intra-environmental T-RF variability within the subglacial environment at JEG between the different sub-environments (basal ice and subglacial waters) and among the different sample sites (B-C and B-F and the early and late season subglacial waters). The dendrogram was created using cluster analysis of all subglacial, supraglacial, and proglacial samples digested with the *Hae*III enzyme, but only the subglacial samples are presented. Cluster analysis was based on the principal component analysis (PCA) factor loadings of each sample on the new variables defined by PCA.

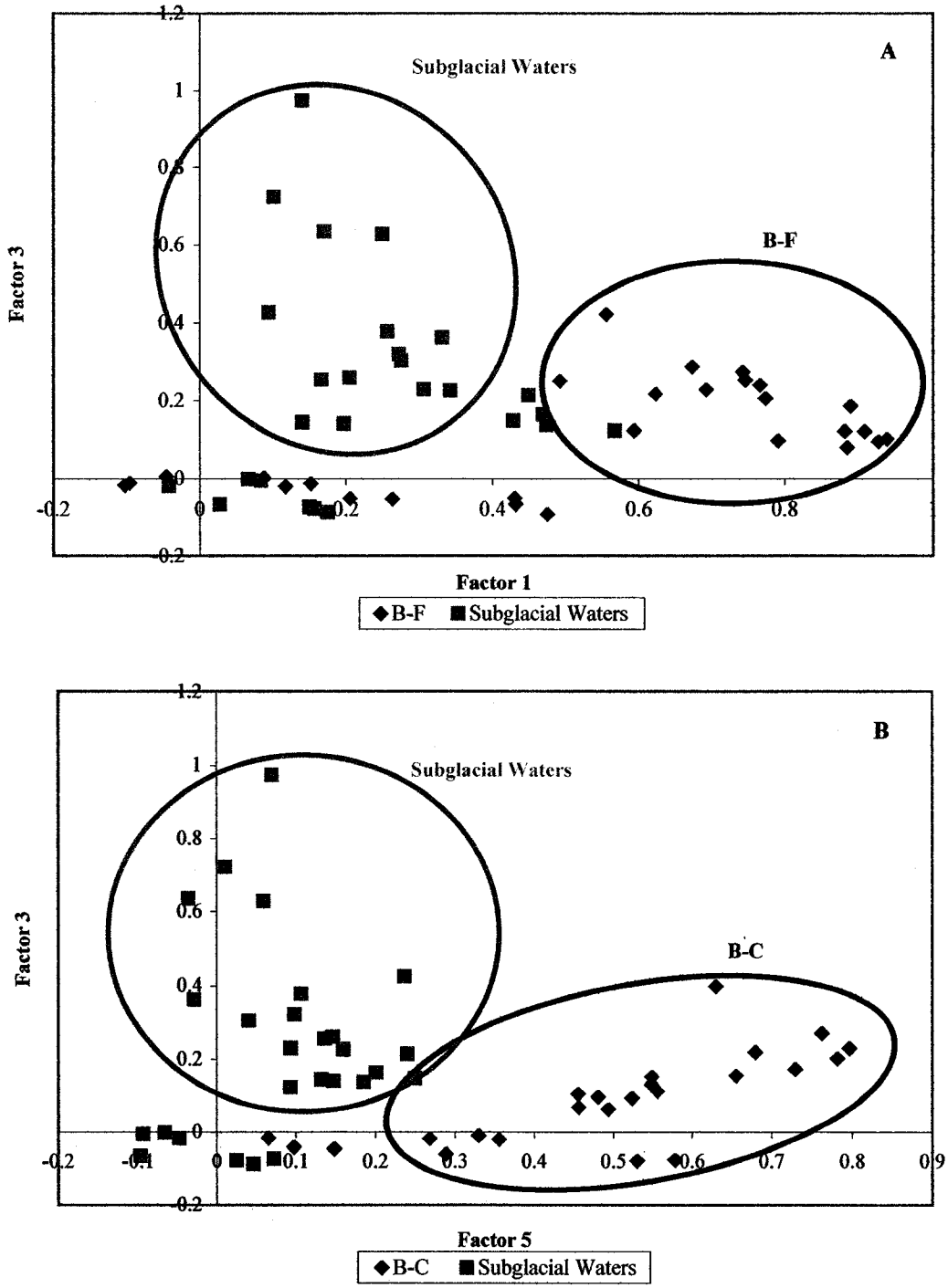

Figure 3.14. Scatter plots of the subglacial sample factor loadings from PCA analysis. Panel A, factors 1 and 3, illustrates that the majority of the subglacial waters and basal ice Fox Junction (B-F) samples are distinct. Panel B, factors 5 and 3, illustrates that the majority of the subglacial waters and basal ice cave (B-C) samples are distinct.

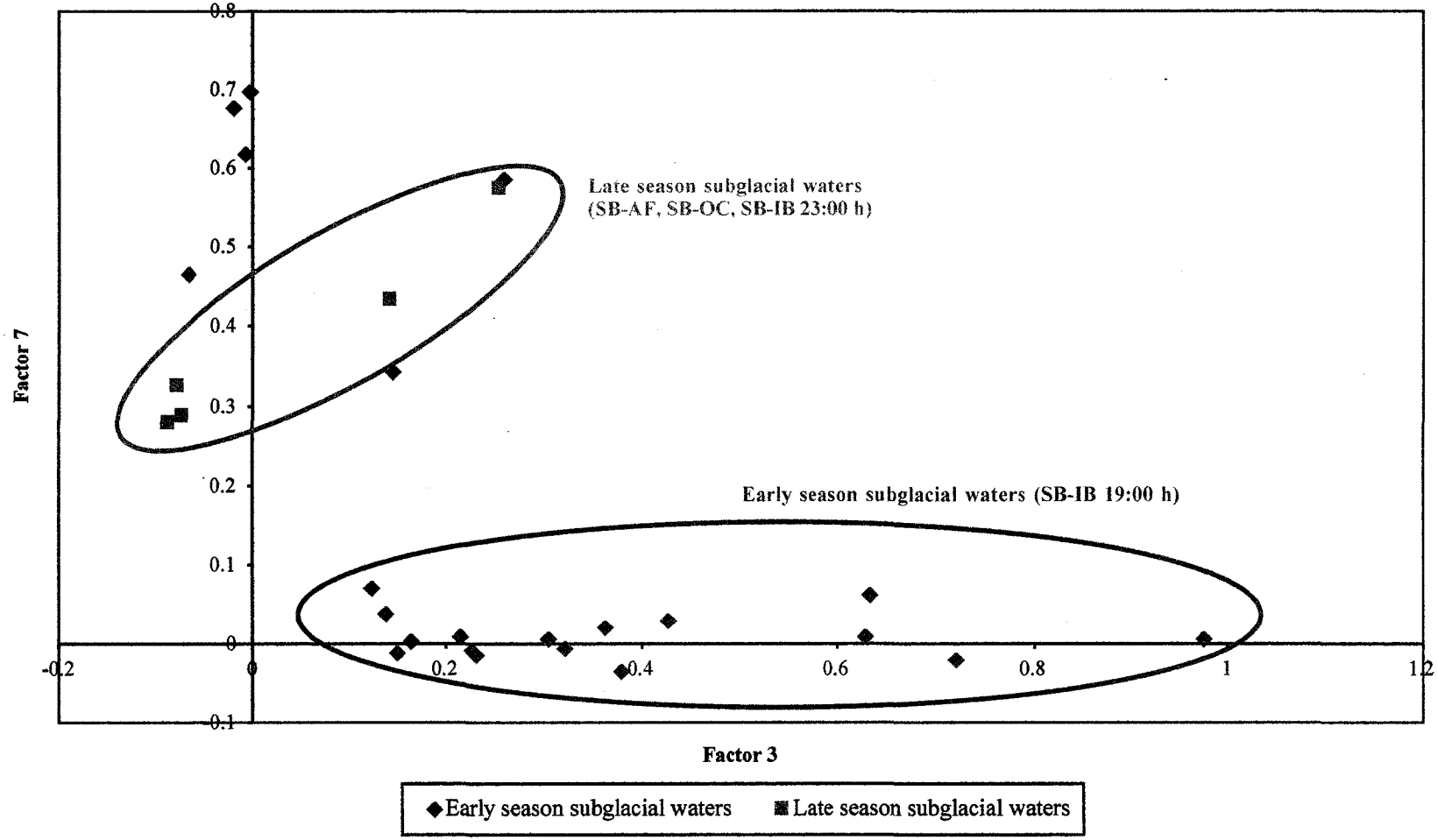

Figure 3.15. Scatter plot of the subglacial water sample factor loadings on factors 3 and 7 from PCA analysis, illustrates that the majority of the early season nitrate depleted subglacial water (SB-IB) samples are distinct from the late season nitrate enriched subglacial water (SB-IB 23:00 h, SB AF, and SB-OC) samples.

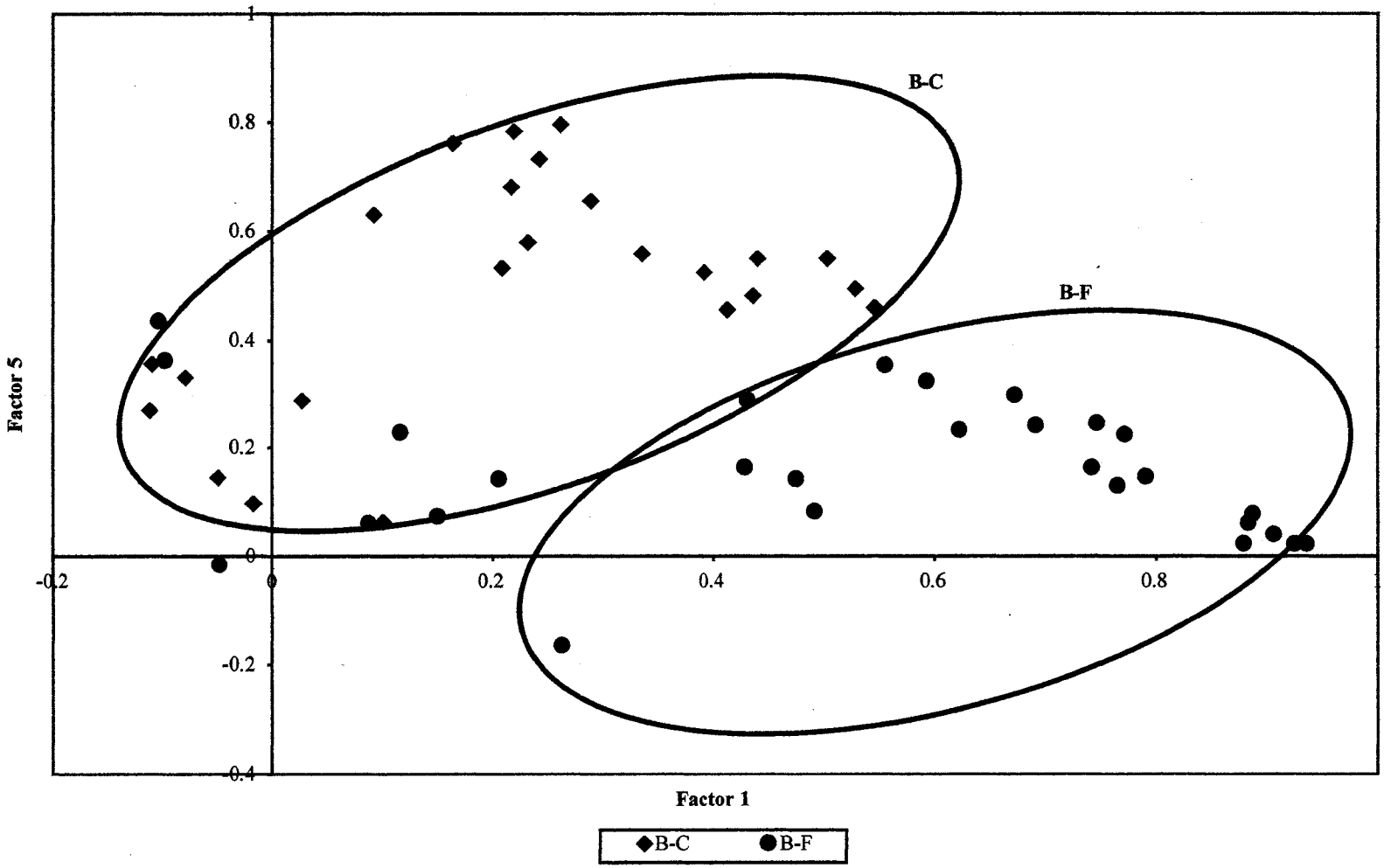

Figure 3.16. Scatter plot of the basal ice sample factor loadings on factors 1 and 5 from PCA analysis, illustrates that though there is some overlap, the majority of the basal ice cave (B-C) samples are distinct from the basal ice fox junction (B-F) samples.

Chapter 4. Discussion

T-RFLP analysis of the bacterial communities found in these glacier environments demonstrated that the T-RF patterns are distinct on inter- and intra-environmental levels, suggesting a heterogeneous distribution of bacteria at JEG. Thus, the T-RFLP and corresponding statistical analyses appeared to be sensitive enough to detect some significant results, despite the inherent limitations and biases within the experimental design of this study. It is likely that the environmental differences among the primary environments and sub-environments, result in a heterogeneous distribution of nutrients and bacteria and the existence of a unique subglacial bacterial component at JEG. The limitations and biases within the molecular techniques used and the experimental design of the study are also discussed. Finally, this chapter concludes by discussing the possible mechanisms by which the subglacial community at JEG may have become established.

4.1. Inter-environmental community differences

The inter-environmental community differences between the subglacial, supraglacial, and proglacial environments may result from differences in energy sources, nutrient availability, and environmental stresses. In terms of energy sources, only the supraglacial environment should contain obligate phototrophs, whereas the subglacial and subsurface proglacial environments should harbour heterotrophs and, potentially, strict chemotrophs. Nutrient localization in the subglacial environment may result in spatial heterogeneity with microenvironments favorable to bacterial colonization, interspersed with oligotrophic macroenvironments. The subglacial environment may also support a more diverse community than that found on the glacier surface because it is protected from extreme temperature fluctuations and freeze-thaw cycles, and likely possesses some anaerobic microhabitats. Thus, specific environmental microcosms may be present at JEG that provide unique bacterial niches based on a temporal scale ("hot moments")

activated by seasonal hydrology, or a spatial scale ("hot spots") as a result of energy or nutrient localization.

4.1.1. Energy Sources

Previous investigations of microbial consortia found in other cold surface environments have identified sunlight as the most obvious and readily available energy source (Carpenter *et al.*, 2000; Grannas and Shepson, 2004; Hoham and Duval, 2004; Tranter *et al.*, 2004). A similar situation would be expected at JEG where the supraglacial communities would depend on photosynthesis to provide energy for growth and therefore should consist mainly of phototrophs that serve as the primary producers for any prokaryotic and eukaryotic heterotrophs. Thus, microbial consortia previously found in glacial meltholes (cryoconites) may resemble the communities present on the surface of JEG. Studies of cryoconite holes on Canada Glacier (Taylor Valley, Antarctica) and White Glacier (Axel Heiberg Island, Canada) discovered simple food webs with microbial photoautotrophs (cyanobacteria, chlorophytes) and heterotrophs (heterotrophic cyanobacteria, tardigrades, and rotifers) (Vincent 1988; Mueller *et al.*, 2001; Tranter *et al.*, 2004). The presence of eukaryotes in JEG supraglacial environments was not addressed in this study.

Conversely, while the communities present in the subglacial and proglacial environments are probably based indirectly on photosynthetic products, these environments have the potential to contain strictly chemotrophic (non-light-requiring) microbes (Siegret *et al.*, 2001). In the subglacial environment, photosynthetic products and biomass may be washed in by the supraglacial meltwaters; similarly, in the proglacial environment photosynthetic products and biomass may percolate down from the surface vegetation layers. Thus, the subglacial bacterial communities should not contain any obligate phototrophs, but would presumably be dominated by heterotrophs (cheomorganotrophs), and possibly also contain some chemoautotrophs (chemolithotrophs). Chemotrophic metabolic types that may be present include nitrate-, sulfate-,

and iron-reducing Bacteria, fermentative microbes, and methanogenic Archaea (Skidmore *et al.*, 2000). Chemotrophy based on sulfide oxidation is also possible, as was discovered at the deep-sea hydrothermal vents (Madigan et al., 2003).

4.1.2. Nutrients

All biological life requires carbon, hydrogen, oxygen, nitrogen, sulfur, and phosphorus, among other trace elements, like iron. At JEG, these nutrients may be released during weathering of the bedrock or sediments or derived from airborne deposition on the surface. Greater rock:water interaction in the subglacial environment compared to the supraglacial environment results in greater solute and suspended sediment concentrations in the subglacial samples (Skidmore *et al.*, 2000). This contrasts with the glacial surface, where atmospheric deposition is probably the primary solute source (Tranter *et al.*, 1993; Toom-Sauntry and Barrie, 2002; Lyons *et al.*, 2003). Thus the subglacial environment is likely a more favorable habitat for microbial growth and diversity than the supraglacial environment where the bacteria are likely to be more nutrient-limited. Previous studies in glacial and other cold environments indicate that microbial activity is positively correlated with sediment concentrations (Sharp *et al.*, 1999; Skidmore *et al.*, 2000; Sheridan *et al.*, 2003; Foght *et al.*, 2004). However, it is unclear whether the microbial communities are physically attached to the fine-grained sediments and debris-rich basal ice. The sediment may therefore serve as a source of nutrients (reduced minerals or OC) and/or as a physical substratum for microbial growth (Sharp *et al.*, 1999; Skidmore *et al.*, 2000).

The subglacial environment may receive supraglacially-derived inputs of nutrients, such as fixed nitrogen, low levels of dissolved gases (especially molecular oxygen and carbon dioxide), and organic particles (airborne material and material derived from microbial mats in supraglacial channels and cryoconites), which can be used by microbes for metabolic processes (Sharp *et al.*, 1999). Although the nutrient concentrations in the supraglacial snow and ice are low, they are still significant because the input is seasonal and short-lived, and the subglacial

communities may become nutrient limited over winter. Surface melting may provide nitrate and ammonium, whereas rock weathering by subglacially routed meltwaters may provide a source of iron (Sharp *et al.,* 1999). Additionally, inorganic sulfide oxidation at the glacier bed produces iron hydroxides, which provide a colloidal iron supply (Sharp *et al.,* 1999). Sulfur is readily available in the subglacial environment at JEG from the dissolution of the gypsum/anhydrite base and the subsequent release of sulfate (Skidmore *et al.,* 2000). Sulfate and methane sulphonate are also available in the snow, and pyrite is present within the carbonates.

It should be noted that phosphate has never been detected in the meltwaters at JEG (Skidmore, 2001) and is probably not readily available from rock sources given that there is no apatite at JEG (the usual source of geologically derived phosphate) (Kerr, 1972). The few plants found in the proglacial area are often associated with bone as a phosphate source, suggesting that the biological systems at JEG are phosphate-limited, and any phosphate present is quickly used and bound to organic matter. In the subglacial environment, the limited phosphate present may have been originally derived from dust particles deposited on the surface snow (M. Sharp, personal communication 2004), which were subsequently transported to the bed, or from recycling of glacially-overridden organic material.

A potential supply of OC in the subglacial environment exists in the bedrock, soils, and plants that have been overridden while the glacier was advancing (Skidmore *et al.,* 2000). Legacy carbon from these sources could sustain and be recycled within subglacial communities for a long time thereafter, even in the absence of new primary production in a light-free environment. Alternatively, subglacial OC may be derived from chemoautotrophic metabolic processes or supraglacial inwash of particulates.

4.1.3. Environmental Stresses

Four fundamental parameters that control microbial survival, growth, and diversity are temperature, pH, water availability, and molecular oxygen abundance. In this study, the pH

values of meltwater samples from each environment at JEG were similar (Appendix 8), so differences in the remaining three factors may have contributed to the observed inter-environmental diversity at JEG.

4.1.3.1. Temperature

The glacial surface air temperature at JEG fluctuates seasonally from ca –40°C to +10°C. Given that the typical growth temperature range of any given organism is approximately 30°C (Madigan *et al.*, 2003), the fluctuations at the surface of JEG do not provide a stable environment to which bacterial communities can adapt. The supraglacial temperature variation serves as a selective pressure favoring growth of transient psychrotolerant species with broad temperature range tolerance and excluding heat-sensitive psychrophiles. Conversely, the subglacial environment is more favorable to long-term bacterial growth because the thick ice layer overlying the glacier bed insulates against the drastic temperature fluctuations that occur at the surface (Sharp *et al.*, 1999). For example, within a tunnel sawed into the glacier base ca. 15 m in from the ice margin, the temperature range was –14°C to -7°C; where the ice is warm-based the range is constant and close to 0°C (M. Sharp, personal communication, 2004).

4.1.3.2. Water Availability

Access to liquid water is essential for all organisms because cells require soluble nutrients for metabolic processes. On the glacier surface, liquid water is readily available to bacterial communities during the summer melt season, but during the winter, the surface snow temperatures are below freezing and only small quantities may be present in the quasi-liquid water layer on the exterior of ice crystals (Carpenter *et al.*, 2000). However, JEG is polythermal and in the subglacial environment liquid water persists in the basal ice, subglacial sediments, and at the ice-bed interface (Skidmore *et al.*, 2000; Sharp *et al.*, 1999; Copland and Sharp, 2001).

The presence of liquid water at the glacial bed also provides protection for microbes against freezing and freeze-thaw cycles, which can cause physical damage by the formation of intracellular ice crystals.

4.1.3.3. Oxygen Availability

The supraglacial streams at JEG should harbor bacterial communities that contain aerotolerant species (e.g. obligate aerobes, facultative anaerobes, microaerophiles, aerotolerant anerobes). However, in the subglacial ice at JEG, Skidmore *et al.,* (2000) observed nitrate and sulfate reduction as well as methanogenesis, and suggested that though the subglacial meltwaters were primarily aerobic (from input of O_2 saturated supraglacial waters, release of dissolved O_2 in melting glacier ice or chemical weathering reactions) (Barker, 1995) the debris-rich basal ice and subglacial sediments had some anaerobic microenvironments. The presumed presence of anaerobic microenvironments in the basal ice samples offers the possibility that these samples may harbor different bacteria (e.g. obligate anaerobes) than those found in the aerobic supraglacial samples. The dissolved oxygen concentrations of potential microenvironments in the subglacial samples were not analyzed in this study. Although it was previously found that the bulk waters draining JEG during the melt season were oxic (Barker, 1995), this is not surprising if anaerobic conditions develop only at the micro-environment level, and the majority of the subglacial waters were routed through major channels that by-pass these micro-environments.

4.2. Intra-environmental community differences

The community differences within the subglacial, supraglacial, and proglacial environments are likely the result of differences in the geological and/or hydrological characteristics of the various sampling sites. The level of intra-environmental variability in the subglacial, supraglacial, and proglacial environments suggests that there may be a large degree of micro- and macro-environmental heterogeneity at JEG. This emphasizes the importance of

sampling a large array of sub-environments to resolve accurately the diversity in nutrient- and energy-limited environments where microbial life can be scattered.

The fact that no bacteria were found in the dry snow samples whereas communities were present in the supraglacial streams, indicates that the onset of the summer melt season may either facilitate the growth of bacterial communities, or concentrate them to a degree that makes them detectable by the molecular methods used in this study. The supraglacial streams may be more favorable environments for microbial growth than the dry snow. Water is more readily available, there are more solutes in the stream water than in the snowpack (especially during the first phases of melt when selective flushing of snowpack solute occurs) (Williams and Melack, 1991; Jenkins *et al.,* 1993), and sediments that are concentrated on the stream beds are more readily accessible than sediments dispersed throughout the snowpack. The apparent lack of bacteria in the dry snow samples may also be related to the sensitivity of the molecular techniques employed in this study, in that the communities in the dry snow were too sparse to be detected by the methods used.

In the supraglacial environment, the SP-IS-a catchment was composed entirely of glacier ice, whereas the SP-MLS-a catchment drained a meltwater lake, fed by two ice marginal channels that transported sediment from an exposed nunatak to the lake. Thus, the SP-IS-a samples are likely dominated by a group of characteristic supraglacial T-RFs, while the SP-MLS-a samples may also contain T-RFs associated with ice marginal sedimentary environments. However, there is very little overlap between the SP-MLS-a communities and the proglacial T-RFs (Table 3.2; cluster 4), thus the SP-MLS-a samples may contain a set of T-RFs unique to this particular sub-environment, though more samples would have to be analyzed to confirm this hypothesis.

In the proglacial environment, the lack of shared T-RFs between the P-S and P-R samples (Figures 3.11 and 3.12) is expected because of the differences in substrate material between these two sites. The P-S samples were taken from glaciofluvial gravels, which contained little fine-grained sediment. Conversely, the P-R samples were taken from sorted rock polygons, developed on cryoturbated tills with a higher fine sediment content. Thus, the observed community

differences between these two proglacial sites most likely reflect the nature of the substrate much more than the degree of soil development, which is very limited in both cases.

In the subglacial environment, samples from basal ice and subglacial meltwater differed (Figures 3.13 and 3.14) because the water generally contained more T-RFs that were also found in the supraglacial environment, while the ice contained more T-RFs that were found in the proglacial environment. The subglacial water samples likely originated as supraglacial waters that penetrated to the glacier bed via crevasses and/or moulins (see 1.3.5 for description of subglacial drainage system at JEG). Thus, it is likely that a larger component of their communities was originally derived from the supraglacial environment compared to the portion derived from the proglacial environment. However, since the early season subglacial waters were probably stored at the glacier bed over winter, they also contain a uniquely subglacial T-RF community component not present in the supraglacial meltwater. The basal ice samples (B-C and B-F) contain glacially overridden material, which was likely originally similar in composition to the present-day proglacial and ice-marginal sediments that contain various types of organic matter, including cyanobacterial mats, and plant material (Skidmore *et al.,* 2000). Thus, these samples contain a larger component of T-RFs that are also present in the proglacial environment, compared to the portion also present in the supraglacial environment.

The T-RF community differences between the early season and late season subglacial waters (Figure 3.15) can be accounted for because the geometry of the subglacial drainage system at JEG evolves over the course of the melt season. The early season subglacial waters drain from a low energy distributed system that extends widely across the bed. This system is the dominant water flow path in the winter, but it transmits only small water fluxes. As the summer progresses, and there is increased meltwater input from the surface, the subglacial drainage system evolves into a high-energy channelized system, which drains most of the meltwater, but occupies only a small fraction of the bed area (Bingham, 2003). The distributed system is likely more hospitable to bacteria due to the low rates of water flow. Waters passing through this system have prolonged

contact with the glacier bed over the winter (approximately 10 months), and the tortuosity of the drainage system ensures that they effectively sample a large fraction of that part of the glacier bed that is at the pressure melting point. Waters stored in the distributed system over winter may become anoxic, when inputs of water from the surface cease at the end of the melt season. The depleted nitrate concentrations in these waters suggest that microbial activity continues during the winter and that nitrate may be used as a terminal electron acceptor in the absence of oxygen (Tranter *et al.,* 2002). In the summer, subglacial meltwater is diluted by supraglacial inflow as crevasses and moulins connect to the subglacial drainage system. Development of major channels confines water flow to a small fraction of the glacier bed, and waters draining through this system may not effectively sample those parts of the bed drained by the distributed system. As a result, the T-RF assemblage of the late season subglacial waters show greater affinity to that of the supraglacial environment compared to some early season waters, which more likely harbor uniquely subglacial members. However, additional late season subglacial water samples would have to be analyzed to confirm this hypothesis. The input of supraglacial waters in the summer replenishes the subglacial nitrate supply, but the majority of waters flow through the glacier too fast for bacteria to use the nitrate (residence times deduced from dye tracing experiments are on the order of a few hours) (Bingham, 2003). This could explain the elevated nitrate concentrations in the later season subglacial waters.

The apparently heterogeneous spatial distribution of OC beneath JEG may account for the observed T-RF pattern differences between the B-C and B-F basal ice sites (Figure 3.16), and the fact that no bacteria were found in the B-S samples. The most likely source of the OC in the subglacial sediments is the permafrozen soils and plant material that were overridden during past glacial advances (Skidmore *et al.,* 2000). Considering that plants are sparsely distributed in the present-day proglacial area, it is not surprising that OC abundance in the subglacial sediments is highly variable. Since OC is required for chemo-organotrophic metabolism, the higher OC concentrations at the B-C site may make it a more favorable microenvironment for a greater array

of bacteria than either the B-F site, where basal ice has much lower OC concentrations, or the B-S site, where the OC concentrations were the lowest observed of the three sites (Appendix 10).

4.3. Limitations and Biases

Although T-RFLP analysis may be used to infer the source of the subglacial bacteria through comparison of community T-RF patterns, there are several limitations associated with the technique and with the experimental design of this study that may bias the results, as discussed below.

Firstly, it is not known whether the amplified community was derived entirely from living organisms or in part from ancient DNA or microbes preserved in the ice (Abyzov 1993; Christner *et al.*, 2003; Sheridan *et al.*, 2003; Miteva *et al.*, 2004). Secondly, the T-RFLP data used in this study were discrete (categorical), and the relative abundance (peak height) of different T-RFs at each site was not analyzed. Thirdly, direct statistical comparisons of community diversity between the subglacial, supraglacial, and proglacial environments are not possible because the datasets analyzed were not identical in size. To determine whether the greater diversity detected in the subglacial environment was simply a function of the greater number of samples analyzed, a rarefaction curve was constructed (Microsoft Excel™ 2000) by plotting the incremental number of new T-RFs appearing with each sample (Figure 4.1). The results of this analysis were inconclusive, as the subglacial, supraglacial, and proglacial plots had similar gradients suggesting that the number of samples analyzed may be the main factor controlling the apparent diversity. Although it appears that the supraglacial and proglacial communities are more closely related to the subglacial community than to each other, this relationship may in part be a function of the subglacial dataset being larger. Analysis of additional supraglacial and proglacial samples may reveal that these two environments share more T-RFs than could be detected by the present study. A more comprehensive analysis of a greater array of samples and of species abundance and evenness would be necessary to confirm that the bacterial distribution at JEG is truly

heterogeneous and not merely a function of sampling strategy. However, the presence in the smaller supraglacial and proglacial datasets of characteristic groups of T-RFs that are generally absent in the larger subglacial dataset is persuasive evidence that these different environmental habitats do indeed harbor distinct bacterial communities. If these characteristic supraglacial and proglacial groups had been present in the subglacial samples, they should have been detected, given the larger size of the latter dataset.

T-RFLP community analysis is also biased in that it is an approach based on detection of dominant populations, thus it is not useful to account for minor or poorly accessible populations (Liu *et al.,* 1997; Ranjard et al., 2003). T-RFs that are rare in the community will not be detected because they have comparatively low quantities of initial template DNA and thus, may not be amplified because more abundant templates may be preferentially amplified (Liu *et al.,* 1997). Furthermore, if they are amplified, the fluorescence peaks of these T-RFs may not be distinguishable from the background peaks, and most likely will fall below the minimum peak height fluorescence threshold of 100 RFU. Thus the diversity reported in this study is likely to be a conservative estimate, as a rigorous peak height fluorescence threshold was used to ensure that the diversity was not overestimated.

The community diversity may also be underestimated because phylogenetically similar bacterial strains have similar 16S rDNA sequences and T-RFs of identical size may arise from single enzymatic digestions (Liu *et al.,* 1997; Osborn *et al.,* 2000; Mummey and Stahl, 2003; Miteva *et al.,* 2004). Sometimes, T-RFLP studies are based on digestion with pairs of restriction enzymes, although other studies have shown that combining results from several single enzymatic digestions is more informative than using double digestions (Dunbar *et al.,* 2001). In this study only two restriction enzymes were used in single digestions, whereas other enzymes may have produced T-RFs that more accurately reflected the community diversity (Engebretson and Moyer, 2003). The ability of different restriction enzymes to detect the actual number of 16S rDNA sequence variants may be especially important in an environment like JEG, which contains a few

specialized habitats represented by a limited number of phylotypes. It should also be noted that this study only utilized two multivariate statistical methods to analyze the T-RF patterns.

Although the physical lysis treatment used in this study, has been utilized successfully in other cold environment studies (Foght *et al.*, 2004), the community diversity may have been underestimated because repeated extractions yielded additional DNA (data not shown). Not all of the cells were lysed with the first extraction procedure; thus, additional extraction procedures may be necessary to obtain a more complete picture of community diversity. In future experiments, extracts from serial treatments should be pooled before analysis.

Regardless of the limitations discussed above, all molecular techniques exhibit similar biases, yet molecular analyses still provide the most advanced tool for examination of microbial communities in their natural environment.

4.4. Subglacial community establishment

Although previous studies of subsurface bacterial consortia in cold environments (e.g. temperate alpine subglacial environments, Greenland glacier ice cores, accreted ice from Lake Vostok) have discerned the community composition through culture techniques and DNA sequencing analysis (Priscu *et al.*, 1999; Christner *et al.*, 2001; Miteva *et al.*, 2004; Foght *et al.*, 2004), none have established the source of truly subglacial communities. Possible mechanisms by which subglacial bacterial communities may become established are by (1) transport to the glacier bed by supraglacial meltwaters flowing down crevasses and moulins, (2) vertical transport by the flow of glacier ice, or (3) basal incorporation of soils and sediments overridden during glacial advance. Given sufficient time, the isolation of the subglacial environment from its surroundings may have allowed the development of a unique bacterial community, regardless of the original source of organisms (Sharp *et al.*, 1999; Miteva *et al.*, 2004). If the subglacial bacterial communities were established and replenished by either the first or second mechanism, it is likely that the subglacial community would consist primarily of supraglacial T-RFs. If the

subglacial communities were established by the third mechanism, it is likely that the majority of the subglacial T-RFs would also be found in the proglacial environment. The T-RFLP analysis indicates that the subglacial environment consists of bacterial communities that may be, to some degree, distinct from those in both the supraglacial and proglacial environments. Though the subglacial community would ultimately have been derived from either or both the supraglacial and proglacial environments, it is interesting that continued inputs from both of these potential source communities do not appear to result in a subglacial T-RF community that mirrors either environment. From the samples analyzed, the T-RFs that dominate the supraglacial and proglacial environments do not appear frequently subglacially. However, there are other T-RFs that occur less commonly supraglacially and proglacially that do occur frequently in the subglacial community. There are also T-RFs that occur only in the subglacial setting. This implies that environmental conditions at the bed may exclude or select against the dominant components of the potential source communities, allow selected minor components to survive, and also may support T-RFs that cannot thrive in these two other environments. Thus, a combination of all three mechanisms present at different times or detected at different times (perhaps as a function of sampling and/or hydrology in addition to time and isolation) is most likely responsible for subglacial bacterial community establishment and development at JEG.

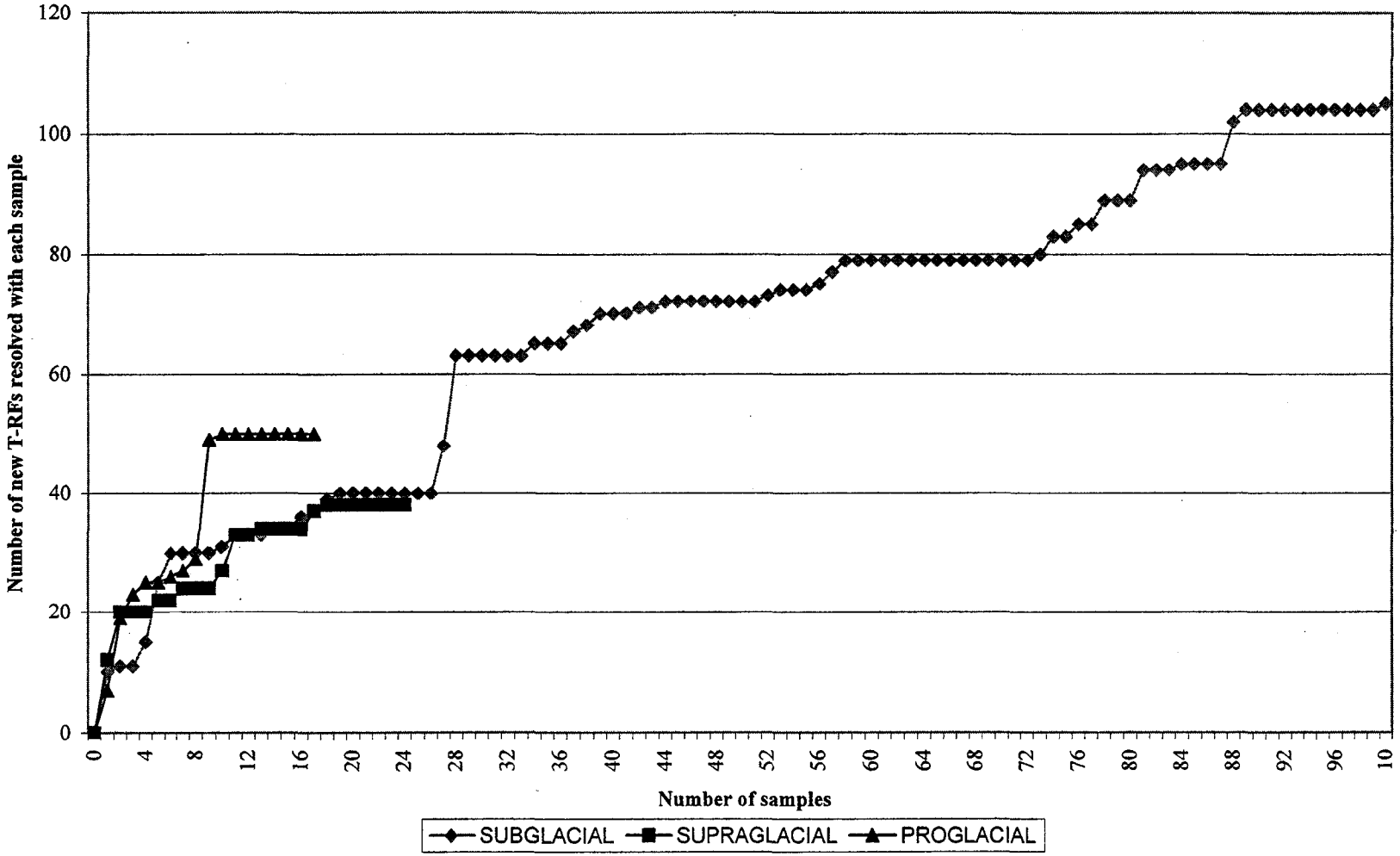

Figure 4.1. A rarefaction curve illustrating the incremental number of new T-RFs appearing with each sample analyzed with the *Hae* III enzyme. One hundred subglacial, 24 supraglacial, and 16 proglacial samples were analyzed.

Chapter 5. Summary and Implications

5.1. Summary

This research has (a) presented the first indication of the source, diversity, and distribution of subglacial bacterial communities, thus providing insight into fundamental questions not answered using any other technique, (b) revealed that some members of the subglacial community are apparently not derived from either the supraglacial or proglacial source communities, and thus may be autochthonous to the subglacial environment, (c) illustrated that the bacterial communities are distinct on inter- and intra-environmental levels, suggesting a heterogeneous and diverse distribution of bacteria dependent on varying physical and chemical characteristics among the different glacial environments and sub-environments, and (d) highlighted the potential association that a unique subglacial community may have with glacial water chemistry, thus possibly suggesting the existence of a functioning ecosystem with biogeochemical significance in the subglacial environment.

5.2. Future Research and Implications

The existence of a uniquely subglacial community may have implications for subglacial biogeochemical cycles, and provides increased understanding of the limitations of life on Earth and, possibly, analogues for extraterrestrial life beneath the Martian polar ice caps.

Although this study has not taxonomically identified any of the T-RFs, a public database of 16S rDNA T-RFs is being constructed (http://rdp.cme.msu.edu/html) (Cole *et al.*, 2003). In the future it may permit genus or species names to be assigned to the T-RFs observed in the JEG samples. This would enable further speculation about the contribution of bacterial metabolic activities to the subglacial chemistry of JEG. Furthermore, the current study has been limited to analysis of Bacteria, but could be expanded to include Archaea and Eukarya, which may also be contributors to the biogeochemical cycles. Additionally, the index of T-RFs identified in this

study could be used to complement culture-based community techniques, which are currently being conducted on JEG samples, by providing information about the environmental distribution of the organisms identified by culture methods. In this way, it may be possible to select particularly widespread organisms for DNA sequencing identification, to determine if they could facilitate subglacial biogeochemical reactions. By combining molecular-based and culture-based community analyses at JEG, it may also be possible to determine if the organisms detected with molecular techniques are the same as those detected with culture-based techniques.

Finally, the presence of communities beneath high Arctic polythermal glaciers uniquely adapted to these environmental conditions further illustrates the extent of prokaryotic diversity and distribution on Earth. These communities may be potential analogues for life in other extreme cold extraterrestrial regions, such as beneath the Martian polar ice caps (Nealson, 1997). It is not unreasonable to speculate that the environmental conditions characteristic of subglacial environments on Earth (access to liquid water and nutrients, protection from temperature fluctuations and UV radiation) formerly or presently resemble those in the basal sediments beneath the Martian polar ice caps (Skidmore *et al.*, 2000). Possibly, the bacterial microhabitats created by the seasonal hydrology at JEG are analogues for subterranean microbial habitats beneath the Martian polar ice caps, which were similarly created by partial melting of the ice caps and periodic effluxes of hydrothermal heat (McKay, 2001; McKay and Stoker, 1989; Clifford *et al.*, 2000).

References

Abyzov, S.S., 1993. Microorganisms in Antarctic ice. In Antarctic Microbiology, E.I. Friedmann (ed). New York, Wiley-Liss: 265 – 297.

Amann, R., W. Ludwig, and K-H. Scheleifer. 1995. Phylogenetic identification and *in situ* detection of individual microbial cells without cultivation. Microbiological Reviews 59 (1): 143 – 169.

Anderson, D.T., W.H. Pollard, C.T. McKay, and C. Omelon. 1998. Perennial springs in the Canadian High Arctic, analogs of past Martian liquid water habitats. Eos Transaction 74(45): 59.

Balakrishnan, S. 2000. Isolation and characterization of sub-glacial microorganisms from Arctic ice samples collected at John Evans Glacier, Nunavut Canada. Biology 498 research paper, Department of Biological Sciences, University of Alberta.

Barker, J.D. 1995. A study of dissolved oxygen in the meltwaters of John Evans Glacier, N.W.T., Canada. Earth and Atmospheric Sciences 426 research paper, Department of Earth and Atmospheric Sciences, University of Alberta.

Becker, S., P. Boger, R. Oehlmann, and A. Ernst. 2000. PCR bias in ecological analysis: a case study of quantitative *Taq* nuclease assays in analysis of microbial communities. Applied and Environmental Microbiology 66 (11): 4945 – 4953.

Bingham, R.G. 2003. The hydrology and dynamics of a high Arctic glacier. PhD thesis. University of Glasgow, p. 254.

Blackwood, C.B., T. Marsh, S-H. Kim, and E.A. Paul. 2003. Terminal restriction fragment length polymorphism data analysis for quantitative comparison of microbial communities. Applied and Environmental Microbiology 69 (2): 926 – 932.

Blatter, H., and K. Hutter. 1991. Polythermal conditions in arctic glaciers. Journal of Glaciology 37 (126): 261 – 269.

Bottrell, S.H., and M. Tranter. 2002. Sulphide oxidation under partially anoxic conditions at the bed of the Haut Glacier d'Arolla, Switzerland. Hydrological Processes 16: 2363 – 2368.

Brosius, J., T.J. Dull, D.D. Sleeter, and H.F. Noller. 1981. Gene organization and primary structure of a ribosomal-RNA operon from *Escherichia coli.* Journal of Molecular Biology 148 (2): 107 – 127.

Brown, G.H., M. Tranter, M.J. Sharp, T.D. Davies, and S. Tsouris. 1994. Dissolved oxygen variations in alpine glacial meltwaters. Earth Surface Processes and Landforms 19 (3): 247 – 253.

Carpenter, E.J., S. Lin, and D.G. Capone. 2000. Bacterial activity in South Pole snow. Applied and Environmental Microbiology 66 (10): 4514 – 4517.

Christner, B.C., E. Mosley Thompson, L.G. Thompson, and J.N. Reeve. 2001. Isolation of bacteria and 16S rDNAs from Lake Vostok accretion ice. Environmental Microbiology 3: 570 – 577.

Christner, B.C., E. Mosley-Thompson, L.G. Thompson, and J.N. Reeve. 2003. Bacterial recovery from ancient glacial ice. Environmental Microbiology 5 (5): 433 – 436.

Clifford, S.M., D. Crisp, D.A. Fisher, K.E. Herkenhoff, S.E. Smrekar, P.C. Thomas, D.D. Wynn-Williams, R.W. Zurek, J.R. Barnes, B.G. Bills, E.W. Blake, W.M., Calvin, J.M. Cameron, M.H. Carr, P.R. Christensen, B.C. Clark, G.D. Clow, J.A. Cutts, D. Dahl-Jensen, W.B. Durham, F.P. Fanale, J.D. Farmer, F. Forgot, K. Gotto-Azuma, R. Grard, R.M. Haberle, W. Harrison, R. Harvey, A.D. Howard, A.P. Ingersoll, P.B. James, J.S. Kargel, H.H. Kieffer, J. Larsen, K. Lepper, M.C. Malin, D.J. McCleese, B. Murray, J.F. Nye, D.A. Paige, S.R. Platt, J.J. Plaut, N. Reeh, J.W. Rice, D.E. Smith, C.R. Stoker, K.L. Tanaka, E. Mosley-Thompson, T. Thorsteinsson, S.E. Wood, A. Zent, M.T. Zuber, and H.J. Zwally. 2000. The state and future of Mars polar science and exploration. Icarus 144: 210 – 242.

Cole J.R., B. Chai, T.L. Marsh, R.J. Farris, Q. Wang, S.A. Kulam, S. Chandra, D.M. McGarrell, T.M. Schmidt, G.M. Garrity, and J.M. Tiedje. 2003. The Ribosomal Database Project (RDP-II): previewing a new autoaligner that allows regular updates and the new prokaryotic taxonomy. Nucleic Acids Research 31(1):442 – 443.

Copland, L., and M. Sharp. 2001. Mapping thermal and hydrological conditions beneath a polythermal glacier with radio-echo sounding. Journal of Glaciology 47 (157): 232 – 242.

Crosby, L.D., and C.S. Criddle. 2003. Understanding bias in microbial community analysis techniques due to *rrn* operon copy number heterogeneity. BioTechniques 34 (4): 2 – 9.

Dunbar, J., L.O. Ticknor, and C.R. Kuske. 2001. Phylogenetic specificity and reproducibility and new method for analysis of terminal restriction fragment profiles of 16S rRNA genes from bacterial communities. Applied and Environmental Microbiology 67 (1): 190 – 197.

Engebretson, J.J., and C.L. Moyer. 2003. Fidelity of select restriction endonucleases in determining microbial diversity by terminal restriction fragment length polymorphism. Applied and Environmental Microbiology 69 (8): 4823 – 4829.

Fairchild, I.J., L. Bradby, and B. Spiro. 1993. Carbonate diagenesis in ice. Geology 21: 901 – 904.

Fairchild, I.J., L. Bradby, M. Sharp, and J.L. Tisson. 1994. Hydrochemistry of carbonate terrains in alpine glacial settings. Earth Surface Processes and Landforms 19: 33 – 54.

Foght, J., J. Aislabie, S. Turner, C.E. Brown, J. Ryburn, D.J. Saul, and W. Lawson. 2004. Culturable bacteria in subglacial sediments and ice from two Southern Hemisphere glaciers. Microbial Ecology 47: 329 – 340.

Fowler, J., L. Cohen, and P. Jarvis. Practical Statistics for Field Biology. 2nd edition. New York: John Wiley and Sons, Inc.

Frostegard, A., S. Courtois, V. Ramisse, S. Clerc, D. Bernillon, F. Le Gall, P. Jeannin, X. Nesme, and P. Simonet. 1999. Quantification of bias related to the extraction of DNA directly from soils. Applied and Environmental Microbiology 65 (12): 5409 – 5420.

Gibbs, M.T., and L.R. Kump. 1994. Global and chemical erosion during the last glacial maximum and the present: sensitivity to changes in lithology and hydrology. Paleoceanography 9: 529 – 543.

Grannas, A.M., and P.B. Shepson. 2004. Photochemistry and nature of organic matter in Arctic and Antarctic snow. Global Biogeochemical Cycles 18: GB1006, DOI: 10.1029/2003GB002133.

Griffiths, A.J., J.H. Miller, D.T. Suzuki, R.C. Lewontin, and W.M. Gelbart. 1997. An introduction to genetic analysis. 6th edition. New York: W.H. Freeman and Company.

Hoham, R.W. and B. Duval. 2001. Microbial ecology of snow and freshwater ice with emphasis on snow algae. In Snow Ecology: an interdisciplinary examination of snow-covered ecosystems. H.G. Jones, J.W. Pomeroy, D.A. Walker, and R.W. Hoham (eds). Cambridge, UK, Cambridge University Press: pp. 168 – 215.

Hubbard, B., and M. Sharp. 1989. Basal ice formation and deformation: a review. Progress in Physical Geography 13 (4): 529 – 558.

Jenkins, A., R. Ferrier, and D. Waters. 1993. Melt water chemistry and its impact on stream water quality. Hydrological Processes 7: 193 – 203.

Karp, G. 1999. Cell and Molecular Biology: Concepts and Experiments. New York: John Wiley and Sons, Inc.

Kerr, J.W. 1972. Map 1358A Geology: Dobbin Bay, District of Franklin 1:250000, Geological Survey of Canada.

Kump, L.R., and R.B. Alley. 1994. Global chemical weathering on glacial timescales. In Material Fluxes on the Surface of the Earth. T. Usselman and W.W. Hay (eds). Washington, D.C., National Academy Press: 46 – 60.

Lafreniere, M., and M. Sharp. 2002. The concentration and spectrofluorometric properties of Dissolved Organic Carbon (DOC) in surface waters: interpreting the flow routing of runoff and DOC sources in glacial and non-glacial catchments. Arctic, Antarctic, and Alpine Research (submitted).

Lafreniere, M., and M. Sharp. 2003. A comparison of solute fluxes and sources from glacial and non-glacial catchments over contrasting melt seasons. Hydrological Processes (submitted).

Lanoil, B.D., M. Sharp, S.P. Anderson, M.T. La Duc, J. Foght, and K.H. Nealson. 2001. A comparative study of microbial communities under two glaciers. 101st Ann. Meeting American Society for Microbiology meeting, Abst #N-208.

Liu, W., T.L. Marsh, H. Cheng, and L.J. Forney. 1997. Characterization of microbial diversity by determining terminal restriction fragment length polymorphisms of genes encoding 16S rRNA. Applied and Environmental Microbiology 63 (11): 4516 – 4522.

Lyons, W.B., K.A. Welch, A.G. Fountain, G.L. Dana, B.H. Vaughn, and D.M. McKnight. 2003. Surface glaciochemistry of Taylor Valley, southern Victoria Land, Antarctica, and its relationship to stream chemistry. Hydrological Processes 17 (1): 115 – 130.

Madigan, M.T., J.M. Martinko, and J. Parker. 2003. Brock Biology of Microorganisms. 10th edition. New Jersey: Pearson Education, Inc.

Madsen, E.L. 2000. Nucleic-acid characterization of the identity and activity of subsurface microorganisms. Hydrogeology Journal 8: 112 – 125.

Martin-Laurent, F., L. Philippot, S. Hallet, R. Chaussod, J.C. Germon, G. Soulas, and G. Catroux. 2001. DNA extraction from soils: old bias for new microbial diversity analysis methods. Applied and Environmental Microbiology 67 (5): 2354 – 2359.

McKay, C.P., and C.R. Stoker. 1989. The early environment and its evolution on Mars: implications for life. Reviews of Geophysics. 27: 189 – 214.

McKay, C.P. 2001. Life in cold and dry limits: Earth, Mars, and beyond. In Journey to Diverse Microbial Worlds: adaptation to exotic environments. J. Seckbach (ed). London: Kluwer Academic Publishers.

Miller, D.N., J.E. Bryant, E.L. Madsen, and W.C. Ghiorse. 1999. Evaluation and optimization of DNA extraction and purification procedures for soil and sediment samples. Applied and Environmental Microbiology 65 (11): 4715 – 4724.

Miteva, V.I., P.P Sheridan, and J.E. Brenchley. 2004. Phylogenetic and physiological diversity of microorganisms isolated from a deep Greenland glacier ice core. Applied and Environmental Microbiology 70 (1): 202 – 213.

More, M.I., J.B. Herrick, M.C. Silva, W.C. Ghiorse, and E.L. Madsen. 1994. Quantitative cell lysis of indigenous microorganisms and rapid extraction of microbial DNA from sediment. Applied and Environmental Microbiology 60 (5): 1572 – 1580.

Mueller, D.R., W.F. Vincent, W.H. Pollard, and C.H. Fritsen. 2001. Glacial cryoconite ecosystems: a bipolar comparison of algal communities and habitats. Nova Hedwigia, Beiheft 123.

Mummey, D.L., and P.D. Stahl. 2003. Spatial and temporal variability of bacterial 16S rDNA-based T-RFLP patterns derived from soil of two Wyoming grassland ecosystems. FEMS Microbiology Ecology 46: 113 – 120.

Nealson, K.H. 1997. The limits of life on Earth and searching for life on Mars. Journal of Geophysical Research 102 (E10): 23,675 – 23,686.

O'Donnell, A.G. and H.E. Borres. 1999. 16S rDNA methods in soil microbiology. Current Opinion in Biotechnology 10 (3): 225 – 229.

Osborn, A.M., E.R. Moore, and K.N. Timmis. 2000. An evaluation of terminal restriction fragment length polymorphism (T-RFLP) analysis for the study of microbial community structure and dynamics. Environmental Microbiology 2 (1): 39 – 50.

Priscu, J.C., E.E. Adams, W.B. Lyons, M.A. Voytek, D.W. Mogk, R.L. Brown, C.P. McKay, C.D. Takacs, K.A. Welch, C.F. Wolf, J.D. Krishtein, and R. Avci. 1999. Geomicrobiology of subglacial ice above Lake Vostok, Antarctica. Science 286: 2141-2144.

Raiswell, R., 1984. Chemical models of solute acquisition in glacial meltwaters. Journal of Glaciology, 30 (104): 49 – 57.

Raiswell, R., and A.G. Thomas. 1984. Solute acquisition in glacial melt waters I. Fjallsjokull (south-east Iceland): bulk melt waters with closed-system characteristics. Journal of Glaciology 30 (104): 35 – 43.

Ranjard, L., D.P. Lejon, C. Mougel, L. Schehrer, D. Merdinoglu, and R. Chaussod. 2003. Sampling strategy in molecular microbial ecology: influence of soil sample size on DNA fingerprinting analysis of fungal and bacterial communities. Environmental Microbiology 5 (11): 1111 – 1120.

Rappe, M.S., and S.J. Giovannoni. 2003. The uncultured microbial majority. Annual Reviews in Microbiology 57: 369 – 394.

Reynolds, R.C., and N.M. Johnson. 1972. Chemical weathering in the temperate glacial environment of the Northern Cascade Mountains. Geochimica Cosmochimica Acta 36: 537 – 554.

Roose-Amsaleg, C.L., E. Garnier-Sillam, and M. Harry. 2001. Extraction and purification of microbial DNA from soil and sediment samples. Applied Soil Ecology 18: 47 – 60.

Schlesinger, W.H. 1997. Biogeochemistry: an analysis of global change. 2nd edition. New York, Academic Press: 90 – 96.

Sharp, M., J. Parkes, B. Cragg, I.J. Fairchild, H. Lamb, and M. Tranter. 1999. Widespread bacterial populations at glacier beds and their relationship to rock weathering and carbon cycling. Geology 27 (2): 107-110.

Sheridan, P.P., V.I. Miteva, and J.E. Brenchley. 2003. Phylogenetic analysis of anaerobic psychrophilic enrichment cultures obtained from a Greenland glacier ice core. Applied and Environmental Microbiology 69 (4): 2153 – 2160.

Siegert, M.J., J.C. Ellis-Evans, M. Tranter, C. Mayer, J-R. Petit, A. Salamatin, and J.C. Priscu. 2001. Physical, chemical, and biological processes in Lake Vostok and other Antarctic subglacial lakes. Nature 414: 603 – 609.

Skidmore, M.L. and M.J. Sharp. 1999. Drainage behaviour of a high Arctic polythermal glacier. Annals of Glaciology 28: 209-215.

Skidmore, M.L., J.M. Foght, and M.J. Sharp. 2000. Microbial life beneath a High Arctic glacier. Applied and Environmental Microbiology 66 (8): 3214-3220.

Skidmore, M. 2001. Hydrology, microbiology and carbon cycling at a high Arctic polythermal glacier (John Evans Glacier, Ellesmere Island, Canada). PhD Thesis, University of Alberta 60 – 115.

Toom-Sauntry, D., and L.A. Barrie. 2002. Chemical composition of snowfall in the high Arctic: 1990-1994. Atmospheric Environment 36: 2683 – 2693.

Tranter, M. 1982. Controls on the chemical composition of Alpine glacial meltwaters. Ph.D. thesis, East Anglia, UK.

Tranter, M., G. Brown, R. Rainswell, M. Sharp, and A. Gurnell. 1993. A conceptual model of solute acquisition by alpine glacial meltwaters. Journal of Glaciology 39 (133): 573 – 581.

Tranter, M., G.H. Brown, A. Hodson, A.M. Gurnell, and M.J. Sharp. 1994. Variations in the nitrate concentration of glacial runoff in Alpine and sub-polar environments. International Association of Hydrological Sciences Publication 233: 299 – 310.

Tranter, M., M.J. Sharp, H.R. Lamb, G.H. Brown, B.P. Hubbard, and I.C. Willis. 2002. Geochemical weathering at the bed of Haut Glacier d'Arolla, Switzerland – a new model. Hydrological Processes 16: 959 – 993.

Tranter, M., A.G. Fountain, C.H. Fritsen, W.B. Lyons, J.C. Priscu, P.J. Statham, and K.A. Welch. 2004. Extreme hydrochemical conditions in natural microcosms entombed within Antarctic ice. Hydrological Processes 18: 379 – 387.

Vincent, W.F. 1988. Microbial ecosystems of Antarctica. Cambridge: Cambridge University Press.

Wadham, J.L., S. Bottrell, M. Tranter, and R. Raiswell. 2003. Stable isotope evidence for microbial sulphate reduction at the bed of a polythermal high Arctic glacier. Earth and Planetary Science Letters 219: 341 – 355.

Welker, J.M., J.T. Fahnestock, G.H.R. Henry, K.W. O'Dea, and R.E. Piper. 2002. Microbial activity discovered in previously ice-entombed arctic ecosystems. EOS 83 (26): 281 and 284.

Williams, M.W., and J.M. Melack. 1991. Solute chemistry of snowmelt and runoff in an alpine basin, Sierra Nevada. Water Resources Research 27 (7): 1575 – 1588.

Wintzingerode, F.V., U.B. Gobel, and E. Stackebrandt. 1997. Determination of microbial diversity in environmental samples: pitfalls of PCR-based rRNA analysis. FEMS Microbiology Reviews 21: 213 – 229.

Woodward, J., M. Sharp, and A. Arendt. 1997. The effect of superimposed ice formation on the sensitivity of glacier mass balance to climate change. Annals of Glaciology 24: 186 – 190.

Zhou, J., M.A. Bruns, and J.M. Tiedje. 1996. DNA recovery from soils of diverse composition. Applied and Environmental Microbiology 62 (2): 316 – 322.

Appendices

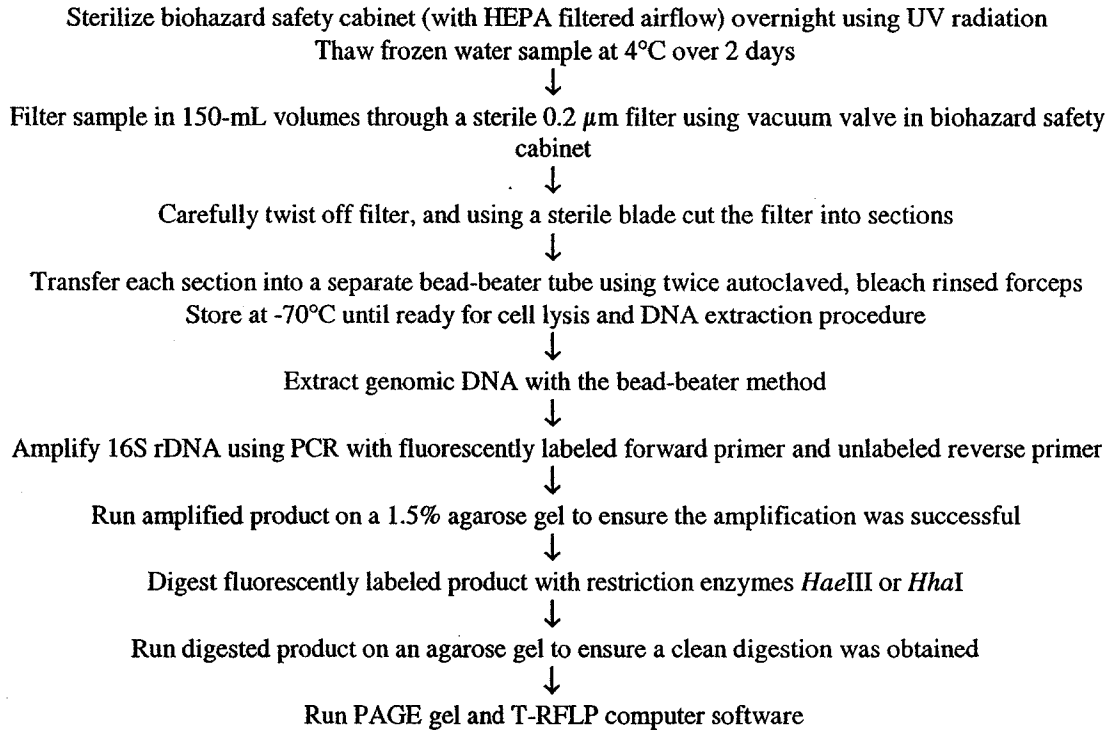

Appendix 1. Aseptic sample processing, DNA extraction and amplification, and digestion of 16S rRNA genes with the bead-beater technique for 1-L subglacial and supraglacial water samples collected at JEG. Note that the procedure for dry and wet snow samples is the same, except that the thawing and filtration steps were conducted in the field.

Sterilize biohazard safety cabinet (with HEPA filtered airflow) overnight using UV radiation
Rinse beakers in DI water and autoclave twice with foil on top

↓

Carefully open WhirlPak™ sample bags and transfer ice chunks into a sterile beaker
Immediately place foil cover back on beaker
Let basal ice thaw in beakers at 4°C until the sample has melted

↓

Filter slurry through a sterile 0.2 μm filter
Keep filtered water for ion, pH, and EC analysis
Keep ~100 mL of the unfiltered slurry/water for DOC analysis

↓

Carefully twist off the filter, and using a sterile blade, cut the filter into sections
Transfer each section into a separate bead-beater tube using twice autoclaved, bleach rinsed forceps
Store tubes at -70°C until ready for cell lysis and DNA extraction procedure

↓

Transfer remaining sediment from the basal ice samples into bead-beater tubes in ~0.50 g aliquots
Store these tubes at -70°C until ready for cell lysis and DNA extraction procedure
If there is an abundance of sediment, transfer a portion into a sterile 50-mL tube and store at -20°C
Pipette any remaining slurry from the beaker and store in bead-beater tubes at -70°C in ~500 μL aliquots

↓

Extract genomic DNA using the bead-beater method

↓

Amplify 16S rDNA using PCR with fluorescently labeled forward primer and unlabeled reverse primer

↓

Run amplified product on a 1.5% agarose gel to ensure the amplification was successful

↓

Digest fluorescently labeled product with restriction enzymes *Hae*III or *Hha*I

↓

Run digested product on an agarose gel to ensure a clean digestion was obtained

↓

Run PAGE gel and T-RFLP computer software

Appendix 2. Aseptic sample processing, DNA extraction and amplification, and digestion of 16S rRNA genes with the bead-beater technique for basal ice samples collected at JEG (2002).

Sterilize biohazard safety cabinet (with HEPA filtered airflow) overnight using UV radiation

↓

Carefully open WhirlPak™ sample bags and using twice autoclaved, bleach rinsed spatulas, transfer the sediment sample into bead-beater tubes in ~ 0.50 g aliquots

Store bead-beater tubes at -70°C until ready for cell lysis and DNA extraction procedure

If there is an abundance of sediment, transfer a portion into a sterile 50-mL tube and store at -20°C

↓

Extract genomic DNA with the bead-beater method

↓

Amplify 16S rDNA using PCR with fluorescently labeled forward primer and unlabeled reverse primer

↓

Run amplified product on a 1.5% agarose gel to ensure the amplification was successful

↓

Digest fluorescently labeled product with restriction enzymes *Hae*III or *Hha*I

↓

Run digested product on an agarose gel to ensure a clean digestion was obtained

↓

Run PAGE gel and T-RFLP computer software

Appendix 3. Aseptic sample processing, DNA extraction and amplification, and digestion of 16S rRNA genes with the bead-beater technique for proglacial sediment samples collected at JEG (2002).

1. Bead-beater extractions and 16S rDNA PCR amplification from pure colonies
↓
2. Bead-beater extractions and 16S rDNA PCR amplification from JEG isolates*
↓
3. Determining the optimum time to bead-beat pure colonies and JEG isolates*
↓
4. Bead-beater time trial using JEG mud samples**
↓
5. Determining minimum concentration of cells necessary to successfully extract and amplify DNA from pure colonies and JEG isolates*
↓
6. Determining if it is possible to extract and amplify DNA directly from a filter from 1 L of subglacial water using the bead-beater method
↓
7. Determining the optimum time to bead-beat subglacial filters
↓
8. Control test to ensure that the filter units are DNA-free
↓
9. Determining if it is possible to extract and amplify DNA directly from a filter from 1 L of supraglacial water and a filter from 5 L of melted dry snow
↓
10. Determining if it is possible to extract and amplify DNA from the basal ice sediments
↓
11. Bead-beater extractions and 16S rDNA PCR amplifications from filters of basal ice slurry
↓
12. Combining genomic DNA from several extractions from basal ice sediments and determining if this yields enough DNA for successful amplification
↓
13. Test PCR amplification of genomic DNA from JEG environmental samples using a fluorescent primer and an unlabeled primer
↓
14. Test digestion of JEG environmental samples using restriction enzymes *Hae*III and *Hha*I

Appendix 4. Flow chart depicting the development of an optimum protocol for DNA extraction, 16S rDNA PCR amplification, and digestion for T-RFLP analysis for samples collected at JEG. Steps 1-5 were completed from November 2001 – March 2002. Steps 6-14 were completed from August 2002 – November 2002, using samples collected during the summer field season (May – July 2002) at JEG.

* - pure bacterial cultures isolated from mud samples collected from JEG in the 2001 field season by J. Barker.
** - mud samples collected from JEG in the 2001 field season by J. Barker.

Appendix 5. Sample list and key of all samples analyzed with T-RFLP analysis with the *Hae* III enzyme. The number preceding the sample name refers to the lane number on the gel. This number is followed by the sample site abbreviation and the bag or bottle number. No bag or bottle number indicates that the sample was taken from the first bag or bottle. The following numbers and letters refer to different aspects of the sample processing and molecular laboratory procedures. A description of samples in the next column explains the sample processing procedures represented by the numbers. The fractions refer to the portion of the filter from which DNA was extracted. "1st filter" represents the initial filtration process, whereas "2nd filter" refers to the second filtration unit used after the first filter became impassable with sediment. Whether the sample was diluted after the DNA extraction process in attempt to gain a better amplicon product is also noted. A description of the type of replicate the sample represents explains the molecular laboratory procedures represened by the letters. The suffixes "a" and "b" represent the first and second PCR amplifications and enzymatic digestions. The suffixes "e" and "f" represent the third and fourth PCR amplifications and enzymatic digestions. The suffixes "aa" and "bb" represent additional PCR amplifications and enzymatic digestions, in which the amount of DNA digested was not yet optimized to 6 ng/μL. Numbers following the letter suffixes indicate replicates of only the enzymatic digestion step using the same PCR amplicon. Finally, the polyacrylamide gel that the sample was run on is also noted. PAGE 1 represents the only 500-bp gel. PAGE 2 - 17 represent 2500-bp gels. Whether the sample represented a "same gel replicate" (identical samples run on the same polyacrylamide gel) or a "between (b/w) gel replicate" (identical samples run on different polyacrylamide gels) is also noted.

Subglacial Samples

Sample No.	Sample Name	Sample Description	Type of replicate	No. of T-RFs in each sample
1	23-B-C#2 - 9 (11/24/02 c)_PAGE 1	bag 1 - combined DNA from several 500 uL muddy slurry tubes	original (1st)	4
2	24-B-C#3 - 10 (11/24/02 c)_PAGE 1	bag 1 - combined DNA from several 500 uL muddy slurry tubes	original (1st)	7
3	01-B-C 1/4 - 1 (11/22/02 a)_PAGE 1	bag 1- 1/4 filter from 250 mL	original (1st)	8
4	17-B-C 1/4 - 3 (11/24/02 c)_PAGE 1	bag 1 - 1/4 filter from 250 mL	original (1st)	18
5	01-B-C1/4a_PAGE 4	bag 1- 1/4 filter from 250 mL	original (1st)	17
6	01-B-C1/4a_PAGE 5	bag 1- 1/4 filter from 250 mL	original (1st), b/w gel replicate (PAGE 4, Lane 1)	11
7	02-B-C1/4b_PAGE 4	bag 1- 1/4 filter from 250 mL	PCR replicate (2nd)	15
8	02-B-C1/4b_PAGE 5	bag 1- 1/4 filter from 250 mL	PCR replicate (2nd), b/w gel replicate (PAGE 4, Lane 2)	13
9	29-B-C-1/4a2_PAGE 6	bag 1- 1/4 filter from 250 mL	digest replicate (2nd)	9
10	25-B-C(1/4)a2_PAGE 8	bag 1- 1/4 filter from 250 mL	digest replicate (2nd), b/w gel replicate (PAGE 6, Lane 29)	9
11	05-B-C(1/4)aa_PAGE 9	bag 1- 1/4 filter from 250 mL	PCR replicate	4
12	10-B-C3/4(1/10x)a_PAGE 4	bag 1 - 3/4 filter from 250 mL (diluted 1/10 after extraction)	original (1st)	13
13	10-B-C3/4(1/10x)a_PAGE 5	bag 1 - 3/4 filter from 250 mL (diluted 1/10 after extraction)	original (1st), b/w gel replicate (PAGE 4, Lane 10)	17
14	11-B-C3/4(1/10x)b_PAGE 4	bag 1 - 3/4 filter from 250 mL (diluted 1/10 after extraction)	PCR replicate (2nd)	10
15	11-B-C3/4(1/10x)b_PAGE 5	bag 1 - 3/4 filter from 250 mL (diluted 1/10 after extraction)	PCR replicate (2nd), b/w gel replicate (PAGE 4, Lane 11)	8
16	06-B-C(3/4)(1/10x)e_PAGE 6	bag 1 - 3/4 filter from 250 mL (diluted 1/10 after extraction)	PCR replicate (3rd)	4
17	02-B-C(3/4)(1/10x)e_PAGE 8	bag 1 - 3/4 filter from 250 mL (diluted 1/10 after extraction)	PCR replicate (3rd); b/w gel replicate (PAGE 6, Lane 6)	13
18	29-B-C(3/4)(1/10x)a2_PAGE 8	bag 1- 3/4 filter from 250 mL	digest replicate (2nd)	17
19	18-B-C2-3a_PAGE 4	bag 2 - 1/16 filter from 180 mL	original (1st)	15
20	18-B-C2-3a_PAGE 5	bag 2 - 1/16 filter from 180 mL	original (1st), b/w gel replicate (PAGE 4, 18)	12
21	05-B-C2-3a _PAGE 7	bag 2 - 1/16 filter from 180 mL	orginal (1st), b/w gel replicate (PAGE 4, Lane 18; PAGE 5, Lane 18)	5
22	37-B-C2-3a2_PAGE 6	bag 2 - 1/16 filter from 180 mL	digest replicate (2nd)	10
23	02-B-C2-3a2_PAGE 7	bag 2 - 1/16 filter from 180 mL	digest replicate (2nd), b/w gel replicate (PAGE 6, Lane 37)	8
24	33-B-C2-3a2_PAGE 8	bag 2 - 1/16 filter from 180 mL	digest replicate (2nd), b/w gel replicate (PAGE 6, Lane 37)	13
25	03-B-C2-2a_PAGE 7	bag 2 - 1/4 filter from 180 mL	original (1st)	1
26	20-B-C2-2a_PAGE 10	bag 2 - 1/4 filter from 180 mL	orignal (1st), b/w gel replicate (PAGE 7, Lane 3)	1
27	07-S-IB2 19:001 - 7 (11/22/02 a)_PAGE 1	bottle 2 - 1/4 filter from 1 L	original (1st)	8
28	25-S-IB2 19:00 1 - 11 (11/24/02 c)_PAGE 1	bottle 2 - 1/4 filter from 1 L	original (1st)	1
29	10-S-IB2-19:00-6/30-1aa_PAGE 9	bottle 2 - 1/4 filter from 1 L	original (1st)	2
30	26-S-IB2 19:00 2 - 12 (11/24/02 c)_PAGE 1	bottle 2 - 1/4 filter from 1 L	original (1st)	7
31	11-S-IB2-19:00-6/30-2aa_PAGE 9	bottle 2 - 1/4 filter from 1 L	original (1st)	1
32	14-S-IB3-19:006/301(1/10x)a_PAGE 4	bottle 3 - 1/4 filter from 950 mL (diluted 1/10 after extraction)	original (1st)	13
33	14-S-IB3-19:006/301(1/10x)a_PAGE 5	bottle 3 - 1/4 filter from 950 mL (diluted 1/10 after extraction)	original (1st), b/w gel replicate (PAGE 4, Lane 14)	12
34	35-S-IB3-19:00-6/30-1(1/10x)a2_PAGE 6	bottle 3 - 1/4 filter from 950 mL (diluted 1/10 after extraction)	digest replicate (2nd)	5
35	31-S-IB3-19:00-6/30-1(1/10x)a2_PAGE 8	bottle 3 - 1/4 filter from 950 mL (diluted 1/10 after extraction)	digest replicate (2nd), b/w gel replicate (PAGE 6, Lane 35)	7
36	15-S-IB3-19:006/301(1/10x)b_PAGE 4	bottle 3 - 1/4 filter from 950 mL (diluted 1/10 after extraction)	PCR replicate (2nd)	7
37	15-S-IB3-19:006/301(1/10x)b_PAGE 5	bottle 3 - 1/4 filter from 950 mL (diluted 1/10 after extraction)	PCR replicate (2nd), b/w gel replicate (PAGE 4, Lane 15)	4
38	08-S-IB3-6/30-19:00-1(1/10x)e_PAGE 7	bottle 3 - 1/4 filter from 950 mL (diluted 1/10 after extraction)	PCR replicate (3rd)	10
39	32-S-IB3-6/30-19:00-1(1/10x)e_PAGE 7	bottle 3 - 1/4 filter from 950 mL (diluted 1/10 after extraction)	PCR replicate (3rd), same gel replicate (PAGE 7, Lane 8)	9
40	26-S-IB3-19:00-6/30-1(1/10x)e_PAGE 10	bottle 3 - 1/4 filter from 950 mL (diluted 1/10 after extraction)	PCR replicate (3rd),b/w gel replicate (PAGE 7, Lanes 8 and 32)	8
41	16-S-IB3-19:006/301(1/50x)a_PAGE 4	bottle 3 - 1/4 filter from 950 mL (diluted 1/50 after extraction)	original (1st)	1
42	16-S-IB3-19:006/301(1/50x)a_PAGE 5	bottle 3 - 1/4 filter from 950 mL (diluted 1/50 after extraction)	original (1st), b/w gel replicate (PAGE 4, Lane 16)	2
43	36-S-IB3-19:00-6/30-1(1/50x)a2_PAGE 6	bottle 3 - 1/4 filter from 950 mL (diluted 1/50 after extraction)	digest replicate (2nd)	5
44	32-S-IB3-19:00-6/30-1(1/50x)a2_PAGE 8	bottle 3 - 1/4 filter from 950 mL (diluted 1/50 after extraction)	digest replicate (2nd), b/w gel replicate (PAGE 6, Lane 36)	1
45	17-S-IB3-19:006/301(1/50x)b_PAGE 4	bottle 3 - 1/4 filter from 950 mL (diluted 1/50 after extraction)	PCR replicate (2nd)	1
46	17-S-IB3-19:006/301(1/50x)b_PAGE 5	bottle 3 - 1/4 filter from 950 mL (diluted 1/50 after extraction)	PCR replicate (2nd), b/w gel replicate (PAGE 4, Lane 17)	1
47	08-S-IB3-6/30-19:00-2a_PAGE 6	bottle 3 - 1/4 filter from 950 mL	original (1st)	2
48	04-S-IB3(6/30)19:00-2a_PAGE 8	bottle 3 - 1/4 filter from 950 mL	original (1st), b/w gel replicate (PAGE 6, Lane 8)	4
49	09-S-IB3-6/30-19:00-2(1/10x)a_PAGE 6	bottle 3 - 1/4 filter from 950 mL (diluted 1/10 after extraction)	original (1st)	3
50	05-S-IB3(6/30)19:00-2(1/10x)a_PAGE 8	bottle 3 - 1/4 filter from 950 mL (diluted 1/10 after extraction)	original (1st), b/w gel replicate (PAGE 6, Lane 9)	5
51	09-S-IB3-6/30-19:00-2b_PAGE 7	bottle 3 - 1/4 filter from 950 mL	PCR replicate (2nd)	4
52	10-S-IB3-6/30-19:00-2(1/10x)b_PAGE 7	bottle 3 - 1/4 filter from 950 mL (diluted 1/10 after extraction)	PCR replicate (2nd)	4

CONTINUED

Subglacial Samples

Sample No.	Sample Name	Sample Description	Type of replicate	No. of T-RFs in each sample
53	14-S-IB3-6/30-19:00-3a_PAGE 7	bottle 3 - 1/2 filter from 950 mL	original (1st)	1
54	22-S-IB3-19:00-6/30-3a_PAGE 10	bottle 3 - 1/2 filter from 950 mL	orignal (1st), b/w gel replicate (PAGE 7, Lane 14)	1
55	20-S-IB3-6/30-19:00-3a_PAGE 7	bottle 3 - 1/2 filter from 950 mL	original (1st), same gel replicate (PAGE 7, Lane 14)	1
56	09-S-IB4-6/30-19:00-3a_PAGE 11	bottle 4 - 1/2 filter from 900 mL	original (1st)	1
57	23-S-IB4-6/30-19:00-3b_PAGE 13	bottle 4 - 1/2 filter from 900 mL	PCR replicate (2nd)	11
58	S-IB4(6/30)19:00-3a_PAGE 17	bottle 4 - 1/2 filter from 900 mL	PCR replicate (3rd)	24
59	11-S-IB-6/30-11PM-3a_PAGE 11	11pm S-IB sample - 1/2 filter from 990 mL	original (1st)	6
60	26-S-OC1-7/4-12:45PM-5b_PAGE 13	S-OC (bottle 1/3) 7/4 sample at 12:45 PM - 1/4 filter from 520 mL	PCR replicate (2nd)	27
61	24-S-AF-7/1-11AM-3b_PAGE 13	Sub AF- 7/1 sample at 11 AM - 1/4 filter from 1 L	PCR replicate (2nd)	12
62	S-AF(7/1)11:00-3a_PAGE 17	Sub AF- 7/1 sample at 11 AM - 1/4 filter from 1 L	original (1st)	22
63	S-AF(7/1)11:00-3b_PAGE 17	Sub AF- 7/1 sample at 11 AM - 1/4 filter from 1 L	PCR replicate (3rd)	16
64	18-B-F (filter #2) 1/4 - 4 (11/24/02 c)_PAGE 1	bag 1 - 1/4 filter from 230 mL (2nd filter)	original (1st)	10
65	04-B-F1/4(f#1)a_PAGE 7	bag 1 - 1/4 filter from 400 mL (1st filter)	original (1st)	1
66	12-B-F3/4(f1)(1/10x)a_PAGE 4	bag 1 - 3/4 filter from 400 mL (1st filter) (diluted 1/10 after extraction)	original (1st)	14
67	12-B-F3/4(f1)(1/10x)a_PAGE 5	bag 1 - 3/4 filter from 400 mL (1st filter) (diluted 1/10 after extraction)	original (1st), b/w gel replicate (PAGE 4, Lane 12)	12
68	13-B-F3/4(f1)(1/10x)b_PAGE 4	bag 1 - 3/4 filter from 400 mL (1st filter) (diluted 1/10 after extraction)	PCR replicate (2nd)	4
69	13-B-F3/4(f1)(1/10x)b_PAGE 5	bag 1 - 3/4 filter from 400 mL (1st filter) (diluted 1/10 after extraction)	PCR replicate (2nd), b/w gel replicate (PAGE 4, Lane 13)	4
70	05-B-F(3/4)(f1)(1/10x)e_PAGE 6	bag 1 - 3/4 filter from 400 mL (1st filter) (diluted 1/10 after extraction)	PCR replicate (3rd)	3
71	01-B-F(3/4)(f#1)(1/10x)e_PAGE 8	bag 1 - 3/4 filter from 400 mL (1st filter) (diluted 1/10 after extraction)	PCR replicate (3rd), b/w gel replicate (PAGE 6, Lane 5)	15
72	03-B-F(f2)1/4a_PAGE 4	bag 1 - 1/4 filter from 230 mL (2nd filter)	original (1st)	13
73	03-B-F(f2)1/4a_PAGE 5	bag 1 - 1/4 filter from 230 mL (2nd filter)	original (1st), b/w gel replicate (PAGE 4, Lane 3)	12
74	30-B-F(f2)1/4a2_PAGE 6	bag 1 - 1/4 filter from 230 mL (2nd filter)	digest replicate (2nd)	10
75	01-B-F(f2)1/4a2_PAGE 7	bag 1 - 1/4 filter from 230 mL (2nd filter)	digest replicate (2nd), b/w gel replicate (PAGE 6, Lane 30)	10
76	26-B-F(f#2)(1/4)a2_PAGE 8	bag 1 - 1/4 filter from 230 mL (2nd filter)	digest replicate (2nd), b/w gel replicate (PAGE 6, Lane 30)	7
77	04-B-F(f2)1/4b_PAGE 4	bag 1 - 1/4 filter from 230 mL (2nd filter)	PCR replicate (2nd)	15
78	04-B-F(f2)1/4b_PAGE 5	bag 1 - 1/4 filter from 230 mL (2nd filter)	PCR replicate (2nd), b/w gel replicate (PAGE 4, Lane 4)	13
79	06-B-F(f#2)1/4b_PAGE 7	bag 1 - 1/4 filter from 230 mL (2nd filter)	PCR replicate (2nd), b/w gel replicate (PAGE 4, Lane 4; PAGE 5, Lane 4)	9
80	06-B-F(f#2)(1/4)aa_PAGE 9	bag 1 - 1/4 filter from 230 mL (2nd filter)	PCR replicate	13
81	03-B-F(3/4)(f#2)(1/10x)a_PAGE 8	bag 1 - 3/4 filter from 230 mL (2nd filter) (diluted 1/10 after extraction)	original (1st)	1
82	07-B-F3/4(1/10x)(f#2)b_PAGE 7	bag 1 - 3/4 filter from 230 mL (2nd filter) (diluted 1/10 after extraction)	PCR replicate (2nd)	4
83	23-B-F2(f1)1(1/50x)a_PAGE 4	bag 2 - 1/8 filter from 460 mL (1st filter) (diluted 1/50 after extraction)	original (1st)	6
84	23-B-F2(f1)1(1/50x)a_PAGE 5	bag 2 - 1/8 filter from 460 mL (1st filter) (diluted 1/50 after extraction)	original (1st), b/w gel replicate (PAGE 4, Lane 23)	7
85	24-B-F2(f1)1(1/50x)b_PAGE 4	bag 2 - 1/8 filter from 460 mL (1st filter) (diluted 1/50 after extraction)	PCR replicate (2nd)	2
86	24-B-F2(f1)1(1/50x)b_PAGE 5	bag 2 - 1/8 filter from 460 mL (1st filter) (diluted 1/50 after extraction)	PCR replicate (2nd), b/w gel replicate (PAGE 4, Lane 24)	2
87	25-B-F2(f1)1(1/100x)a_PAGE 4	bag 2 - 1/8 filter from 460 mL (1st filter) (diluted 1/100 after extraction)	original (1st)	8
88	25-B-F2(f1)1(1/100x)a_PAGE 5	bag 2 - 1/8 filter from 460 mL (1st filter) (diluted 1/100 after extraction)	original (1st), b/w gel replicate (PAGE 4, Lane 25)	6
89	26-B-F2(f1)1(1/100x)b_PAGE 4	bag 2 - 1/8 filter from 460 mL (1st filter) (diluted 1/100 after extraction)	PCR replicate (2nd)	4
90	26-B-F2(f1)1(1/100x)b_PAGE 5	bag 2 - 1/8 filter from 460 mL (1st filter) (diluted 1/100 after extraction)	PCR replicate (2nd), b/w gel replicate (PAGE 4, Lane 26)	3
91	21-B-F2(f1)3(1/50x)a_PAGE 4	bag 2 - 1/16 filter from 460 mL (1st filter) (diluted 1/50 after extraction)	original (1st)	8
92	21-B-F2(f1)3(1/50x)a_PAGE 5	bag 2 - 1/16 filter from 460 mL (1st filter) (diluted 1/50 after extraction)	original (1st), b/w gel replicate (PAGE 4, Lane 21)	13
93	39-B-F2(f1)3(1/50x)a2_PAGE 6	bag 2 - 1/16 filter from 460 mL (1st filter) (diluted 1/50 after extraction)	digest replicate (2nd)	9
94	35-B-F2(f1)3(1/50x)a2_PAGE 8	bag 2 - 1/16 filter from 460 mL (1st filter) (diluted 1/50 after extraction)	digest replicate (2nd); b/w gel replicate (PAGE 6, Lane 39)	7
95	22-B-F2(f1)3(1/100x)a_PAGE 4	bag 2 - 1/16 filter from 460 mL (1st filter) (diluted 1/100 after extraction)	original (1st)	8
96	22-B-F2(f1)3(1/100x)a_PAGE 5	bag 2 - 1/16 filter from 460 mL (1st filter) (diluted 1/100 after extraction)	original (1st), b/w gel replicate (PAGE 4, Lane 22)	9
97	10-B-F2-5a_PAGE 6	bag 2 - 0.56 g of sediment	original (1st)	5
98	06-B-F2-5a_PAGE 8	bag 2 - 0.56 g of sediment	original (1st), b/w gel replicate (PAGE 6, Lane 10)	1
99	21-M-N 1/4 - 7 (11/24/02 c)_PAGE 1	bag 1 - 1/4 filter from 20 mL	original (1st)	5
100	07-M-N(1/4)aa_PAGE 9	bag 1 - 1/4 filter from 20 mL	original (1st)	6

Supraglacial Samples

Sample No.	Sample Name	Sample Description	Type of replicate	No. of T-RFs in each sample
101	03-SP-IS-a 1/4 - 3 (11/22/02 a)_PAGE 1	bottle 1 - 1/4 filter from 1 L	original (1st)	7
102	19-SP-IS-a 1/4 - 5 (11/24/02 c)_PAGE 1	bottle 1 - 1/4 filter from 1 L	original (1st)	13
103	20-SP-IS-a 3/4 - 6 (11/24/02 c)_PAGE 1	bottle 1 - 3/4 filter from 1 L	original (1st)	7
104	05-SP-IS-a1/4a_PAGE 4	bottle 1 - 1/4 filter from 1 L	original (1st)	12
105	05-SP-IS-a1/4a_PAGE 5	bottle 1 - 1/4 filter from 1 L	original (1st), b/w gel replicate (PAGE 4, Lane 5)	11
106	31-SP-IS-a-1/4a2_PAGE 6	bottle 1 - 1/4 filter from 1 L	digest replicate (2nd)	10
107	27-SP-IS-a(1/4)a2_PAGE 8	bottle 1 - 1/4 filter from 1 L	digest replicate (2nd), b/w gel replicate (PAGE 6, Lane 31)	9
108	06-SP-IS-a1/4b_PAGE 4	bottle 1 - 1/4 filter from 1 L	PCR replicate (2nd)	12
109	06-SP-IS-a1/4b_PAGE 5	bottle 1 - 1/4 filter from 1 L	PCR replicate (2nd), b/w gel replicate (PAGE 4, Lane 6)	12
110	07-SP-IS-a3/4a_PAGE 4	bottle 1 - 3/4 filter from 1 L	original (1st)	19
111	07-SP-IS-a3/4a_PAGE 5	bottle 1 - 3/4 filter from 1 L	original (1st), b/w gel replicate (PAGE 4, Lane 7)	19
112	32-SP-IS-a-3/4a2_PAGE 6	bottle 1 - 3/4 filter from 1 L	digest replicate (2nd)	6
113	28-SP-IS-a(3/4)a2_PAGE 8	bottle 1 - 3/4 filter from 1 L	digest replicate (2nd), b/w gel replicate (PAGE 6, Lane 32)	12
114	08-SP-IS-a3/4b_PAGE 4	bottle 1 - 3/4 filter from 1 L	PCR replicate (2nd)	9
115	08-SP-IS-a3/4b_PAGE 5	bottle 1 - 3/4 filter from 1 L	PCR replicate (2nd), b/w gel replicate (PAGE 4, Lane 8)	11

CONTINUED

Supraglacial Samples

Sample No.	Sample Name	Sample Description	Type of replicate	No. of T-RFs in each sample
116	19-SP-IS-a2-6/161a_PAGE 4	bottle 2 - 1/4 filter from 1 L	original (1st)	9
117	19-SP-IS-a2-6/161a_PAGE 5	bottle 2 - 1/4 filter from 1 L	original (1st), b/w gel replicate (PAGE 4, Lane 19)	10
118	38-SP-IS-a2-6/16-1a2_PAGE 6	bottle 2 - 1/4 filter from 1 L	digest replicate (2nd)	8
119	34-SP-IS-a2-6/16-1a2_PAGE 8	bottle 2 - 1/4 filter from 1 L	digest replicate (2nd), b/w gel replicate (PAGE 6, Lane 38)	10
120	20-SP-IS-a2-6/161b_PAGE 4	bottle 2 - 1/4 filter from 1 L	PCR replicate (2nd)	10
121	20-SP-IS-a2-6/161b_PAGE 5	bottle 2 - 1/4 filter from 1 L	PCR replicate (2nd), b/w gel replicate (PAGE 4, Lane 20)	9
122	SP-MLS-a(6/28)-3a_PAGE 17	SP-MLS-a - pre subglacial burst sample - 1/4 filter	original (1st)	11
123	SP-MLS-a(6/28)-3b_PAGE 17	SP-MLS-a - pre subglacial burst sample - 1/4 filter	PCR replicate (2nd)	4
124	13-SP-MLS-a-7/5-3a_PAGE 11	SP-MLS-a 7/5 - post-subglacial burst sample - 1/4 filter from1000 mL	original (1st)	4

Proglacial Samples

Sample No.	Sample Name	Sample Description	Type of replicate	No. of T-RFs in each sample
125	27-P-S 5 1x - 13 (11/24/02 c)_PAGE 1	bag 1 - 0.56 g of subsurface P-S sediments	original (1st)	23
126	09-P-S5(1x)a_PAGE 4	bag 1 of 0.56 g of subsurface P-S sediments	original (1st)	6
127	09-P-S5(1x)a_PAGE 5	bag 1 of 0.56 g of subsurface P-S sediments	original (1st), b/w gel replicate (PAGE 4, Lane 9)	2
128	P-S-2a_PAGE 17	bag 1 - 0.61 g of subsurface P-S sediments	original (1st)	7
129	P-S-2b_PAGE 17	bag 1 - 0.61 g of subsurface P-S sediments	PCR replicate (2nd)	7
130	01-P-R1-1a_PAGE 15	bag 1 - 0.41 g of subsurface P-R seds	original (1st)	3
131	02-P-R1-2a_PAGE 15	bag 1- 0.54 g of subsurface P-R seds	original (1st)	4
132	07-P-R1-3a_PAGE 15	bag 1 - 0.52 g of subsurface P-R seds	original (1st)	12
133	08-P-R1-4a_PAGE 15	bag 1 - 0.60 g of subsurface P-R seds	original (1st)	11
134	09-P-R1-5a_PAGE 15	bag 1 - 0.55 g of subsurface P-R seds	original (1st)	8
135	10-P-R1-6a_PAGE 15	bag 1 - 0.52 g of subsurface P-R seds	original (1st)	12
136	19-P-R1-1b_PAGE 15	bag 1 - 0.41 g of subsurface P-R seds	PCR replicate (2nd)	6
137	20-P-R1-2b_PAGE 15	bag 1- 0.54 g of subsurface P-R seds	PCR replicate (2nd)	4
138	25-P-R1-3b_PAGE 15	bag 1 - 0.52 g of subsurface P-R seds	PCR replicate (2nd)	12
139	26-P-R1-4b_PAGE 15	bag 1 - 0.60 g of subsurface P-R seds	PCR replicate (2nd)	10
140	27-P-R1-5b_PAGE 15	bag 1 - 0.55 g of subsurface P-R seds	PCR replicate (2nd)	14
141	28-P-R1-6b_PAGE 15	bag 1 - 0.52 g of subsurface P-R seds	PCR replicate (2nd)	15

Appendix 6. Sample list and key of all samples analyzed with T-RFLP analysis with the *Hha* I enzyme. The number preceding the sample name refers to the lane number on the gel. This number is followed by the sample site abbreviation and the bag or bottle number. No bag or bottle number indicates that the sample was taken from the first bag or bottle. The following numbers and letters refer to different aspects of the sample processing and molecular laboratory procedures. A description of samples in the next column explains the sample processing procedures represented by the numbers. The fractions refer to the portion of the filter from which DNA was extracted. "1st filter" represents the initial filtration process, whereas "2nd filter" refers to the second filtration unit used after the first filter became impassable with sediment. Whether the sample was diluted after the DNA extraction process in attempt to gain a better amplicon product is also noted. A description of the type of replicate the sample represents explains the molecular laboratory procedures represened by the letters. The suffixes "c" and "d" represent the first and second PCR amplifications and enzymatic digestions. The suffixes "g" and "h" represent the third and fourth PCR amplifications and enzymatic digestions. The suffixes "cc" and "dd" represent additional PCR amplifications and enzymatic digestions, in which the amount of DNA digested was not yet optimized to 6 ng/μL. Numbers following the letter suffixes indicate replicates of only the enzymatic digestion step using the same PCR amplicon. Finally, the polyacrylamide gel that the sample was run on is also noted. PAGE 1 represents the only 500-bp gel. PAGE 2 - 17 represent 2500-bp gels. Whether the sample represented a "same gel replicate" (identical samples run on the same polyacrylamide gel) or a "between (b/w) gel replicate" (identical samples run on different polyacrylamide gels) is also noted.

Subglacial Samples Sample No.	Sample Name	Sample Description	Type of replicate	No. of T-RFs in each sample
1	38-B-C #2 - 24 (11/24/02 c)_PAGE 1	bag 1 - combined DNA from several 500 uL muddy slurry tubes	original (1st)	2
2	39-B-C #3 - 25 (11/24/02 c)_PAGE 1	bag 1 - combined DNA from several 500 uL muddy slurry tubes	original (1st)	5
3	10-B-C#2cc_PAGE 10	bag 1 - combined DNA from several 500 uL muddy slurry tubes	original (1st)	5
4	11-B-C#3cc_PAGE 10	bag 1 - combined DNA from several 500 uL muddy slurry tubes	original (1st)	5
5	30-B-C 1/4 - 16 (11/24/02 c)_PAGE 1	bag 1 - 1/4 filter fr. 250 mL	original (1st)	7
6	01-B-C1/4c_PAGE 2	bag 1- 1/4 filter fr. 250 mL	original (1st)	6
7	01-B-C1/4c_PAGE 3	bag 1- 1/4 filter fr. 250 mL	original (1st), b/w gel replicate (PAGE 2, Lane 1)	7
8	02-B-C1/4d_PAGE 2	bag 1- 1/4 filter fr. 250 mL	PCR replicate (2nd)	10
9	02-B-C1/4d_PAGE 3	bag 1- 1/4 filter fr. 250 mL	PCR replicate (2nd), b/w gel replicate (PAGE 2, Lane 2)	11
10	19-B-C(1/4)cc_PAGE 9	bag 1- 1/4 filter fr. 250 mL	PCR replicate	4
11	02-B-C(1/4)dd_PAGE 10	bag 1- 1/4 filter fr. 250 mL	PCR replicate	12
12	10-B-C3/4(1/10x)c_PAGE 2	bag 1 - 3/4 filter fr. 250 mL (diluted 1/10 after ext.)	original (1st)	9
13	10-B-C3/4(1/10x)c_PAGE 3	bag 1 - 3/4 filter fr. 250 mL (diluted 1/10 after ext.)	original (1st), b/w gel replicate (PAGE 2, Lane 10)	8
14	11-B-C3/4(1/10x)d_PAGE 3	bag 1 - 3/4 filter fr. 250 mL (diluted 1/10 after ext.)	PCR replicate (2nd)	6
15	14-B-C(3/4)(1/10x)g_PAGE 8	bag 1 - 3/4 filter fr. 250 mL (diluted 1/10 after ext.)	PCR replicate (3rd), b/w gel replicate (PAGE 6, Lane 18)	4
16	18-B-C2-3c_PAGE 2	bag 2 - 1/16 filter fr. 180 mL	original (1st)	8
17	18-B-C2-3c_PAGE 3	bag 2 - 1/16 filter fr. 180 mL	original (1st), b/w gel replicate (PAGE 2, Lane 18)	9
18	14-S-IB2 19:001 - 14 (11/22/02 a)_PAGE 1	bottle 2 - 1/4 filter fr. 1 L	original (1st)	6
19	41-S-IB2 19:00 1 - 27 (11/24/02 c)_PAGE 1	bottle 2 - 1/4 filter fr. 1 L	original (1st)	2
20	42-S-IB2 19:00 2 - 28 (11/24/02 c)_PAGE 1	bottle 2 - 1/4 filter fr. 1 L	original (1st)	5
21	24-S-IB2-19:00-6/30-1cc_PAGE 9	bottle 2 - 1/4 filter fr. 1 L	original (1st)	4
22	25-S-IB2-19:00-6/30-2cc_PAGE 9	bottle 2 - 1/4 filter fr. 1 L	original (1st)	2
23	13-S-IB2-19:00-6/30-1cc_PAGE 10	bottle 2 - 1/4 filter fr. 1 L	PCR replicate	3
24	14-S-IB2-19:00-6/30-2cc_PAGE 10	bottle 2 - 1/4 filter fr. 1 L	PCR replicate	6
25	14-S-IB3-19:006/301(1/10x)c_PAGE 2	bottle 3 - 1/4 filter fr. 950 mL (diluted 1/10 after ext.)	original (1st)	10
26	14-S-IB3-19:006/301(1/10x)c_PAGE 3	bottle 3 - 1/4 filter fr. 950 mL (diluted 1/10 after ext.)	original (1st), b/w gel replicate (PAGE 2, Lane 14)	9
27	15-S-IB3-19:006/301(1/10x)d_PAGE 2	bottle 3 - 1/4 filter fr. 950 mL (diluted 1/10 after ext.)	PCR replicate (2nd)	10
28	15-S-IB3-19:006/301(1/10x)d_PAGE 3	bottle 3 - 1/4 filter fr. 950 mL (diluted 1/10 after ext.)	PCR replicate (2nd), b/w gel replicate (PAGE 2, Lane 15)	12
29	02-S-IB3-6/30-19:00-1(1/10x)g_PAGE 6	bottle 3 - 1/4 filter fr. 950 mL (diluted 1/10 after ext.)	PCR replicate (3rd), b/w gel replicate (PAGE 7, Lanes 33 and 11; PAGE 10, Lane 27)	5
30	11-S-IB3-6/30-19:00-1(1/10x)g_PAGE 7	bottle 3 - 1/4 filter fr. 950 mL (diluted 1/10 after ext.)	PCR replicate (3rd), same and b/w gel replicate (PAGE 6, Lane 2; PAGE 7, Lane 33; PAGE 10, Lane 2	11
31	33-S-IB3-6/30-19:00-1(1/10x)g_PAGE 7	bottle 3 - 1/4 filter fr. 950 mL (diluted 1/10 after ext.)	PCR replicate (3rd), same and b/w gel replicate (PAGE 6, Lane 2; PAGE 7, Lane 11; PAGE 10, Lane 2	10
32	27-S-IB3-19:00-6/30-1(1/10x)g_PAGE 10	bottle 3 - 1/4 filter fr. 950 mL (diluted 1/10 after ext.)	PCR replicate (3rd), b/w gel replicate (PAGE 6, Lane 2; PAGE 7, Lanes 11 and 33)	15
33	16-S-IB3-19:006/301(1/50x)c_PAGE 2	bottle 3 - 1/4 filter fr. 950 mL (diluted 1/50 after ext.)	original (1st)	4
34	16-S-IB3-19:006/301(1/50x)c_PAGE 3	bottle 3 - 1/4 filter fr. 950 mL (diluted 1/50 after ext.)	original (1st), b/w gel replicate (PAGE 2, Lane 16)	4
35	17-S-IB3-19:006/301(1/50x)d_PAGE 2	bottle 3 - 1/4 filter fr. 950 mL (diluted 1/50 after ext.)	PCR replicate (2nd)	3
36	17-S-IB3-19:006/301(1/50x)d_PAGE 3	bottle 3 - 1/4 filter fr. 950 mL (diluted 1/50 after ext.)	PCR replicate (2nd), b/w gel replicate (PAGE 2, Lane 17)	3
37	20-S-IB3-6/30-19:00-2c_PAGE 6	bottle 3 - 1/4 filter fr. 950 mL	original (1st)	1
38	16-S-IB3-6/30-19:00-2c_PAGE 8	bottle 3 - 1/4 filter fr. 950 mL	original (1st), b/w gel replicate (PAGE 6, Lane 20)	10
39	21-S-IB3-6/30-19:00-2(1/10x)c_PAGE 6	bottle 3 - 1/4 filter fr. 950 mL (diluted 1/10 after ext.)	original (1st)	2
40	17-S-IB3-6/30-19:00-2(1/10x)c_PAGE 8	bottle 3 - 1/4 filter fr. 950 mL (diluted 1/10 after ext.)	original (1st), b/w gel replicate (PAGE 6, Lane 21)	4
41	12-S-IB3-6/30-19:00-2c_PAGE 7	bottle 3 - 1/4 filter fr. 950 mL	original (1st), b/w gel replicate (PAGE 6, Lane 20; PAGE 8, Lane 16)	9
42	13-S-IB3-6/30-19:00-2(1/10x)c_PAGE 7	bottle 3 - 1/4 filter fr. 950 mL (diluted 1/10 after ext.)	original (1st), b/w gel replicate (PAGE 6, Lane 21; PAGE 8, Lane 17)	3
43	35-S-IB3-19:00-6/30-3c_PAGE 10	bottle 3 - 1/2 filter fr. 950 mL	original (1st)	1
44	23-S-IB4-6/30-19:00-3c_PAGE 11	bottle 4 - 1/2 filter from 900 mL	original (1st)	3
45	S-IB4(6/30)19:00-3c_PAGE 17	bottle 4 - 1/2 filter from 900 mL	original (1st)	25
46	S-IB4(6/30)19:00-3d_PAGE 17	bottle 4 - 1/2 filter from 900 mL	PCR replicate (2nd)	8
47	24-S-AF-7/1-11AM-3c_PAGE 11	Sub AF- 7/1 sample at 11 AM - 1/4 filter fr. 1 L	original (1st)	1
48	S-AF(7/1)11:00-3c_PAGE 17	Sub AF- 7/1 sample at 11 AM - 1/4 filter fr. 1 L	original (1st)	24
49	S-AF(7/1)11:00-3d_PAGE 17	Sub AF- 7/1 sample at 11 AM - 1/4 filter fr. 1 L	PCR replicate (2nd)	13
50	25-S-IB-6/30-11PM-3c_PAGE 11	11pm S-IB sample - 1/2 filter from 990 mL	original (1st)	6
51	26-S-OC1-7/4-12:45PM-3c_PAGE 11	S-OC (bottle 1/3) 7/4 sample at 12:45 PM - 1/4 filter fr. 520 mL	original (1st)	1
52	12-B-F3/4(f1)(1/10x)c_PAGE 2	bag 1 - 3/4 filter fr. 400 mL (1st filter) (diluted 1/10 after ext.)	original (1st)	11
53	12-B-F3/4(f1)(1/10x)c_PAGE 3	bag 1 - 3/4 filter fr. 400 mL (1st filter) (diluted 1/10 after ext.)	orignial (1st), b/w gel replicate (PAGE 2, Lane 12)	12
54	13-B-F3/4(f1)(1/10x)d_PAGE 2	bag 1 - 3/4 filter fr. 400 mL (1st filter) (diluted 1/10 after ext.)	PCR replicate (2nd)	5
55	13-B-F3/4(f1)(1/10x)d_PAGE 3	bag 1 - 3/4 filter fr. 400 mL (1st filter) (diluted 1/10 after ext.)	PCR replicate (2nd), b/w gel replicate (PAGE 2, Lane 13)	4
56	17-B-F(3/4)(f1)(1/10x)g_PAGE 6	bag 1 - 3/4 filter fr. 400 mL (1st filter) (diluted 1/10 after ext.)	PCR replicate (3rd)	4
57	13-B-F(3/4)(f#1)(1/10x)g_PAGE 8	bag 1 - 3/4 filter fr. 400 mL (1st filter) (diluted 1/10 after ext.)	PCR replicate (3rd), b/w gel replicate (PAGE 6, Lane 17)	8
58	19-B-F(3/4)(f2)(1/10x)c_PAGE 6	bag 1 - 3/4 filter fr. 230 mL (2nd filter) (diluted 1/10 after ext.)	original (1st)	1
59	15-B-F(3/4)(f#2)(1/10x)e_PAGE 8	bag 1 - 3/4 filter fr. 230 mL (2nd filter) (diluted 1/10 after ext.)	original (1st), b/w gel replicate (PAGE 6, Lane 19)	2
60	09-B-F (filter #2) 1/4 - 9 (11/22/02 a)_PAGE 1	bag 1 - 1/4 filter fr. 230 mL (2nd filter)	original (1st)	5
61	31-B-F (filter #2) 1/4 - 17 (11/24/02 c)_PAGE 1	bag 1 - 1/4 filter fr. 230 mL (2nd filter)	original (1st)	7
62	03-B-F(f2)1/4c_PAGE 2	bag 1 - 1/4 filter fr. 230 mL (2nd filter)	original (1st)	12

CONTINUED

Subglacial Samples

Sample No.	Sample Name	Sample Description	Type of replicate	No. of T-RFs in each sample
63	03-B-F(f2)1/4c_PAGE 3	bag 1 - 1/4 filter fr. 230 mL (2nd filter)	orinigal (1st), b/w gel replicate (PAGE 2, Lane 3)	12
64	04-B-F(f2)1/4d_PAGE 3	bag 1 - 1/4 filter fr. 230 mL (2nd filter)	PCR replicate (2nd)	10
65	02-B-F(f#2)(1/4)cc_PAGE 9	bag 1 - 1/4 filter fr. 230 mL (2nd filter)	PCR replicate	8
66	20-B-F(f#2)(1/4)dd_PAGE 9	bag 1 - 1/4 filter fr. 230 mL (2nd filter)	PCR replicate	15
67	03-B-F(f#2)(1/4)gg_PAGE 10	bag 1 - 1/4 filter fr. 230 mL (2nd filter)	PCR replicate	7
68	23-B-F2(f1)1(1/50x)c_PAGE 2	bag 2 - 1/8 filter fr. 460 mL (1st filter) (diluted 1/50 after ext.)	original (1st)	8
69	23-B-F2(f1)1(1/50x)c_PAGE 3	bag 2 - 1/8 filter fr. 460 mL (1st filter) (diluted 1/50 after ext.)	original (1st), b/w gel replicate (PAGE 2, Lane 23)	6
70	24-B-F2(f1)1(1/50x)d_PAGE 2	bag 2 - 1/8 filter fr. 460 mL (1st filter) (diluted 1/50 after ext.)	PCR replicate (2nd)	2
71	24-B-F2(f1)1(1/50x)d_PAGE 3	bag 2 - 1/8 filter fr. 460 mL (1st filter) (diluted 1/50 after ext.)	PCR replicate (2nd), b/w gel replicate (PAGE 2, Lane 24)	2
72	25-B-F2(f1)1(1/100x)c_PAGE 3	bag 2 - 1/8 filter fr. 460 mL (1st filter) (diluted 1/100 after ext.)	original (1st), b/w gel replicate (PAGE 2, Lane 25)	17
73	26-B-F2(f1)1(1/100x)d_PAGE 2	bag 2 - 1/8 filter fr. 460 mL (1st filter) (diluted 1/100 after ext.)	PCR replicate (2nd)	2
74	26-B-F2(f1)1(1/100x)d_PAGE 3	bag 2 - 1/8 filter fr. 460 mL (1st filter) (diluted 1/100 after ext.)	PCR replicate (2nd), b/w gel replicate (PAGE 2, Lane 26)	5
75	21-B-F2(f1)3(1/50x)c_PAGE 2	bag 2 - 1/16 filter fr. 460 mL (1st filter) (diluted 1/50 after ext.)	original (1st)	13
76	21-B-F2(f1)3(1/50x)c_PAGE 3	bag 2 - 1/16 filter fr. 460 mL (1st filter) (diluted 1/50 after ext.)	original (1st), b/w gel replicate (PAGE 2, Lane 21)	16
77	22-B-F2(f1)3(1/100x)c_PAGE 2	bag 2 - 1/16 filter fr. 460 mL (1st filter) (diluted 1/100 after ext.)	original (1st)	14
78	22-B-F2(f1)3(1/100x)c_PAGE 3	bag 2 - 1/16 filter fr. 460 mL (1st filter) (diluted 1/100 after ext.)	original (1st), b/w gel replicate (PAGE 2, Lane 22)	7
79	22-B-F2-5c_maya 9	bag 2 - 0.56 g of sediment	original (1st)	2
80	18-B-F2-5c_maya 11	bag 2 - 0.56 g of sediment	original (1st); b/w gel replicate (PAGE 6, Lane 22)	2
81	34-M-N 1/4 - 20 (11/24/02 e)_PAGE 1	bag 1 - 1/4 filter fr. 20 mL	original (1st)	1
82	21-M-N(1/4)cc_PAGE 9	bag 1 - 1/4 filter fr. 20 mL	original (1st)	12
83	06-M-N(1/4)dd_PAGE 10	bag 1 - 1/4 filter fr. 20 mL	PCR replicate	8

Supraglacial Samples

Sample No.	Sample Name	Sample Description	Type of replicate	No. of T-RFs in each sample
84	10-SP-IS-a 1/4 - 10 (11/22/02 a)_PAGE 1	bottle 1 - 1/4 filter fr. 1 L	original (1st)	4
85	32-SP-IS-a 1/4 - 18 (11/24/02 c)_PAGE 1	bottle 1 - 1/4 filter fr. 1 L	original (1st)	6
86	05-SP-IS-a1/4c_PAGE 2	bottle 1 - 1/4 filter fr. 1 L	original (1st)	12
87	05-SP-IS-a1/4c_PAGE 3	bottle 1 - 1/4 filter fr. 1 L	original (1st), b/w gel replicate (PAGE 2, Lane 5)	9
88	06-SP-IS-a1/4d_PAGE 2	bottle 1 - 1/4 filter fr. 1 L	PCR replicate (2nd)	6
89	06-SP-IS-a1/4d_PAGE 3	bottle 1 - 1/4 filter fr. 1 L	PCR replicate (2nd), b/w gel replicate (PAGE 2, Lane 6)	9
90	04-SP-IS-a(1/4)cc_PAGE 10	bottle 1 - 1/4 filter fr. 1 L	PCR replicate	10
91	33-SP-IS-a 3/4 - 19 (11/24/02 c)_PAGE 1	bottle 1 - 3/4 filter fr. 1 L	original (1st)	5
92	46-SP-IS-a 3/4 - 32 (11/24/02 c)_PAGE 1	bottle 1 - 3/4 filter fr. 1 L	original (1st)	6
93	47-SP-IS-a 3/4 x2 DNA - 33 (11/24/02 c)_PAGE 1	bottle 1 - 3/4 filter fr. 1 L	original (1st)	7
94	07-SP-IS-a3/4c_PAGE 2	bottle 1 - 3/4 filter fr. 1 L	original (1st)	11
95	07-SP-IS-a3/4c_PAGE 3	bottle 1 - 3/4 filter fr. 1 L	original (1st), b/w gel replicate (PAGE 2, Lane 7)	12
96	08-SP-IS-a3/4d_PAGE 2	bottle 1 - 3/4 filter fr. 1 L	PCR replicate (2nd)	11
97	08-SP-IS-a3/4d_PAGE 3	bottle 1 - 3/4 filter fr. 1 L	PCR replicate (2nd), b/w gel replicate (PAGE 2, Lane 8)	10
98	05-SP-IS-a(3/4)cc_PAGE 10	bottle 1 - 3/4 filter fr. 1 L	PCR replicate	11
99	18-SP-IS-a(3/4)dd_PAGE 10	bottle 1 - 3/4 filter fr. 1 L	PCR replicate	12
100	19-SP-IS-a(3/4)(2xDNA)dd_PAGE 10	bottle 1 - 3/4 filter fr. 1 L	PCR replicate	12
101	19-SP-IS-a2-6/161c_PAGE 2	bottle 2 - 1/4 filter fr. 1 L	original (1st)	15
102	19-SP-IS-a2-6/161c_PAGE 3	bottle 2 - 1/4 filter fr. 1 L	original (1st), b/w gel replicate (PAGE 2, Lane 19)	6
103	20-SP-IS-a2-6/161d_PAGE 2	bottle 2 - 1/4 filter fr. 1 L	PCR replicate (2nd)	8
104	20-SP-IS-a2-6/161d_PAGE 3	bottle 2 - 1/4 filter fr. 1 L	PCR replicate (2nd), b/w gel replicate (PAGE 2, Lane 20)	14
105	SP-IS-a(july5)-1c_PAGE 16	SP-IS-a 7/5 - post subglacial burst sample - 1/4 filter	original (1st)	2
106	SP-IS-a(july5)-2c_PAGE 16	SP-IS-a 7/5 - post subglacial burst sample - 1/4 filter	original (1st)	2
107	SP-IS-a(july5)-3c_PAGE 16	SP-IS-a 7/5 - post subglacial burst sample - 1/4 filter	original (1st)	1
108	SP-IS-a(july5)-4c_PAGE 16	SP-IS-a 7/5 - post subglacial burst sample - 1/4 filter	original (1st)	1
109	SP-MLS-a-(6/28)-3d_PAGE 17	SP-MLS-a - pre subglacial burst sample - 1/4 filter	original (1st)	7
110	27-SP-MLS-a-7/5-3c_PAGE 11	SP-MLS-a 7/5 - post-subglacial burst sample - 1/4 filter fr. 1000 mL	original (1st)	3

Proglacial Samples

Sample No.	Sample Name	Sample Description	Type of replicate	No. of T-RFs in each sample
111	P-S(1)(1/50x)d_PAGE 16	bag 1 - 0.57 g of P-S subsurface sediments (diluted 1/50x after extraction)	original (1st)	2
112	34-P-S2c_PAGE 11	bag 1 - 0.61 g of P-S subsurface sediments	original (1st)	1
113	P-S-2c_PAGE 17	bag 1 - 0.61 g of P-S subsurface sediments	original (1st)	16
114	P-S-2d_PAGE 17	bag 1 - 0.61 g of P-S subsurface sediments	PCR replicate (2nd)	16
115	13-P-S 4 1/100x - 13 (11/22/02 a)_PAGE 1	bag 1 - 0.49 g of P-S subsurface sediments (diluted 1/100 after ext.)	original (1st)	4
116	35-P-S 4 1/100x - 21 (11/24/02 c)_PAGE 1	bag 1 - 0.49 g of P-S subsurface sediments(diluted 1/100 after ext.)	original (1st)	1
117	11-P-S 5 1x - 11 (11/22/02 a)_PAGE 1	bag 1 - 0.56 g of P-S subsurface sediments	original (1st)	6
118	43-P-S 5 1x - 29 (11/24/02 c)_PAGE 1	bag 1 - 0.56 g of P-S subsurface sediments	original (1st)	1
119	45-P-S 5 1x - 31 (11/24/02 e)_PAGE 1	bag 1 - 0.56 g of P-S subsurface sediments	original (1st)	11
120	07-P-S5(1x)dd_PAGE 10	bag 1 - 0.56 g of P-S subsurface sediments	PCR replicate	2
121	06-P-S13d_PAGE 11	bag 1 - 0.09 g of P-S subsurface sediments	PCR replicate (2nd)	1
122	32-P-S13g_PAGE 11	bag 1 - 0.09 g of P-S subsurface sediments	PCR replicate (3rd)	1
123	33-P-S14d_PAGE 11	bag 1 - 0.13 g of P-S subsurface sediments	PCR replicate (2nd)	2
124	31-P-S18e_PAGE 11	bag 1 - 0.23 g of P-S subsurface sediments	original (1st)	3
125	15-P-S5(1x)(5%DMSO)cc_PAGE 10	bag 1 - 0.56 g of P-S subsurface sediments	PCR replicate	4
126	17-P-S5(1x)(5%DMSO)dd_PAGE 10	bag 1 - 0.56 g of P-S subsurface sediments	PCR replicate	23

Appendix 7. Category base pair sizes of all T-RFs resolved with both the *Hae* III and *Hha* I enzymes.

T-RF No.	T-RF Name	Base pair sizes of categories
1	A(1)02-03	Highest peak from 57.28 to 57.59 bp
2	A(1)04	Highest peak at 59.52 ± 0.05 bp
3	A(1)05-08	Highest peak from 61.97 to 62.98 bp
4	A(1)09	Highest peak from 65.31 to 65.47 bp
5	A(1)10	Highest peak at 67.79 ± 0.05 bp
6	A(1)11	Highest peak at 68.87 ± 0.05 bp
7	A(1)12	Highest peak at 75.00 ± 0.05 bp
8	Q(01)1-2	Highest peak from 80.21 to 80.39 bp
9	Q(01)3-4	Highest peak from 80.55 to 80.77 bp
10	A(1)13-J(1)02	Highest peak from 81.12 to 81.57 bp
11	Q(01)08-C(1)03	Highest peak from 82.20 to 82.40 bp
12	A(1)15-B(1)05	Highest peak from 82.48 to 83.53 bp
13	C(1)08-C(1)09	Highest peak from 84.22 to 84.61 bp
14	B(1)08	Highest peak at 85.23 ± 0.05 bp
15	C(1)10	Highest peak at 85.45 ± 0.05 bp
16	C(1)11-A(1)21	Highest peak from 86.22 to 87.30 bp
17	F(01)01-A(1)24	Highest peak from 89.03 to 89.46 bp
18	Q(01)15	Highest peak at 91.71 ± 0.05 bp
19	G(1)04-H(1)05	Highest peak from 93.05 to 93.25 bp
20	Q(01)17	Highest peak from 93.95 to 94.17 bp
21	G(1)05-C(1)23	Highest peak from 95.03 to 95.52 bp
22	C(1)24-C(1)25	Highest peak from 97.71 to 97.88 bp
23	B(1)15-16	Highest peak from 99.14 to 99.44 bp
24	C(1)29	Highest peak at 112.79 ± 0.05 bp
25	C(1)30-E(1)01	Highest peak from 114.51 to 114.71 bp
26	M(01)01	Highest peak at 119.28 ± 0.05 bp
27	B(1)17	Highest peak from 154.73 to 154.94 bp
28	E(1)02	Highest peak at 178.01 ± 0.05 bp
29	E(1)03-H(1)09	Highest peak from 178.94 to 179.19 bp
30	A(1)26	Highest peak at 179.50 ± 0.05 bp
31	A(1)27	Highest peak at 191.55 ± 0.05 bp
32	M(01)02	Highest peak at 193.69 ± 0.05 bp
33	Q(01)24	Highest peak at 194.38 ± 0.05 bp
34	A(1)28	Highest peak at 194.84 ± 0.05 bp
35	H(1)10	Highest peak at 195.05 ± 0.05 bp
36	A(1)29	Highest peak at 195.83 ± 0.05 bp
37	H(1)11-C(1)54	Highest peak from 196.04 to 196.27 bp
38	A(1)30	Highest peak at 196.82 ± 0.05 bp
39	D(1)05-H(1)12	Highest peak from 197.31 to 197.63 bp
40	A(1)31	Highest peak at 197.92 ± 0.05 bp
41	A(1)32	Highest peak at 198.31 ± 0.05 bp
42	D(1)07-09	Highest peak from 198.62 to 198.99 bp
43	Q(1)27-D(1)10	Highest peak from 199.08 to 199.98 bp
44	M(01)04-C(1)58	Highest peak from 200.09 to 200.36 bp
45	Q(01)28-30	Highest peak from 200.47 to 200.82 bp
46	Q(1)31-I(1)07	Highest peak from 200.86 to 201.39 bp
47	K(1)02-C(1)66	Highest peak from 201.47 to 202.55 bp
48	Q(01)37-G(1)12	Highest peak from 202.85 to 203.56 bp
49	B(1)24-C(1)67	Highest peak from 204.01 to 204.28 bp
50	M(01)09-O(01)20	Highest peak from 204.31 to 204.76 bp
51	Q(01)44	Highest peak at 204.95 ± 0.05 bp
52	A(1)40-Q(01)45	Highest peak from 205.16 to 205.30 bp
53	Q(01)46-47	Highest peak from 205.36 to 205.54 bp
54	F(01)07-Q(01)51	Highest peak from 205.88 to 206.58 bp
55	F(01)08-Q(01)53	Highest peak from 206.66 to 207.10 bp
56	A(1)41-42	Highest peak from 207.14 to 207.44 bp
57	O(01)22-C(1)76	Highest peak from 207.46 to 208.28 bp
58	Q(01)62-63	Highest peak from 208.76 to 208.92 bp
59	A(1)43-A(1)45	Highest peak from 209.04 to 210.75 bp
60	Q(01)70-J(1)28	Highest peak from 211.15 to 211.94 bp
61	I(1)15	Highest peak from 212.07 to 212.24 bp
62	Q()1)75-F(01)19	Highest peak from 212.32 to 212.52 bp
63	A(add1)	Highest peak at 212.75 ± 0.05 bp
64	A(1)47-Q(01)78	Highest peak from 213.20 to 213.48 bp
65	Q(01)79-80	Highest peak from 213.61 to 213.81 bp
66	A(1)48-Q(1)81	Highest peak from 214.71 to 214.86 bp
67	M(01)11	Highest peak at 215.52 ± 0.05 bp
68	O(01)28-29	Highest peak from 215.79 to 215.97 bp
69	A(1)49	Highest peak at 216.16 ± 0.05 bp
70	A(1)50	Highest peak at 216.95 ± 0.05 bp
71	A(1)51	Highest peak at 217.82 ± 0.05 bp
72	H(1)27-D(1)21	Highest peak from 217.99 to 219.06 bp
73	M(01)13-M(01)15	Highest peak from 219.21 to 219.79 bp
74	M(01)16-I(1)20	Highest peak from 219.98 to 220.68 bp
75	Q(01)86-A(1)57	Highest peak from 221.01 to 221.63 bp
76	Q(01)88-89	Highest peak from 222.18 to 222.44 bp
77	Q(01)90	Highest peak at 222.68 ± 0.05 bp
78	D(1)25-26	Highest peak from 223.28 to 223.48 bp
79	M(01)20	Highest peak at 223.71 ± 0.05 bp
80	D(1)27-29	Highest peak from 224.58 to 224.86 bp
81	M(01)21-I(1)21	Highest peak from 225.43 to 226.45 bp
82	M(01)22-G(1)23	Highest peak from 226.56 to 227.74 bp
83	A(1)61-J(1)31	Highest peak from 228.21 to 229.19 bp
84	A(1)62-K(1)09	Highest peak from 229.37 to 229.71 bp
85	A(1)65-G(1)28	Highest peak from 229.97 to 230.86 bp
86	I(1)29	Highest peak at 231.07 ± 0.05 bp
87	A(1)66	Highest peak at 232.38 ± 0.05 bp
88	O(01)35-36	Highest peak from 233.12 to 233.40 bp
89	O(01)37-39	Highest peak from 234.06 to 234.34 bp
90	O(01)40-41	Highest peak from 234.77 to 234.92 bp
91	O(01)42-I(1)31	Highest peak from 235.45 to 235.65 bp
92	M(01)23	Highest peak at 236.26 ± 0.05 bp
93	O(01)43-D(1)44	Highest peak from 236.98 to 237.19 bp
94	G(1)29-D(1)47	Highest peak from 237.47 to 237.65 bp
95	G(add1)	Highest peak at 238.42 ± 0.05 bp
96	E(1)30-D(1)47	Highest peak from 243.08 to 243.34 bp

CONTINUED

T-RF No.	T-RF Name	Base pair sizes of categories
97	M(01)25	Highest peak at 243.75 ± 0.05 bp
98	Q(01)92-93	Highest peak from 243.98 to 244.18 bp
99	A(1)67	Highest peak at 244.70 ± 0.05 bp
100	Q(01)94	Highest peak at 245.93 ± 0.05 bp
101	M(01)26	Highest peak at 253.09 ± 0.05 bp
102	Q(01)95	Highest peak at 253.26 ± 0.05 bp
103	Q(01)96	Highest peak at 255.17 ± 0.05 bp
104	K(1)11	Highest peak at 257.25 ± 0.05 bp
105	M(01)27	Highest peak at 257.44 ± 0.05 bp
106	M(01)28	Highest peak at 261.44 ± 0.05 bp
107	C(1)90	Highest peak at 267.85 ± 0.05 bp
108	D(1)48-49	Highest peak from 269.80 to 270.10 bp
109	A(1)68	Highest peak at 271.00 ± 0.05 bp
110	D(1)50-51	Highest peak from 276.08 to 276.28 bp
111	D(1)52	Highest peak at 278.24 ± 0.05 bp
112	H(1)40-F(01)38	Highest peak from 279.20 to 279.64 bp
113	E(1)31-32	Highest peak from 280.48 to 280.77 bp
114	E(1)33-D(1)55	Highest peak from 282.45 to 282.73 bp
115	A(1)73	Highest peak at 282.90 ± 0.05 bp
116	E(1)34-F(01)40	Highest peak from 283.28 to 283.86 bp
117	D(1)59-I(1)33	Highest peak from 285.37 to 285.56 bp
118	A(1)76	Highest peak at 291.24 ± 0.05 bp
119	I(1)34	Highest peak at 292.26 ± 0.05 bp
120	A(1)77	Highest peak from 292.65 to 292.87 bp
121	I(1)35	Highest peak at 293.12 ± 0.05 bp
122	D(1)60-Q(01)99	Highest peak from 294.08 to 294.36 bp
123	O(01)47-M(01)29	Highest peak from 294.37 to 294.54 bp
124	Q(1)100-O(1)48	Highest peak from 296.22 to 296.41 bp
125	E(1)38	Highest peak from 298.25 to 298.41 bp
126	O(1)49-A(1)79	Highest peak from 299.13 to 299.32 bp
127	E(1)39-I(2)1	Highest peak from 299.83 to 301.18 bp
128	C(2)1	Highest peak at 306.12 ± 0.10 bp
129	Q(2)1	Highest peak at 312.85 ± 0.10 bp
130	E(2)2-A(2)02	Highest peak from 314.39 to 314.82 bp
131	A(2)03-J(2)1	Highest peak from 315.53 to 316.35 bp
132	E(2)5-F(02)4	Highest peak from 316.64 to 317.24 bp
133	M(02)1	Highest peak at 317.51 ± 0.10 bp
134	A(2)05	Highest peak from 322.58 to 322.92 bp
135	E(2)7-D(2)7	Highest peak from 323.84 to 324.46 bp
136	Q(2)4	Highest peak at 325.97 ± 0.10 bp
137	M(02)2	Highest peak at 330.11 ± 0.10 bp
138	O(2)4-5	Highest peak from 330.64 to 331.20 bp
139	Q(2)5	Highest peak at 334.14 ± 0.10 bp
140	Q(2)6	Highest peak at 337.57 ± 0.10 bp
141	Q(2)7	Highest peak at 344.12 ± 0.10 bp
142	J(2)2	Highest peak at 352.27 ± 0.10 bp
143	J(2)3	Highest peak at 356.87 ± 0.10 bp
144	A(2)06	Highest peak at 363.87 ± 0.10 bp
145	J(2)4-B(2)2	Highest peak from 364.83 to 365.26 bp
146	A(2)07	Highest peak at 365.83 ± 0.10 bp
147	I(2)3-Q(2)8	Highest peak from 366.74 to 367.67 bp
148	Q(2)9-A(add4)	Highest peak from 367.81 to 368.45 bp
149	C(2)5-J(2)7	Highest peak from 368.93 to 369.42 bp
150	Q(2)12-13	Highest peak from 370.08 to 370.43 bp
151	P(2)7	Highest peak at 370.90 ± 0.10 bp
152	A(add5)	Highest peak at 372.81 ± 0.10 bp
153	Q(add1)	Highest peak from 373.35 to 373.85 bp
154	C(2)6-C(2)7	Highest peak from 373.98 to 374.54 bp
155	K(2)1-Q(2)24	Highest peak from 374.80 to 375.31 bp
156	C(2)8	Highest peak at 376.26 ± 0.10 bp
157	Q(2)25	Highest peak at 376.84 ± 0.10 bp
158	Q(2)26-A(add2)	Highest peak from 377.53 to 377.84 bp
159	Q(2)27	Highest peak at 380.47 ± 0.10 bp
160	P(2)21-A(2)08	Highest peak from 381.01 to 381.28 bp
161	P(2)22	Highest peak at 382.04 ± 0.10 bp
162	I(2)5	Highest peak at 382.49 ± 0.10 bp
163	A(2)09	Highest peak at 397.75 ± 0.10 bp
164	A(2)10	Highest peak at 399.35 ± 0.10 bp
165	Q(3)1	Highest peak from 400.20 to 400.75 bp
166	F(03)1-D(3)1	Highest peak from 400.85 to 401.32 bp
167	M(03)1	Highest peak at 402.28 ± 0.15 bp
168	A(3)1	Highest peak at 403.37 ± 0.15 bp
169	A(add6)	Highest peak at 403.65 ± 0.15 bp
170	A(3)2-Q(3)2	Highest peak from 403.91 to 404.43 bp
171	H(3)2-D(3)4	Highest peak from 404.49 to 406.02 bp
172	M(03)2-A(3)4	Highest peak from 406.33 to 407.50 bp
173	M(03)3	Highest peak at 407.79 ± 0.15 bp
174	H(3)5-Q(3)5	Highest peak from 408.50 to 409.52 bp
175	Q(3)6-8	Highest peak from 410.16 to 411.40 bp
176	F(03)4	Highest peak at 412.86 ± 0.15 bp
177	F(03)5	Highest peak at 414.63 ± 0.15 bp
178	F(03)6	Highest peak at 416.98 ± 0.15 bp
179	I(3)2	Highest peak at 464.34 ± 0.15 bp
180	C(3)03-05	Highest peak from 464.73 to 465.88 bp
181	B(3)03	Highest peak at 467.05 ± 0.15 bp
182	C(3)06-B(3)04	Highest peak from 469.36 to 470.45 bp
183	A(3)5-A(3)6	Highest peak from 471.54 to 472.47 bp
184	C(3)09-B(3)07	Highest peak from 473.18 to 474.83 bp
185	B(3)08	Highest peak at 475.81 ± 0.15 bp
186	C(3)11	Highest peak at 482.58 ± 0.15 bp
187	C(4)1-B(4)1	Highest peak from 514.85 to 515.54 bp
188	C(4)3	Highest peak at 545.95 ± 0.20 bp
189	Q(4)1	Highest peak at 560.14 ± 0.20 bp
190	Q(4)2	Highest peak at 562.34 ± 0.20 bp
191	J(4)1-C(4)4	Highest peak from 562.86 to 564.17 bp
192	D(4)1-Q(4)4	Highest peak from 564.24 to 565.31 bp
193	J(4)2-P(4)5	Highest peak from 565.98 to 568.29 bp
194	J(4)4-Q(4)13	Highest peak from 568.74 to 571.64 bp
195	Q(4)16	Highest peak at 594.95 ± 0.20 bp
196	Q(5)1	Highest peak at 601.14 ± 0.25 bp

CONTINUED

T-RF No.	T-RF Name	Base pair sizes of categories
197	Q(5)2-F(add1)	Highest peak from 602.94 to 604.16 bp
198	F(add2)-Q(5)5	Highest peak from 604.68 to 605.67 bp
199	P(05)1	Highest peak at 606.58 ± 0.25 bp
200	F(add3)	Highest peak at 607.42 ± 0.25 bp
201	Q(5)6-E(5)3	Highest peak from 609.57 to 611.66 bp
202	E(5)4-E(5)6	Highest peak from 611.70 to 613.70 bp
203	M(05)2	Highest peak at 614.17 ± 0.25 bp
204	F(add4)	Highest peak at 615.64 ± 0.25 bp
205	E(5)7-8	Highest peak from 616.63 to 619.24 bp
206	D(5)5	Highest peak at 621.39 ± 0.25 bp
207	G(5)3	Highest peak at 622.42 ± 0.25 bp
208	F(05)05	Highest peak at 663.32 ± 0.25 bp
209	B(5)01	Highest peak at 668.65 ± 0.25 bp
210	J(5)1-B(5)10	Highest peak from 669.66 to 673.80 bp
211	B(5)11	Highest peak at 678.23 ± 0.25 bp
212	C(add1)	Highest peak at 681.95 ± 0.25 bp
213	F(05)11	Highest peak at 697.36 ± 0.25 bp
214	F(06)3	Highest peak at 707.25 ± 0.35 bp
215	F(06)6	Highest peak at 775.62 ± 0.35 bp
216	Q(6)1	Highest peak at 786.62 ± 0.35 bp
217	P(6)2	Highest peak at 790.24 ± 0.35 bp
218	J(7)1	Highest peak at 843.88 ± 0.50 bp
219	D(7)1	Highest peak from 870.13 to 871.80 bp
220	D(7)2-D(7)3	Highest peak from 871.70 to 873.22 bp
221	C(8)1	Highest peak at 905.54 ± 0.75 bp
222	F(08)3	Highest peak at 917.58 ± 0.75 bp
223	J(8)1-J(8)2	Highest peak from 964.71 to 967.95 bp
224	B(add1)	Highest peak at 982.61 ± 0.75 bp
225	C(8)2-J(8)5	Highest peak from 988.29 to 994.52 bp
226	C(8)6-8	Highest peak from 993.88 to 999.45 bp
227	J(9)1-C(9)1	Highest peak from 1000.29 to 1005.18 bp
228	I(9)1-K(add1)	Highest peak from 1006.11 to 1014.80 bp
229	J(9)6	Highest peak from 1015.56 to 1018.57 bp
230	D(10)1-2	Highest peak from 1116.01 to 1122.93 bp
231	K(11)1	Highest peak at 1231.89 ± 2.00 bp

Appendix 8. EC (μS/cm) and pH values of supraglacial snow, supraglacial waters, subglacial waters, and basal ice samples.

Sample Location (Date)	EC value (μS/cm)	pH value
Supraglacial Snow		
Wet snow (SP-IS-a stream bank) (6/19/02)	3.4	6.8
Wet snow (Lower glacier) (6/19/02)	11	8.6
Wet snow (Middle glacier) (6/20/02)	21	8.7
Supraglacial Waters		
SP-IS-a (7/5/02)	4.3	7.8
SP-IS-a (7/18/02)	6.6	No measurement
SP-MLS-b (7/5/02)	7.5	7.5
SP-MLS-b (6/16/02)	8.2	7.9
SP-MLS-b (6/28/02)	8.4	7.6
SP-IS-a (6/16/02)	9.3	7.0
SP-IS-b (6/18/02)	11	7.7
SP-IS-a (6/28/02)	11	7.3
SP-MLS-a (6/28/02)	11	7.3
SP-MLS-a (7/18/02)	20	6.7
SP-MLS-a (7/5/02)	29	7.5
SP-ML-a (7/5/02)	40	7.7
SP-MLS-b (7/13/02)	41	8.1
SP-ML-a (6/28/02)	48	7.3
SP-ML-a (6/28/02)	49	6.4
Subglacial Waters		
SB-OC 12:45 h (7/4/02)	185	7.4
SB-AF 11:55 h (7/4/02)	210	7.4
SB-OC 17:00 h (7/23/02)	236	8.8
SB-AF 23:00 h (7/2/02)	240	No measurement
SB-OC 14:00 h (7/19/02)	262	8.6
SB-OC 17:00 h (7/16/02)	310	7.9
SB-OC 23:00 h (7/2/02)	340	No measurement
SB-OC 14:15 h (7/12/02)	361	7.7
SB-AF 15:30 h (7/1/02)	390	8.5
SB-AF 14:30 h (7/1/02)	423	8.5
SB-IB 7:00 h (7/1/02)	436	8.2
SB-AF 13:30 h (7/1/02)	437	8.4
SB-AF 12:30 h (7/1/02)	453	8.4
SB-AF 10:00 h (7/1/02)	454	8.3
SB-IB 9:00 h (7/1/02)	470	8.3
SB-AF 11:00 h (7/1/02)	470	8.3
SB-IB 8:00 h (7/1/02)	473	8.2
SB-IB 5:00 h (7/1/02)	482	8.1
SB-IB 24:00 h (6/30/02)	491	8.3
SB-AF 9:00 h (7/1/02)	492	8.3
SB-IB 6:00 h (7/1/02)	508	8.1
SB-IB 4:00 h (7/1/02)	534	8.1
SB-IB 3:00 h (7/1/02)	562	8.1
SB-IB 21:00 h (6/30/02)	577	8.0
SB-IB 2:00 h (7/1/02)	587	8.0
SB-IB 20:00 h (6/30/02)	594	7.9
SB-IB 23:00 h (6/30/02)	603	7.9
SB-IB 1:00 h (7/1/02)	618	8.0
SB-IB 19:00 h (6/30/02)	646	7.9
SB-IB 19:00 h (6/30/02)	646	7.9
SB-IB 22:00 h (6/30/02)	694	7.9
Basal Ice		
B-F (bag 1) (7/31/02)	62	7.4
B-C (bag 2) (7/15/02)	68	7.6
B-S (bag 1) (5/31/02)	114	8.2
B-F (bag 2) (7/31/02)	223	7.0
B-C (bag 1) (7/15/02)	235	6.4

Appendix 9. Nitrate and sulfate concentrations in supraglacial snow, supraglacial waters, subglacial waters, and basal ice samples. The early season nitrate depleted subglacial water samples are indicated with an asterik.

Sample Location (Date)	Nitrate Amount (μeq/L)	Sulfate Amount (μeq/L)
Supraglacial Snow		
Wet snow (Middle glacier) (6.20.02)	0	2.4
Wet snow (SP-IS-a bank) (6.19.02)	0	0.6
Wet snow (Lower glacier) (6.18.02)	1.8	2.8
Supraglacial Waters		
SP-IS-a (7.18.02)	0.2	1.6
SP-MLS-b (7.5.02)	0.5	2.9
SP-MLS-b (6.16.02)	0.6	5.2
SP-MLS-a (7.5.02)	0.6	2.4
SP-MLS-b (6.28.02)	0.7	3.0
SP-MLS-a (7.18.02)	0.7	5.3
SP-MLS- a (7.18.02)	0.8	5.1
SP-ML-a (7.5.02)	0.8	6.4
SP-ML-a (7.5.02)	1.0	6.9
SP-MLS-b (7.13.02)	1.1	8.6
SP-MLS-a (6.28.02)	1.2	4.1
SP-IS-a (6.16.02)	1.2	6.6
SP-IS-b (6.18.02)	1.4	6.4
SP-ML-a (6.28.02)	1.6	7.7
SP-ML-a (6.28.02)	1.9	9.4
SP-IS-a (6.28.02)	1.9	5.3
Subglacial Waters		
SB-AF 14:30 h (7.1.02)*	0.1	3830
SB-AF 12:30 h (7.1.02)*	0.2	3788
SB-IB 8:00 h (7.1.02)*	0.2	3775
SB-IB 7:00 h (7.1.02)*	0.2	3816
SB-IB 4:00 h (7.1.02)*	0.2	4436
SB-IB 10:00 h (7.1.02)*	0.2	4063
SB-IB 5:00 h (7.1.02)*	0.3	4180
SB-IB 9:00 h (7.1.02)*	0.3	3872
SB-IB 6:00 h (7.1.02)*	0.3	4373
SB-IB 21:00 h (6.30.02)*	0.3	3587
SB-IB 20:00 h (6.30.02)*	0.3	5446
SB-IB 2:00 h (7.1.02)*	0.3	5409
SB-IB 19:00 h (6.30.02)*	0.3	6328
SB-IB 19:00 h (6.30.02)*	0.4	5872
SB-OC 17:00 h (7.23.02)	0.4	1527
SB-IB 1:00 h (7.1.02)*	0.4	5353
SB-IB 3:00 h (7.1.02)*	0.4	5005
SB-IB 22:00 h (6.30.02)*	0.5	6674
SB-OC 16:50 h (7.16.02)	0.7	1994
SB-OC 14:00 h (7.19.02)	0.7	2094
SB-AF 11:55 h (7.4.02)	1.0	1586
SB-OC 12:45 h (7.5.02)	1.1	1341
SB-OC 12:45 h (7.5.02)	1.1	1339
SB-OC 15:00 h (7.12.02)	1.6	2995
SB-AF 13:30 h (7.1.02)	2.5	3820
SB-IB 23:00 h (6.30.02)	2.8	5007
SB-AF 15:30 h (7.1.02)	2.8	3414
SB-AF 9:00 h (7.1.02)	3.1	4388
SB-IB 24:00 h (6.30.02)	3.1	4232
SB-AF 11:00 h (7.1.02)	3.6	4297
Basal Ice		
B-S (bag 1) (5.31.02)	0	197
B-C (bag 1) (6.15.02)	0	1308
B-F (bag 1) (8.1.02)	0	5.9
B-F (bag 2) (8.1.02)	0.8	9.1
B-C (bag 2) (6.15.02)	1.1	1343

Appendix 10. Dissolved organic carbon (DOC) concentrations in parts per million (ppm) in supraglacial snow, supraglacial waters, subglacial waters, and basal ice samples.

Sample Location (Date)	DOC amount (ppm)
Supraglacial Snow	
Wet snow (Middle glacier) (6.20.02)	0.38
Wet snow (Lower glacier) (6.19.02)	1.23
Wet snow (SP-IS-a) (6.19.02)	1.35
Supraglacial Waters	
SP-MLS-a (7.5.02)	0.26
SP-IS-a (7.5.02)	0.35
SP-MLS-a (7.5.02)	0.55
SP-IS-a (6.30.02)	0.57
SP-MLS-b (7.13.02)	0.67
SP-MLS-b (6.16.02)	0.95
SP-IS-a (6.16.02)	1.01
SP-IS-b (6.18.02)	1.21
SP-MLS-b (7.13.02)	1.85
SP-MLS-a (7.18.02)	2.47
SP-IS-a (7.18.02)	3.42
Subglacial Waters	
SB-AF 15:30 h (7.1.02)	0.24
SB-OC (7.23.02)	0.25
SB-AF 11:55 h (7.4.02)	0.34
SB-IB 19:00 h (6.30.02)	0.35
SB-OC 12:45 h (7.4.02)	0.46
SB-OC 12:45 h (7.4.02)	0.65
SB-OC (7.16.02)	2.28
SB-OC (7.12.02)	2.83
SB-OC (7.19.02)	3.71
Basal Ice	
B-S (bag 1) (5.31.02)	0.55
B-F (bag 1) (7.31.02)	1.17
B-F (bag 2) (7.31.02)	0.76
B-C (bag 1) (6.15.02)	62.9
B-C (bag 2) (6.15.02)	244

Appendix 11. Table summarising the T-RF occurrences of each sample analyzed with the *Hae* III enzyme. For each sample, the percentage occurrence values of all T-RFs present in samples from each primary environment were summed, and divided by the total number of T-RFs present in the sample. Percent occurrences greater than 10% in any environment are in boldface. The environmental presence is also summarised. "All" signifies that the sample contains at least one T-RF that was found in all three primary environments. "SB" denotes the subglacial environment. "SP" denotes the supraglacial environment. "P" denotes the proglacial environment. Samples 1-26 are B-C samples. Samples 27-63 are subglacial water samples. Samples 64-98 are B-F samples. Samples 99-100 are M-N samples. Samples 101-121 are SP-IS-a samples. Samples 122-124 are SP-MLS-a samples. Samples 125-129 are P-S samples. Samples 130-141 are P-R

Hae III sample key no.	Occurrences Subglacial (%)	Occurences Supraglacial (%)	Occurences Proglacial (%)	Environmental Presence
1	**17**	4	6	ALL
2	**14**	13	8	ALL
3	**15**	12	7	ALL
4	**13**	17	8	ALL
5	**28**	14	13	ALL
6	**35**	9	12	ALL
7	**30**	14	15	ALL
8	**32**	15	17	ALL
9	**26**	11	12	ALL
10	**34**	13	12	ALL
11	**38**	24	24	ALL
12	**34**	20	12	ALL
13	**31**	20	10	ALL
14	**10**	8	10	ALL
15	**17**	7	13	ALL
16	**38**	24	24	ALL
17	**33**	20	12	ALL
18	**30**	16	10	ALL
19	**27**	18	10	ALL
20	**29**	24	9	ALL
21	**38**	7	5	ALL
22	**33**	19	11	ALL
23	**35**	23	13	ALL
24	**30**	21	9	ALL
25	**27**	92	0	SBSP
26	**27**	92	0	SBSP
27	**10**	6	5	ALL
28	**17**	0	6	SBP
29	**55**	4	21	ALL
30	**9**	7	2	ALL
31	**66**	4	0	SBSP
32	**33**	20	12	ALL
33	**28**	32	8	ALL
34	**45**	22	0	SBSP
35	**45**	17	18	ALL
36	**40**	27	6	ALL
37	**44**	25	10	ALL
38	**35**	27	13	ALL
39	**38**	23	14	ALL
40	**34**	34	15	ALL
41	**66**	4	0	SBSP
42	**37**	42	0	SBSP
43	**32**	4	19	ALL
44	**66**	4	0	SBSP
45	**66**	4	0	SBSP
46	**66**	4	0	SBSP
47	**25**	4	0	SBSP
48	**46**	5	10	ALL
49	**19**	4	2	ALL
50	**42**	23	8	ALL
51	**46**	5	10	ALL
52	**46**	5	10	ALL
53	**66**	4	0	SBSP
54	**66**	4	0	SBSP
55	**66**	4	0	SBSP
56	**66**	4	0	SBSP
57	**20**	2	14	ALL
58	**14**	9	6	ALL
59	**29**	26	8	ALL
60	**13**	4	5	ALL
61	**18**	1	14	ALL
62	**11**	10	7	ALL
63	**15**	11	8	ALL
64	**15**	12	5	ALL
65	**58**	0	0	SB
66	**31**	9	11	ALL

CONTINUED

Hae III sample key no.	Occurrences Subglacial (%)	Occurences Supraglacial (%)	Occurences Proglacial (%)	Environmental Presence
67	34	10	12	ALL
68	52	2	21	ALL
69	52	2	21	ALL
70	2	0	27	SBP
71	27	10	12	ALL
72	33	10	11	ALL
73	35	9	12	ALL
74	34	10	10	ALL
75	26	13	8	ALL
76	40	7	12	ALL
77	31	15	10	ALL
78	33	10	11	ALL
79	34	15	9	ALL
80	33	10	11	ALL
81	58	0	0	SB
82	52	2	21	ALL
83	45	3	21	ALL
84	41	2	18	ALL
85	46	0	0	SB
86	46	0	0	SB
87	11	6	12	ALL
88	14	8	16	ALL
89	36	5	3	ALL
90	45	1	14	ALL
91	41	2	15	ALL
92	32	11	10	ALL
93	14	10	12	ALL
94	15	11	14	ALL
95	37	4	16	ALL
96	33	4	14	ALL
97	10	12	19	ALL
98	58	0	0	SB
99	11	3	8	ALL
100	22	3	23	ALL
101	8	28	3	ALL
102	9	26	2	ALL
103	8	28	3	ALL
104	9	58	1	ALL
105	9	63	1	ALL
106	9	57	1	ALL
107	10	69	1	ALL
108	8	60	1	ALL
109	9	60	7	ALL
110	11	43	5	ALL
111	11	45	5	ALL
112	12	76	0	SBSP
113	11	60	1	ALL
114	9	69	1	ALL
115	9	63	1	ALL
116	8	71	1	ALL
117	7	68	1	ALL
118	17	41	12	ALL
119	12	65	5	ALL
120	8	66	8	ALL
121	8	71	1	ALL
122	13	23	2	ALL
123	5	39	0	SBSP
124	12	40	0	SBSP
125	8	3	14	ALL
126	14	17	33	ALL
127	15	8	12	ALL
128	3	0	11	SBP
129	3	0	11	SBP
130	20	7	78	ALL
131	15	5	74	ALL
132	10	2	52	SBP
133	10	2	54	ALL
134	8	3	62	ALL
135	9	3	50	ALL
136	10	4	59	ALL
137	15	5	74	ALL
138	10	2	52	ALL
139	11	3	55	ALL
140	9	2	47	ALL
141	11	4	48	ALL